UNIVERSITÉ GRENOBLE ALPES
Observatoire des Sciences de l'Univers de Grenoble
UNIVERSITY OF THESSALY
Civil Engineering Department

Drought Analysis using Meteorological Drought Indices, in Thessaly region, Greece

Author: Theodoros Karampatakis
Supervisor: Dr. Lampros Vasiliades

Greek-French program of postgraduate studies
"Management of Hydrometeorological Hazards-Hydrohasards"

2017

ACKNOWLEDGMENTS

This project represents the final part of my master degree, in the Greek-French postgraduate program "Hydrohasards".

First of all I would like to thank my main supervisor, Dr. Lampros Vasiliades, for making this project possible, for his encouraging attitude, constructive criticism and inspiring discussions during this period. Moreover, I would like to express my sincere gratitude to the coordinators of the program, Athanasios Loukas from University of Thessaly in Greece and Gilles Molinié from Université Joseph Fourier (Grenoble Alpes) in France for my selection, giving me the opportunity to fulfill my ambitions and goals. Furthermore, their help and guidance during the semesters was crucial for my adaptation to the program.

Finally, I would like to thank my family and my friends for their boundless support along with all the people in the department, who established a very friendly and creative working environment.

ABSTRACT

Droughts constitute perhaps the most complex natural phenomenon. Their inevitable nature in combination with the prolonged and nonstructural effects cause confusion in the scientific society apropos the formation of a concrete definition and consequently rendering their deeper understanding infeasible. In an effort to monitor and assess droughts there are many indices suggested, based on one or more hydro-climatic parameters in order to identify different aspects which contribute to the intensification of the phenomenon. In this dissertation, the behavior of four meteorological drought indices with different structure is discussed, analyzing drought episodes in Thessaly. More specifically the widely used indices SPI and SPEI and two produced multivariate models MSDI(Pr-PET), MSDI(SPI-SPEI) which are motivated by the promising MSDI index, are selected for the comparative drought analysis of the region. The first model is structured combining probabilistically the hydro-climatic variables of precipitation and potential evapotranspiration (PET), while the second is formed combining probabilistically the indices SPI and SPEI. Main purpose of this multivariate synthesis is to generate two new indices capable of being used as supplementary tools in monitoring and assessing droughts. The monthly precipitation and temperature data, covering the hydrological period 1960-2002, were used for the calculation of the considered indices at time scales: 1, 3, 6, 9 and 12 months. In order to obtain equal amount of precipitation and temperature data, the lapse rate method is applied, forming a total of 78 meteorological stations in the region. The results of the time series and a drought classification for all the stations are cited, presenting the main similarities/differences in the behavior of the four indices in the drought analysis of Thessaly. Additionally, a correlation analysis is conducted, displaying scatter plots and spatial patterns of the correlation values for the possible combinations of the examined indices. SPI and SPEI indices seem to be the most appropriate for the detection of drought episodes in the region, whereas the weakness of the two multivariate models to capture extremely drought events is obvious. Furthermore, it was ascertained that SPI and SPEI indices are more strongly correlated in the mountainous regions where the influence of the potential evapotranspiration is not so noticeable and therefore they mainly respond to the rainfall fluctuations. In the last part of this thesis a Principal Component Analysis (PCA) is performed for the most efficient indices SPI and SPEI, at time scales 3 and 12. According to this methodology, a reduction in the dimensionality of the initial SPI and SPEI series can be achieved, providing information for the drought variability of the region and thus, it can be construed as a new index for the aforementioned meteorological drought measures. The outcomes indicate two similar homogeneous patterns for both indices, expressing the temporal evolution of droughts in Thessaly for the 42 hydrological years. The most extreme drought events were recorded in the end of 70s and in the beginning of 90s considering the short term drought conditions. Examining the hydrological drought conditions, the most extreme drought episodes were detected in the end of 70s and in the end of 80s. An orthogonal rotation of the axes is conducted, providing several distinctive small regions for our study area. The results suggest that the inclusion of potential evapotranspiration especially in the drought monitoring of low-altitude regions, is crucial for the identification of spatial drought patterns, at least in a local scale.

ΠΕΡΙΛΗΨΗ

Οι ξηρασίες αποτελούν ίσως το πιο περίπλοκο φυσικό φαινόμενο. Η αναπόφευκτη φύση τους, σε συνδυασμό με τις εκτενείς και μη δομημένες επιδράσεις επιφέρουν μια σύγχυση στην επιστημονική κοινότητα σχετικά με την απόδοση μιας σαφής εννοίας, καθιστώντας ανέφικτη τη βαθύτερη κατανόηση τους. Σε μια προσπάθεια παρακολούθησης και αξιολόγησης του φαινομένου, πολλοί δείκτες ξηρασίας έχουν προταθεί, βασιζόμενοι σε μια ή περισσότερες υδρο-κλιματικές παραμέτρους προκειμένου να προσδιοριστούν διάφορες πτυχές που συμβάλουν στην εντατικοποίηση του φαινομένου. Στην παρούσα διατριβή, εξετάζεται η συμπεριφορά τεσσάρων μετεωρολογικών δεικτών ξηρασίας με διαφορετική δομή, αναλύοντας τα επεισόδια ξηρασίας στην περιοχή της Θεσσαλίας. Συγκεκριμένα οι διαδεδομένοι δείκτες SPI και SPEI επιλέγονται, λαμβάνοντας υπόψη την παράμετρο της βροχόπτωσης και της δυνητικής εξατμισοδιαπνοής αντίστοιχα. Η συγκριτική ανάλυση πλαισιώνεται από δυο παραγόμενα πολυμεταβλητά μοντέλα MSDI(Pr-PET) και MSDI(SPI-SPEI), προερχόμενα από τον υποσχόμενο δείκτη MSDI. Το πρώτο μοντέλο δομείται συνδυάζοντας πιθανολογικά τις υδρο-κλιματικές μεταβλητές της βροχόπτωσης και της δυνητικής εξταμισοδιαπνοής, ενώ το δεύτερο, συνδυάζοντας τους δείκτες SPI και SPEI. Κύριος σκοπός αυτής πολυμεταβλητής σύνθεσης, είναι να δημιουργηθούν δυο νέοι ικανοί δείκτες που να μπορούν να χρησιμοποιηθούν ως επιπρόσθετα εργαλεία στην παρακολούθηση και εκτίμηση των ξηρασιών. Τα μηναία βροχομετρικά και θερμοκρασιακά δεδομένα της υδρολογικής περιόδου 1960-2002 χρησιμοποιήθηκαν για τον υπολογισμό των εξεταζόμενων δεικτών, κατά τις χρονικές κλίμακες: 1, 3, 6, 9 και 12. Προκειμένου να εξασφαλιστεί ισάξιος αριθμός βροχομετρικών και θερμοκρασιακών δεδομένων, η μέθοδος της κατακόρυφης θερμοβαθμίδας εφαρμόζεται, σχηματίζοντας συνολικά 78 μετεωρολογικούς σταθμούς στην περιοχή. Τα αποτελέσματα των χρόνο-σειρών και η ταξινόμηση των γεγονότων ξηρασίας για όλους τους σταθμούς παρατίθενται, παρουσιάζοντας τις βασικές ομοιότητες/διαφορές στην συμπεριφορά των τεσσάρων δεικτών. Επιπλέον, μια ανάλυση συσχέτισης των τεσσάρων δεικτών διεξάγεται, προβάλλοντας διαγράμματα σκεδασμού και χωρικά μοτίβα συσχετίσεων για τους δυνατούς(εφικτούς) συνδυασμούς των εξεταζόμενων δεικτών. Οι δείκτες SPI και SPEI εμφανίζονται να είναι οι πιο κατάλληλοι για την ανίχνευση των επεισοδίων ξηρασίας της περιοχής, ενώ παρατηρείται η αδυναμία των δύο πολυμεταβλητών μοντέλων στον εντοπισμό επεισοδίων ξηρασίας εξαιρετικής επικινδυνότητας. Επίσης διαπιστώθηκε, ότι οι δείκτες SPI, SPEI εμφανίζονται πιο ισχυρά συσχετισμένοι στις ορεινές περιοχές όπου η επίδραση της δυνητικής εξατμισοδιαπνοής δεν είναι τόσο αισθητή, και κατά συνέπεια ανταποκρίνονται κυρίως στις διακυμάνσεις της βροχόπτωσης. Στο τελευταίο μέρος της παρούσας διατριβής διενεργήθηκε η Ανάλυση των Κυρίων Συνιστωσών (ΑΚΣ) στους δυο πιο αποτελεσματικούς δείκτες SPI και SPEI για τις χρονικές κλίμακες 3 και 12. Σύμφωνα με αυτή τη στατιστική διεργασία, επιτυγχάνεται η μείωση της διαστασιοποίησης των αρχικών δεδομένων των δυο δεικτών· παρέχοντας σημαντικές πληροφορίες για τη μεταβλητότητα των ξηρασιών στην εξεταζόμενη περιοχή, και επομένως η μέθοδος αυτή μπορεί να ερμηνευθεί ως ένας νέος δείκτης για κάθε ένα από τα δυο προαναφερθέντα μέτρα μετεωρολογικής ξηρασίας. Τα αποτελέσματα της μεθόδου ΑΚΣ υπέδειξαν δύο παρόμοια ομοιογενή πρότυπα και για τους δύο δείκτες, εκφράζοντας την χρονική εξέλιξη της ξηρασιών στη Θεσσαλία για τα 42 υδρολογικά έτη. Λαμβάνοντας υπόψη τις βραχυπρόθεσμες συνθήκες ξηρασίας, τα πιο ακραία γεγονότα ξηρασίας καταγράφηκαν στο τέλος της δεκαετίας του '70 και στις αρχές της δεκαετίας του '90, ενώ εξετάζοντας πιο μακροπρόθεσμες συνθήκες, τα πιο ακραία επεισόδια εντοπίστηκαν στο τέλος της δεκαετίας του '70 και στο τέλος της δεκαετίας του '80. Επιπλέον μια τεχνική, ορθογώνιας περιστροφής των αξόνων διεξάγεται· προβάλλοντας αρκετές διακριτές υπο-περιοχές για την περιοχή μελέτης μας. Τα αποτελέσματα υποδεικνύουν ότι η ενσωμάτωση της δυνητικής εξατμισοδιαπνοής, ειδικότερα για την παρακολούθηση των ξηρασιών σε

περιοχές χαμηλού υψομέτρου, είναι καθοριστικής σημασίας για την αναγνώριση χωρικών μοντέλων ξηρασίας, τουλάχιστον σε τοπική κλίμακα.

RESUME

Les sécheresses constituent peut-être le phénomène naturel le plus complexe. Leur nature inévitable en combinaison avec les effets prolongés et non structurels entraîne une confusion dans la société scientifique à propos de la formation d'une définition concrète et, par conséquent, rendent leur compréhension plus profonde impossible. Dans le but de surveiller et d'évaluer les sécheresses, de nombreux indices sont suggérés, sur la base d'un ou plusieurs paramètres hydro-climatiques afin d'identifier différents aspects qui contribuent à l'intensification du phénomène. Dans cette thèse, on discute le comportement de quatre indices météorologiques de sécheresse avec une structure différente, en analysant les épisodes de sécheresse en Thessalie. Plus précisément, les indices largement utilisés SPI et SPEI et deux modèles multivariés : MSDI(Pr-PET), MSDI(SPI-SPEI) qui sont motivés par l'indice prometteur MSDI, sont sélectionnés pour l'analyse comparative de la sécheresse de la région. Le premier modèle est structuré en combinant de manière probabiliste les variables hydro-climatiques de la précipitation et l'évapotranspiration potentielle (PET), tandis que la seconde est formée combinant de manière probabiliste les indices SPI et SPEI. Le but principal de cette synthèse multivariée est de générer deux nouveaux indices susceptibles d'être utilisés comme outils complémentaires pour la surveillance et l'évaluation des sécheresses. Les données mensuelles sur les précipitations et la température, couvrant la période hydrologique 1960-2002, ont été utilisées pour le calcul des indices considérés aux échelles de temps: 1, 3, 6, 9, et 12 mois. Afin d'obtenir une quantité égale de données sur les précipitations et la température, une méthode de gradient thermique adiabatique a été appliqué pour obtenir 78 stations météorologiques dans la région. Les résultats des séries chronologiques et une classification de la sécheresse pour toutes les stations sont cités, présentant les principales similitudes / différences dans le comportement des quatre indices dans l'analyse de la sécheresse en Thessalie. En outre, une analyse de corrélation est effectuée, affichant des diagrammes de dispersion et des motifs spatiaux des valeurs de corrélation pour les combinaisons possibles des indices examinés. Les indices SPI et SPEI semblent être les plus appropriés pour la détection des épisodes de sécheresse dans la région, alors que la faiblesse des deux modèles multivariés pour capturer des événements extrêmement séchés est évidente. En outre, il a été constaté que les indices SPI et SPEI sont plus fortement corrélés dans les régions montagneuses où l'influence de l'évapotranspiration potentielle n'est pas si perceptible et, par conséquent, elles répondent principalement aux fluctuations des précipitations. Dans la dernière partie de cette thèse, une analyse des composantes principales (ACP) est effectuée pour les indices SPI et SPEI les plus efficaces, aux échelles de temps 3 et 12. Selon cette méthodologie, une réduction de la dimension des séries SPI et SPEI initiales peut être fourni, fournir des informations sur la variabilité de la sécheresse de la région et donc, il peut être interprété comme un nouvel indice pour les indices de sécheresse météorologique précitées. Les résultats indiquent deux modèles homogènes similaires pour les deux indices, exprimant l'évolution temporelle des sécheresses en Thessalie pour les 42 années hydrologiques. Les événements de sécheresse les plus extrêmes ont été enregistrés à la fin des années 70 et, au début des années 90, examinant les conditions de sécheresse à court terme. En examinant les conditions hydrologiques de la sécheresse, les épisodes de sécheresse les plus extrêmes ont été détectés à la fin des années 70 et à la fin des années 80. Une rotation orthogonale des axes est réalisée, fournissant plusieurs petites régions distinctives pour notre zone d'étude. Les résultats suggèrent que l'inclusion de l'évapotranspiration potentielle, en particulier dans la surveillance de la sécheresse des régions à basse altitude, est cruciale pour l'identification des schémas de sécheresse spatiale, au moins à l'échelle locale.

TABLE OF CONTENTS

1 INTRODUCTION

1.1 Droughts

Drought is universally regarded as a natural hazard of great severity that can occur under any climatic condition. It is differentiated from the other natural disasters because its implications lack structure and disperse in vast geographical regions *(Wilhite and Glantz, 1985; Wilhite, 1992, 2000; Wilhite* and Pulwart, *2005)*.

Furthermore, the phenomenon of drought is characterized by slow development spreading through the full hydrological cycle and its relentless consequences are often shown after its completion *(Vogt et al., 2011b)*. Hence, contrasting to other natural hazards, it is challenging to determine both the onset and the end of a drought. For this reason, drought is frequently described as a creeping phenomenon *(Tannehill, 1947)*.

Society, environment and economy are sectors that are severely afflicted by the results of droughts. The following examples are indicative of this situation. Firstly, the social sector has suffered great repercussions as, according to findings of the UN Global Assessment Report, *(UNISDR, 2011)* more than 11 million fatalities were caused and more than 2 billion people have been affected by droughts. The numbers exceed those of any other natural hazard. The droughts that were reported in Sub-Saharan Africa in the early to mid-1980s have had adverse effects in the lives of more than 40 million people *(OFDA, 1990)*. Secondly, the ecosystem has been extremely burdened by the phenomenon. For instance, the Amazon River was hit by a drought in 2005 which seriously affected both the transportation of the river and the total crop yield *(Marengo et al., 2008)*. *Guarin and Taylor (2005)* have pointed out that that tree mortality in Northern California is mainly caused by fire in the years of drought and in Southern Europe significant correlations between wildfires and drought index SPI *(Standardized Precipitation Index; McKee et al.,1993)* were found *(Bifulco et al., 2014; Gudmundsson et al., 2014)*. Finally, in reference to the economic sector, Australia suffered huge losses of about 20% in the income owing to the severe drought of 2002-2003 *(Horridge et al., 2005)*. Moreover, the European droughts from 1976 to 2006 caused damage that was estimated approximately at 100 billion Euros *(Vogt et al., 2011a)*.

Furthermore, the lack of an accurate and globally accepted definition of drought leads to confusions about the existence and the severity of the phenomenon. The definition of drought differs considering the climatic and topographical characteristics of each region. In addition, the definition of drought is modified depending on the objectives of each scientific field. More specifically, in meteorology drought is defined as the precipitation deficit for a long period of time compared to the average amount of precipitation; in agriculture this means low crop production as there is inadequate soil moisture to cover the transpiration needs of the plants in their crucial stages of cultivation; in hydrology, drought means a drop in the water level of lakes, rivers and aquifers (i.e. groundwater) below a certain limit for a specified length of time, while for social-economic science, it expresses the vulnerability of society to water shortage.

All the above explain the vast number of definitions that have been recorded during the recent years *(World Meteorological Organization (WMO), 1975; Wilhite and Glantz, 1985; Wilhite, 1992, 2000; Wilhite* and Pulwart, *2005)*. *Wilhite and Glantz* reported in 1985 that more than 150 definitions have been used to provide explanation for the phenomenon of drought.

The aforementioned support the notion that drought is a perplexing phenomenon and sets the least accessible natural hazard. Furthermore, the difficulty in developing highly effective and immediate measures in an effort to mitigate the damage on human activities caused by drought can be explained by its inevitable nature. Thus, it is essential to achieve a comprehensive knowledge of the problem in order to eliminate any misunderstandings about drought and society's capacity to moderate its effects *(Keyantash and Dracup 2002)*. By comprehensive, it is implied that the understanding of such a phenomenon is impossible to be based on a single research objective alone (e.g. meteorology). In this case, the cooperation of several sectors is required such as meteorology, hydrology, agriculture and economy in order to accomplish a thorough analysis of the phenomenon aiming at understanding, assessing and explaining the causes of its formation and consequently its implications. Such an attempt focuses on collecting and processing historical hydro-climatic data for the purpose of creating the appropriate tools which will contribute to the improvement of monitoring and assessing the phenomenon and lead to a more timely prediction.

Finally, several organizations like the European Drought Centre (EDC) and the National Drought Mitigation Center (NDMC) have been established in order to inform and guide people and institutes, providing strategies and implement measures through which the moderation in vulnerability to drought can be achieved.

1.2 Drought Characteristics

As above mentioned, droughts differ a lot from the other natural hazards due to complexity of the phenomenon. However, they seem to share some characteristics according to which they can be classified and evaluated over their significance. Three major characteristics of droughts are adduced below, as were analyzed by *Wilhite (1992, 2000; Wilhite and Pulwart, 2005)*.

The intensity of drought renders the first characteristic and basically refers to the precipitation shortfall and the significance of its deficit. Generally, it can be defined by the calculation of climatic indices, which are reckoned with regard to the "regular" values of precipitation *(Wilhite, 1992, 2000; Wilhite and Pulwart, 2005)*.

The second distinctive feature of droughts is their duration. A drought event may have a short lag time (few weeks/months) in its manifestation regarding the first signal of precipitation shortage; but then it can last for long periods such as months or even years through the consequences it can cause (though rainfalls of low significance may be recorded during this period of time). For instance, when the onset of the dry period is in the late fall and proceeds through winter, it will probably have insignificant impacts. Nevertheless, if the dry period continues into the spring and the beginning of summer, there is a dramatic increase in the demand of water supplies for agricultural and urban purposes. Persisting drought conditions for more than a growing season lead to substantial magnifying of the repercussions as a result of a decline in surface and subsurface water supplies and expand the cycle of impacts *(Wilhite, 1992, 2000; Wilhite and Pulwart, 2005)*.

The third characteristic of drought is the spatial distribution. The areas that are influenced by severe drought events are gradually increasing as long as drought persists longer. Large countries such as the United States of America, China, Brazil, and India are rarely affected by a drought episode throughout their territory (*Wilhite, 1992, 2000; Wilhite* and Pulwart, *2005)*. On the contrary, it is not rare to observe a drought event in a country, during a whole year; *(Wilhite, 2000)* as drought is the result of regional or large-scale atmospheric abnormalities *(Tallaksen et al. 2011)* which are generated and obstinately repeat for prolonged time over different districts. For example, in the USA, on average 14% of the country is affected by severe to extreme drought every year. *(Wilhite and Pulwart, 2005).*

1.3 Drought Indices

In the process of monitoring and assessing droughts, drought indices play an essential role because their use assists the simplification of the perplexing relationships between climate and climate-related parameters. A drought index is acceptable when it presents a clear, simple and qualitative analysis of the main drought characteristics namely the intensity, the duration and the special extent *(Hayes, 2000)*.

Drought indices incorporate several variables related to drought, (e.g. precipitation, temperature, potential evapotranspiration, soil moisture, snowpack) into a single number, the use of which is more efficient in the decision making process than raw data *(Hayes et al., 2007).*

Several meteorological drought indices have been proposed based on the hydro-climatic variable of precipitation. An illustration of this classification is the Standardized Precipitation Index *(SPI; McKee et al., 1993)* which is acclaimed by an increasing number of scientists around the world and has been recommended by the World Meteorological Organization as the primary tool for monitoring meteorological droughts. However, in some cases a single variable may not provide adequate information for the assessment of droughts because droughts constitute a complex process associated with multiple variables. Thus, apart from precipitation the parameter of temperature can be included in a meteorological drought assessment. The first attempt was made in 1965 when Palmer Drought Severity Index *(PDSI; Palmer, 1965)* was developed. The PDSI is calculated based on precipitation data, temperature and the Available Water Content (AWC), and its original purpose was to identify droughts in crop-producing regions of the United States. In 2007, *Tsakiris et al.* developed the Reconnaissance Drought Index *(RDI; Tsakiris et al., 2007)* considering, except for precipitation, a temperature component - the Potential Evapotranspiration (PET) - aiming to provide an effective index for monitoring droughts. On the same grounds, Vicente-Serrano et al. (2010) suggested the index Standardized Precipitation Evapotranspiration Index *(SPEI; Vicente-Serrano et al, 2010)* in order to examine the effect of temperature on drought analysis through a water balance concept. This final approach is great significance, especially for studies which are related to climate change as, according to *Mavromatis (2007),* the constant indications of increasing temperature in the recent years lead to more severe drought episodes.

Drought indices like Aggregated Drought Index *(ADI; Keyantash and Dracup, 2004)* and Joint Deficit Index *(JDI; Kao and Govindaraju, 2010)* provide a multivariate attempt in the analysis of the phenomenon by using more than a single drought-related variable. Finally, according to *Hao and AghaKouchak (2013)* it is pointed out, that no one of the existing single indices is able to represent all aspects of meteorological, agricultural, and hydrological droughts. Consequently, a new approach based on the combination of several drought indices should be conducted for an overall drought assessment. In this view, they suggested the Multivariate Standardized Drought Index *(MSDI; Hao and AghaKouchak, 2013)* which not only has the capacity to combine the drought information from the drought-related variables, but from the drought indices as well.

In the subsection below, special emphasis will be laid on the two meteorological drought indices SPI, SPEI and the new promising index MSDI because they have been chosen for the purposes of the present dissertation.

1.3.1 The Standardized Precipitation Index (SPI)

The Standardized Precipitation Index (SPI) was designed by *McKee et al. (1993)* at University of Colorado. Their main purpose was to develop a flexible index that has the ability to identify different drought types, considering that the time response on rainfall abnormalities among the various hydrological subsystems differs considerably. This effort was accomplished by quantifying the rainfall deficit at multiple time scales. More specifically, *McKee et al. (1993)* estimated the SPI for the time scales of 3, 6, 12, 24, and 48 months. Short time scales (no more than 3 months) are appropriate to reflect the impact of drought on soil moisture, snowpack, and stream flows of small rivers; medium term aggregated values (3–12 months) are suitable to assess the drought on stream flow and reservoir storage whereas long time scales (12–24 months) can be used for long-term processes (e.g. groundwater recharge) *(Spinoni et al, 2013).* Therefore, this multi-temporal approach of SPI provides "a macroscopic insight of the impacts of drought on the availability of water resources" *(Angelidis et al., 2012)*.

Calculation of the SPI is based on the long-term precipitation record for a desired period. This long-term record is fitted to a probability distribution, which is then transformed into a normal distribution. Positive SPI values signify greater than median precipitation, and negative values signify less than median precipitation *(Edwards and McKee, 1997)*. Apart from the previously mentioned mathematical approach of this transformation, a meteorological point of view can be determined, representing the drought and flood events in a similar probabilistic style *(Wu et al., 2007)*. All the aforementioned characteristics can lead to tenable advantages of the SPI index. These advantages explain the reasons why SPI represents the most widespread index and are cited as they were presented by *Hayes et al. (1999)*. Specifically, the first advantage of index is its simplicity, as it is based only on precipitation data. Secondly, the standardization of the index ensures the consistency of the frequency of extreme events at any location and on any time scale allowing the researchers to compare drought conditions among different time periods and regions with diverse climatic conditions.Thirdly, the ability to be calculated over multiple time scales. This last feature justifies the characterization as temporally flexible index, as it can adjust to the needs of the research by the use of the appropriate time scale and therefore the detection of the preferable drought type can be achieved.

Finally, special emphasis should be laid on the quantity and reliability of the data which are used to form the distribution. It has been stated by *McKee et al. (1993)* that the ideal required length of rainfall period used in the calculation of SPI is an uninterrupted period of at least 30 years. Another recommendation made by *Guttman's* approach *(1991, 1993, 1998 and 1999),* states that at least a 50 years long dataset is essential for the definition of the SPI on time scales smaller than 12 months, while 24, 36 or 48-month periods require longer datasets.

1.3.2 The Standardized Precipitation Evapotranspiration Index (SPEI)

Vicente-Serrano et al. (2010) have recently proposed the Standardized Precipitation Evapotranspiration Index *(SPEI; Vicente-Serrano et al., 2010)* as an enhanced index, based on a monthly (or weekly) climatic water balance (precipitation minus potential evapotranspiration). Due to inclusion of potential evapotranspiration, SPEI offers the ability to indicate the role of temperature variability on drought assessment *(Vicente- Serrano et al., 2010).*

The effectiveness of SPEI was confirmed, using the data from 11 observatories around the world, under several climate characteristics *(Vicente-Serrano et al., 2010).* Therefore, considering the temperature as an integral part of the index, SPEI can be characterized as an appealing indicator in the process of drought monitoring associated to potential climate changes (*Vicente-Serrano et al., 2010; Hao and Singh, 2015).*

Another advantage of SPEI is that the simplicity of calculation and the multi-temporal nature of SPI are combined *(Vicente-Serrano et al., 2010)*. In specific, similarly to SPI, it can be calculated at different time scales, allowing the user to decide upon the suitable time scale, in view of the corresponding type of drought. Furthermore, it is expressed as "a standardized Gaussian variate with a mean of zero and a standard deviation of one" *(Begueria et al., 2010)*. Therefore, it has the ability to assess the drought severity with respect to intensity and duration, and can detect the onset and end of drought events *(Vicente-Serrano et al., 2010)*.

1.3.3 The Multivariate Standardized Drought Index (MSDI)

Hao and AghaKouchak (2013), relied on the view that drought monitoring and prediction should be based on multiple sources of information, proposed in 2013, a new multivariate index, the Multivariate Standardized Drought Index *(MSDI; Hao and AghaKouchak, 2013).* More specifically, due to the complexity of drought as phenomenon, because it is associated with many hydro-climatic variables, there is a need to develop a measure, capable of characterizing the overall drought condition. MSDI constitutes an effective way to construct multivariate drought indices, combining the drought information from drought-related variables (e.g. precipitation, potential evapotranspiration, soil moisture, runoff) or from drought indices (e.g. SPI, SPEI, SSI).

The proposed multi-index drought model was motivated by the recommended Standardized Precipitation Index and can be developed through constructing the joint distribution of two or more univariate variables or indices of interest. Similarly to the SPI, a multi-scalar accumulation of data can be conducted at multiple time scales (e.g. 1, 3, 6, 9 and 12 months) in order to determine and monitor drought events. Therefore, the multi-scalar property of MSDI confers a significant benefit as it is recognized as a flexible and comparable measure in the process of analyzing droughts.

Approaching the effectiveness of MSDI, two attempts have been made based on standardization of the joint probability of accumulated precipitation and soil moisture and following different computational methods *(Hao and AghaKouchak, 2013; Hao and AghaKouchak, 2014).* In an analysis conducted in 2013 entitled "Multivariate Standardized Drought Index: A parametric multi-index model", *Hao and AghaKouckak (2013)* assumed that Copulas functions are appropriate to obtain estimation of the joint probability of the two abovementioned variables.The estimated MSDI then was compared with the most commonly used standardized drought indices namely, SPI and SSI at different time scales. The results have shown that MSDI represents a logical model in which multiple indices can be combined probabilistically. It should be stressed that MSDI was applied in California and North Carolina, considering drought conditions under several climate zones.

A second approach was performed by the same authors *(Hao and AghaKouchak, 2014)*. The first one, based on Copula concept was replaced by an alternative nonparametric method, providing a new modified version of the multivariate standardized index. In this analysis, data were provided by NASA with the use of MERRA-Land version, in order to describe two major droughts which struck the United States in 2007 and 2009.Then the construction of MSDI, SPI and SSI indices

was followed, and a comparison along them was conducted. In the end, MSDI along with the other indices were evaluated against U.S. Drought Monitor (USDM) data.

In view of the outcomes of the aforementioned study, it is demonstrated for one more time that MSDI is appropriate for drought monitoring. *Hao and AghaKouchak (2014)* concluded that MSDI and USMD data, concur well, examining their spatiotemporal consistency. Another interesting characteristic of MSDI is also reflected in this research, and this is the aspect that by using the multivariate index higher probabilities of drought detection can be accomplished, juxtaposed with univariate drought indices SPI and SSI. Additionally, as it is mentioned by the authors, MSDI is able to provide further information for drought analysis, as it can combine the properties of both SPI and SSI, and in some cases detect the spatial extend of drought.

In conclusion, MSDI constitutes a very promising index as it offers new approach to the overall drought assessment. However, it should be pointed out that it is not the main purpose of this index to be used as a measure indicating the weak points of other indices, but it has to be used as a corroborative source of information in order to provide further insights into the drought monitoring process *(Hao and AghaKouchak, 2013, 2014)*.

1.4 Droughts in Greece

As far as the phenomenon of drought in Greece is concerned, a major characteristic that has to be pointed out, is the unbalanced rainfall distribution on both spatial and temporal analysis. This is because of the geo-morphological relief of the country combined with the prevailing climatic conditions. More specifically, the western parts of Greece and the eastern Aegean Sea seem to experience higher amounts of precipitation compared to the central and southern Aegean, whilst the mountainous regions have higher amounts of precipitation and snowfall contrasting to plain areas. Moreover, lower amounts of precipitation are recorded in the summer compared to other seasons (*Anagnostopoulou, 2003).*

Anagnostopoulou (2003) based on the presence or absence of drought episodes, provided evidence that Greece can be divided spatially into four main regions namely, west and mainland of Greece, south and southeastern Greece (Crete and Dodecanese), eastern insular Greece (east Aegean islands) and finally the main axis of Greece which constitutes of the central Macedonia, the eastern mainland of the country, Sporades and Cyclades islands. This spatial distribution, with some variations, remains the same in every season all year round, apart from winter when Greece is divided into three regions (In Appendix-A the corresponding Figure, is provided). Drought can be presented in one of the above regions alone, but it can also extend to more with lower or the same intensity.

In terms of time, droughts in Greece have a strong seasonal character. Except for the permanent drought which develops during summer when long periods of dry spells are observed almost over the entire country, the other seasons experience specific drought episodes. It should be stressed that the driest year is not accompanied by drought events throughout its course, but only in certain time periods. For example, the driest year in the west and mainland of Greece is the hydrological year 1992-1993, the classification of which was based on the absence of rainfall during the winter (1992-1993). On the contrary, the driest year of the Eastern Greece (1986-1987) is characterized by the general reduction of rainfall, though no season seems to experience extreme depletion.

Moreover, according to *Anagnostopoulou (2003)* the characteristics of drought of the Greek territory are the following:

- A dry day in Greece is the one in which precipitation is lower or equal to 0.1mm.
- A drought episode in Greece, especially during winter time, is defined as the period when the consecutive days of dry conditions last for more than 10 days. Shorter periods of dry days are considered normal.
- As extreme droughts are described those drought episodes when there are consecutive months with values of the index SPI<-2.0.
- Droughts rarely occur in the entire Greek territory. Despite the fact that Greece is a small country, the unique topography and the varied relief result in variations in the rainfall distribution and consequently the non concurrent development of droughts in the whole country.

Concerning the drought events in Thessaly, extreme and persistent drought episodes have been observed from mid to late 1970s and from late 1980s to early 1990s. The average cumulative areal precipitation during these two periods is compared to the normal cumulative areal precipitation in Figure 1 where the lack is obvious. More specifically, the hydrological years 1976-1977 and 1989-1990 are the first and the second driest years respectively, for the era 1960-1993. The extended and significant reduction of monthly and annual precipitation has a dramatic influence on the water resources of the region. Normally, the dry periods are followed by high temperatures, something that leads to higher rates of evapotranspiration and dry soils. These conditions have a negative impact on the vegetation and agriculture of Thessaly. Further consequences involve deficiency of irrigation and overexploitation of ground water. For example, during the hydrological year 1989-1990 the water supply from Plastiras dam declined by 70% and the arable by surface water lands declined by 90% *(Loukas and Vasiliades, 2004).*

Consequently, the potential occurrence of harsher drought incidents is very crucial. Such events could worsen the existing situation. Therefore, the phenomenon of drought, which is globally recognized as a natural disaster with immeasurable and multifarious repercussions, should be thoroughly analyzed in studies concerning the water resources management of Thessaly.

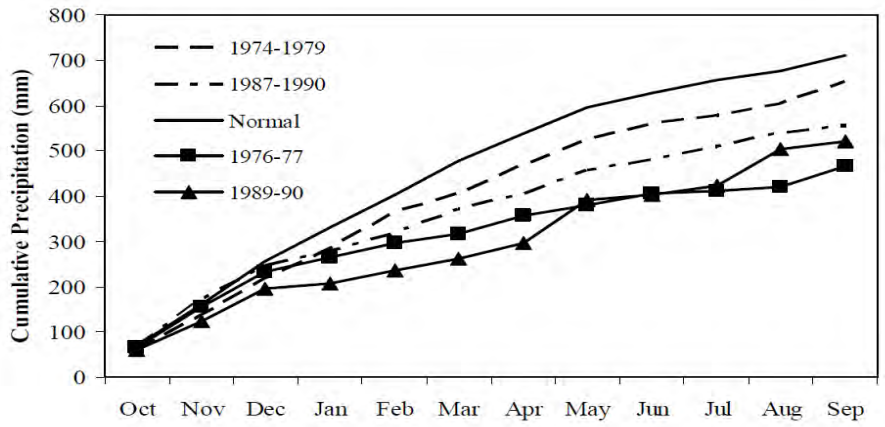

Figure 1: Cumulative areal precipitation for selected dry years and periods (Loukas and Vasiliades, 2004).

1.5 Purpose of the Study

Droughts in the region of Thessaly can be regarded as a meteorological phenomenon accompanied by prolonged periods of abnormal precipitation deficit *(Loukas and Vasiliades, 2004)*. Relied on this view, a meteorological drought assessment of the region can be accomplished, considering the drought-related variables of precipitation and potential evapotranspiration.

Precipitation and temperature data will be used for the purposes of this research. Precipitation observations are provided by 78 precipitation stations uniformly distributed over Thessaly. In order to derive the temperature data, the temperature lapse rate method is applied, as there is a limited number of meteorological stations at the desirable locations.

The main aim of this study is to examine the behaviour of four meteorological indices with different structure, detecting the drought events for 42 years in Thessaly region. It should be mentioned that the selection of these indices was encouraged considering their multi-temporal nature and their similar probabilistic approach (similar probabilistic style). More specifically, the identification of drought events in Thessaly is attempted using the widely used index SPI, the more recent index SPEI, and two produced multivariate indices, motivated by the new promising index MSDI. It is highlighted that the first produced multivariate index is derived, combining probabilistically the hydro-climatic variables, precipitation and potential evapotranspiration, while the second it is generated, combining probabilistically the standardized meteorological drought indices SPI and SPEI. Therefore, it has been provided an effective way to construct multivariate indices, considering the joint distribution of two univariate variables or indices, as proposed by *Hao and AghaKouchak (2014)*.

In the last part of this thesis, a Principal Component Analysis (PCA) is performed for the indices SPI and SPEI. This statistical method was applied providing a new dataset with fewer variables to the aforementioned indices, in order to identify spatial patterns of droughts for the area of Thessaly. Furthermore a comparison between the two indices can be conducted, examining their possible differences.

2 STUDY AREA-DATABASE

2.1 Study Area

The study area of this research is the region of Thessaly, Greece. It is located in the central department of the mainland of Greece forming the greatest plain of the country. It is surrounded by large mountainous masses, among which Mount Olympus, rising to over than 2800 m, situated at the northern part of the plain. In the west, there is the Pindus mountain range, which is approximately 230 km long and reaches a width of over 70 km. Mountains Kissavos and Pelion are located in the east. In the south, there is the Othrys mountain range. The total acreage of the region is 13377 km^2 while the average elevation is estimated at 500 m above sea level.

As far as the climate of the area is concerned, two different areas can be distinguished, namely the coastal eastern side of Thessaly, with a Mediterranean climate which is characterized by warm and dry summers and cold and humid winters – and the western lowland-hilly side, with a typical continental climate with great temperature variations between summer and winter time. The annual average temperature fluctuates from 16^o to 17^o C. The annual thermometric range is over

22^{o} C. The warmest months are July and August and the coldest ones are January, February and December. The average precipitation is relatively high in the west – more than 1850 mm – and decreases in the plain region by 400 mm. The rainiest months are from October to January whilst July and August are the driest ones. Snowfall is very common especially in the mountainous areas of the region and becomes more intense from the south to the north and from the east to the west. Snowfalls are more frequent during February and January. Additionally, hailstorms are frequent in the north of the region during May and June and in the south-eastern part from February to April. The annual average humidity relatively fluctuates from 67% to 72%. In the eastern parts, there is a dry period of 4 to 5 months which gradually diminishes to 2 to 4 months in the central and western lowland parts and to 1 to 2 months in the western mountainous areas.

The main drainage basin of the hydrological department of Thessaly is the basin of the river Pinios which extends across an area of about 9500 km^2. The closed basin of Karla as well as other smaller tributaries are also included in the hydrological department.

A remarkable characteristic of the plain of Thessaly is the intensive agricultural activity. The main crops commonly cultivated in the area, are cotton, barley, and wheat which contribute significantly to the growth of the local economy. Thus, the constant reduction of the amount of water due to extensive use of the land and utilization of the water resources by the hydroelectric dam of Smokovo, in combination with inadequate irrigation projects render the observation of the aquatic reserve in the region imperative *(Loukas and Vasiliades, 2004)*.

2.2 Database

Monthly precipitation data (mm), from 78 precipitation stations, can be used for the estimation of SPI. The stations are uniformly distributed over Thessaly region (Figure 2) and their characteristics are shown in Table 1. In this project except for precipitation data, the inclusion of temperature data at the same positions of precipitation stations must be considered for the estimation of PET, and therefore of SPEI. Monthly temperature data can be derived using the temperature lapse rate method, as there is a limited number of meteorological stations at the desirable locations. This method will be analyzed in the next section.

The precipitation and temperature data of the region were provided by the Laboratory of Hydrology and Aquatic Systems Analysis of the University of Thessaly (Department of Civil Engineering) and cover 42 hydrological years, from October 1960 to September 2002. It should be noted that the length of the period fully satisfies the requirements of the indices of this research. The selection of the specific hydrological years ensures the quality and the reliability of the data, as a lot of research has been conducted by the University of Thessaly based in this period.

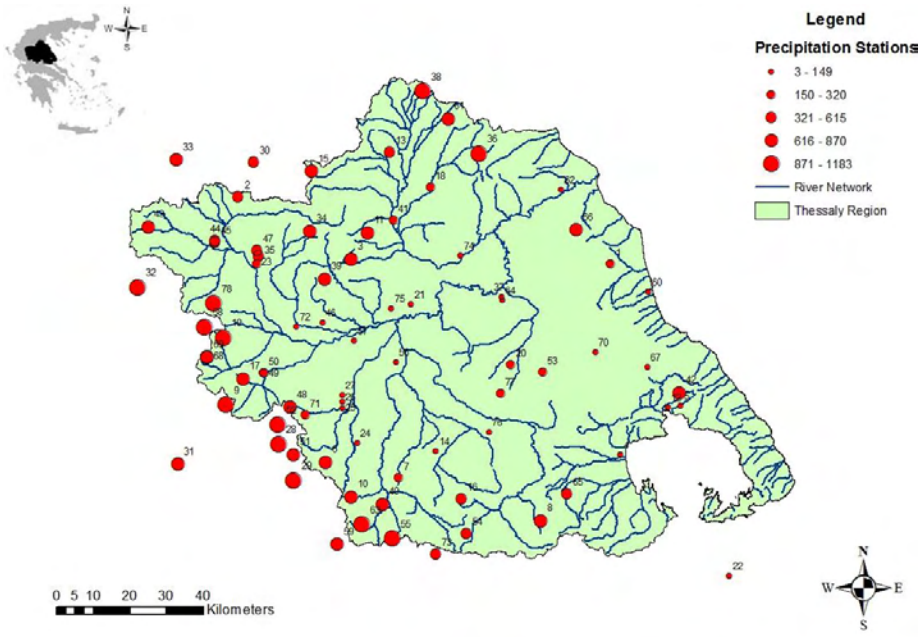

Figure 2: Location and elevation of the precipitation stations of Thessaly Water Department.

Table 1: Precipitation Stations and their characteristics of Thessaly Water Department.

Id	Name of Station	Elevation (m)	Latitude (°)	Id	Name of Station	Elevation (m)	Latitude (°)
1	AGIA	180	39.715	40	LOYTROPHGH	730	39.113
2	AGIOFYLLOS	581	39.859	41	MAGOYLA	180	39.813
3	AGRIELIA	700	39.713	42	MAKRYNITSA	690	39.399
4	AGXIALOS	15	39.246	43	MALAKASIO	842	39.780
5	ALLH MERIA	120	39.368	44	MEG. KERASIA_YPGE	560	39.752
6	AMARANTOS	800	39.213	45	MEG. KERASIA	500	39.746
7	ANABRA_KARDITSAS	208	39.180	46	MEGALOXVRI	100	39.557
8	ANABRA_MAGNISIAS	700	39.080	47	METEORA	596	39.730
9	ARGITHEA	980	39.348	48	MORFOVOUNI	780	39.346
10	BATHILAKOS	800	39.130	49	MOUZAKI_YPGE	226	39.429
11	VERDIKOYSA	863	39.780	50	MOUZAKI_YPEXODE	226	39.430
12	VOLOS	3	39.363	51	MOYXA	870	39.230
13	GIANNOTA	578	39.980	52	MPEZOYLA	901	39.302
14	GRAMMATIKON	95	39.247	53	MYRA	320	39.446
15	DESKATI	830	39.927	54	JYNIADA	456	39.046
16	DOMOKOS	615	39.130	55	P. GIANNITSOY	960	39.030
17	DRAKOTRYPA	680	39.413	56	PALAMAS	95	39.464
18	ELASSONA	314	39.896	57	PEDINON	95	39.514
19	ELATI	900	39.513	58	PERTOYLI	1160	39.538
20	ZAPPEIO	170	39.463	59	PITSIOTA	800	39.012
21	ZARKO	120	39.608	60	POLYDENDRI	100	39.646
22	ISTIAIA	45	38.952	61	PYTHIO	750	40.063
23	KALAMPAKA	222	39.696	62	PYRGETOS	31	39.896
24	KALIFONI	100	39.264	63	RENTINA	903	39.062
25	KAPNIKOS_STATHMOS	110	39.347	64	SEKFO	80	39.621
26	KARDITSA	138	39.363	65	SKOPIA	580	39.146
27	KARDITSOMAGOYLA	95	39.381	66	SPHLIA	813	39.796
28	KARITSA	900	39.255	67	STEFANODIKEIO	80	39.463
29	KAROPLESI	910	39.166	68	STOYRNAREIKA_DEH	860	39.463
30	KARPERO	510	39.946	69	STOYRNAREIKA_YPGE	860	39.464
31	KATAFYLLIO	698	39.199	70	SOTIRIO	51	39.496
32	KATAFYTO	980	39.631	71	TAYROPOS	220	39.330
33	KHPOYRGIO	868	39.946	72	TRIKALA	149	39.546
34	KONISKOS	860	39.780	73	TRILOFO	580	38.994
35	KRATIKO_KTHMA	532	39.715	74	TIRNAVOS	92	39.730
36	KRYOVRISI	1030	39.980	75	FARKADONA	87	39.596
37	LARISA	73	39.630	76	FARSALA	148	39.296
38	LIVADI	1183	40.130	77	XALKIADES	250	39.392
39	LIOPRASO	740	39.663	78	XRYSOMILIA	940	39.596

3 METHODOLOGY

3.1 Data Processing

In the area of Thessaly there are 26 meteorological stations available. The characteristics for every station and the mean annual temperature (℃) from 42 hydrological years (October 1960 - September 2002) are provided, as shown in the Table 2.

Table 2: Meteorological Stations and their characteristics of Thessaly Water Department.

Id	Station	Elevation (m)	Mean Temperature (℃)
4	AGXIALOS	15	16.2
9	ARGITHEA	980	12.3
79	VAKARI	1150	11.0
12	VOLOS	3	17.1
14	GRAMMATIKON	95	16.6
16	DOMOKOS	615	14.1
23	KALAMPAKA	222	16.1
24	KALIFONI	100	16.0
25	KAPNIKOS_STATHMOS	110	15.9
27	KARDITSOMAGOYLA	95	16.5
35	KRATIKO_KTHMA	532	13.8
37	LARISA	73	15.7
80	LEONTITO	950	12.4
38	LIVADI	1183	11.0
41	MAGOYLA	180	14.6
53	MYRA	320	16.0
56	PALAMAS	95	16.1
81	PAXTOURI	950	12.4
57	PEDINON	95	16.4
82	POLYNERI	730	13.2
65	SKOPIA	580	14.8
70	SOTIRIO	51	15.1
83	FRAGMA_TAYROPOY	850	11.3
72	TRIKALA	149	16.3
76	FARSALA_EMY	148	16.2
84	FARSALA_YPGE	434	15.4

According to the purposes of this study, the small number of meteorological stations in the area (26 meteorological stations) and therefore, the limited number of meteorological stations at the locations of precipitation gauges (only 20 meteorological stations), necessitates the use of temperature lapse rate method for the estimation of temperature data at the desirable positions (locations of precipitation stations).

The temperature lapse rate method relied on the assumption that temperature decreases linearly with increasing altitude. Based on this assumption, a linear regression line can be fitted to the mean annual temperature data of the available meteorological stations of Thessaly.

The linear regression equation (1) is given below:

$$y = b * x + a \quad (1)$$

Where y represents the predicted mean annual temperature, b is the slope of the regression line, x is the elevation of each station and a represents the intecept of regreassion line.

The slope b, and the intercept a, are estimated using the equations (2) and (3) respectively:

$$b = \frac{\sum x*y - \sum x \sum y}{\sum x^2 - (\sum x)^2} \quad (2)$$

$$a = \frac{1}{n}(\sum y - b * \sum x) \quad (3)$$

The proportion of variance explained by the regression model, can be calculated, using the square of Pearson correlation or coefficient of determination, r^2.

Pearson correlation coefficient r, is a measure of the linear dependence between two or more variables (x and y in this case). Its values ranges between +1 and −1, where a value of +1 indicates that there is a perfect positive relationship between the variables, a value of -1 represents a perfect negative relationship of the variables, and a 0 value indicates that there is no a linear correlation between them. The Pearson correlation coefficient is estimated, according to the following equation:

$$r = \frac{n(\sum xy) - (\sum x)(\sum y)}{\sqrt{[n(\sum x^2) - (\sum x)^2][(n(\sum y^2) - (\sum y)^2)]}} \quad (4)$$

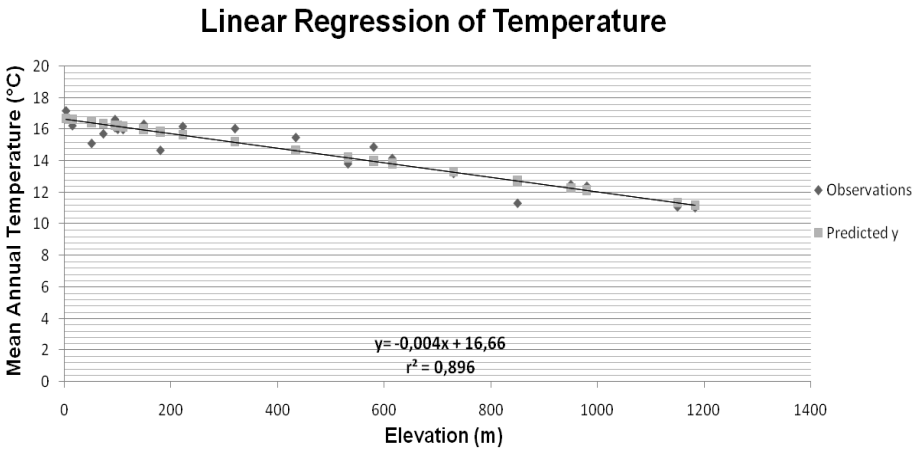

Figure 3: Linear regression of mean annual temperature for 26 meteorological stations in Thessaly.

As the linear regression of temperature for the region of Thessaly is extracted (Figure 3), the method of temperature lapse rate will follow. In this thesis, 8 out of the 26 available meteorological stations are selected in order to form meteorological stations at the same positions of precipitation gauges. It must be stressed that the selection of the location for each of these eight meteorological stations, is conducted in order to include the nearest precipitation stations.

The temperature lapse rate method can be performed, considering the following equations:

$$T_2 = T_1 + \left(-\frac{dT}{dh}\right)(h_2 - \mathrm{h}_1) \quad \text{if} \quad h_2 > h_1 \tag{5}$$

$$T_2 = T_1 - \left(-\frac{dT}{dh}\right)(h_1 - \mathrm{h}_2) \quad \text{if} \quad h_1 > h_2 \tag{6}$$

Where T_2 is the annual temperature of the formed meteorological station, T_1 represents the annual temperature from one of the eight selected meteorological stations, $-\frac{dT}{dh}$ is the negative rate of temperature with altitude, and in this case is represented by the slope b of the linear regression, h_2 represents the altitude of the formed station, and h_1 is the altitude of the selected meteorological station.

Applying the temperature lapse rate method as described by the equations (5) and (6), 78 meteorological stations can be formed in the same positions with the precipitation stations, providing the annual temperature for each hydrological year.

Having estimated the annual temperature data, the monthly temperature data of the formed meteorological stations can easily be derived for each hydrological year. This can be accomplished by multiplying each value of monthly temperature of the selected station, with the estimated annual temperature of the formed station and dividing this amount by the annual temperature of the selected station.

3.2 SPI – SPEI – MSDI Indices

In this study four meteorological drought indices with different structure have been introduced, considering their multi-temporal nature, and their similar probabilistic style.Specifically, the recommended standardized drought index SPI and its enhanced version SPEI, have been selected for a drought analysis in Thessaly region, taking into account, except from the parameter of precipitation, a temperature component (potential evapotranspiration, PET), through a water balance concept. This analysis is accompanied by two standardized bivariate indices, motivated by the promising index MSDI. The two bivariate models MSDI(Pr-PET) and MSDI(SPI-SPEI), have been developed through constructing the joint distribution function of two meteorological variables (precipitation and PET) and two meteorological drought indices (SPI and SPEI) respectively, purposing to obtain two effective meteorological drought measures which can be used as supplementary tools in the drought monitoring process.

The four standardized drought indices are calculated at time scales 1, 3, 6, 9 and 12 months, in order to assess short and medium term drought conditions in our study area.

3.2.1 Computation of The Standardized Precipitation Index (SPI)

A series of accumulated precipitation for a fixed time scale of interest is the basis for the calculation of the SPI for any location. Therefore, an overriding concern, is the aggregation of monthly precipitation data at different time scales, employing the advantage of the flexibility of the index. It should be mentioned that the precipitation value, $P_{i,j}^{k}$ in a given month j and year i, depends on the chosen time scale k. In the following example is calculated the accumulated precipitation for one month in a particular year i , considering a 12-month time scale.

$$P_{i,j}^{k} = \sum_{l=13-k+j}^{12} p_{i-1,l} + \sum_{l=1}^{j} p_{i,l} \quad \text{if } j<k, \tag{7}$$

and

$$P_{i,j}^{k} = \sum_{l=j-k+1}^{j} p_{i,l} \quad \text{if } j \geq k \tag{8}$$

Where $p_{i,l}$ is the precipitation in the first month of the year i, in millimeters (mm).

Therefore, according to the equations (7) and (8), the aggregation of the precipitation data for all months can be accomplished, at the desirable time scales (in our case at: 1, 3, 6, 9 and 12 months).

The next step of the SPI calculation involves a series of transformation based on the two parameter Gamma distribution. Gamma distribution is suitable for the analysis of rainfall records, as according to *Thom (1958)* in the majority of the cases precipitation time series using this distribution, can be well adapted.

The gamma distribution, is defined by its frequency or probability density function as:

$$g(x) = \frac{1}{\beta^{\alpha}\Gamma(\alpha)} x^{\alpha-1} e^{-\frac{x}{\beta}} \; for \; x > 0 \tag{9}$$

where α, β stand for shape and scale parameters respectively, x describes the amount of precipitation, and $\Gamma(\alpha)$ is the gamma function defined by

$$\Gamma(\alpha) = \int_0^{\infty} y^{\alpha-1} e^{-y}\, dy \tag{10}$$

Fitting the gamma probability density function to the precipitation data, makes it necessary the estimation of alpha and beta parameters. So the two parameters are calculated for each station, for each month of the year, and for each time scale of interest (in our case at: 1, 3, 6, 9 and 12 months).

Maximum likelihood solutions are used to optimally estimate α and β

$$\alpha = \frac{1}{4A}\left(1 + \sqrt{1 + \frac{4A}{3}}\right), \qquad \beta = \frac{\bar{x}}{a} \tag{11}$$

where $A = \ln(\bar{x}) - \frac{\sum \ln(x)}{n}$, and n is the number of observations.

The probability density function can be integrated with respect to x, in order to find the cumulative probability $G(x)$. So $G(x)$ can be defined as:

$$G(x) = \int_0^X g(x)\, dx = \frac{1}{\beta^{\alpha}\Gamma(\alpha)} \int_0^x \chi^{\alpha-1} e^{-\chi/\beta}\, dx \tag{12}$$

Letting $t = \frac{x}{\hat{\beta}}$, the last equation (12) is reduced to:

$$G(x) = \frac{1}{\Gamma(\alpha)} \int_0^X t^{a-1}\, \mathrm{e}^{-1} \mathrm{dt} \tag{13}$$

Since the gamma distribution is undefined for x=0 and considering that the monthly precipitation data may contain several zero values, the cumulative probability can be modified, taking into account the probability of zero values, according to the following equation:

$$H(x) = q + (1 - q)G(x) \tag{14}$$

Where q is the probability of zero and $G(x)$ the cumulative probability of the incomplete gamma function. If m is the number of zeros in precipitation time series, q can be estimated by m/n. Finally, the cumulative probability distribution $H(x)$, is transformed into the standard normal distribution Z (mean zero and variane one), relied on the classical approximation of Abramowitz and Stegun (1965) in order to obtain the SPI values.

$$Z = SPI = -\left(t - \frac{c_0 + c_1 t + c_2 t^2}{1 + d_1 t + d_2 t^2 + d_3 t^3}\right),\ t = \sqrt{ln\left(\frac{1}{(H(x))^2}\right)} \tag{15}$$

For $0 < H(x) < 0.5$

$$Z = SPI = +\left(t - \frac{c_0 + c_1 t + c_2 t^2}{1 + d_1 t + d_2 t^2 + d_3 t^3}\right),\ t = \sqrt{ln\left(\frac{1}{(1.0 - H(x))^2}\right)} \tag{16}$$

For $0.5 < H(x) < 1$

The constants are:

$$C_0 = 2.515517, \qquad C_{1=}0.802853, \qquad C_2 = 0.010328$$

$$d_1 = 1.432788, \qquad d_2 = 0.189269, \qquad d_3 = 0.001308$$

Once standardized the strength of the anomaly, is classified as set out in Table 3. More specifically, a drought event occurs when the SPI continuously reaches an intensity of -1.0 or less. The event ends when the SPI becomes positive. Each drought event therefore, has a duration defined by its beginning and ending. The positive sum of the SPI for all the months during a drought event, it is called as drought magnitude *(Hayes et al., 2007)*. In this table, the corresponding probabilities are also provided.

Table 3: Drought classification by SPI values and corresponding event probabilities.

SPI	Classification	Probability (%)
2 or more	Extremely wet	2.3
1.5 to 1.99	Very wet	4.4
1 to 1.49	Moderately wet	9.2
0 to 0.99	Mildly wet	34.1
0 to -0.99	Mildly drought	34.1
-1 to -1.49	Moderately drought	9.2
-1.5 to -1.99	Severely drought	4.4
-2 or less	Extremely drought	2.3

3.2.2 Computation of The Standardized Precipitation Evapotranspiration Index (SPEI)

Calculation of SPEI index, is based on the difference between monthly precipitation P_j and monthly potential evapotranspiration, PET_j. This amount represents a simplified concept of climate water balance and expresses a simple measure of the water surplus or deficit for each month *(Vicente-Serrano et al., 2010).*

A climate water balance for the analyzed month J can be calculated according to the following equation:

$$D_j = P_j - PET_j \tag{17}$$

The estimation of PET can be obtained by using either the simple method of Thornthwaite *(Thornthwaite, 1948)*, which is mainly based on the temperature data – or using a more complicated equation, associated with more parameters, the Penman-Monteith method, PM. In the present study, the Thornthwaite method was used as it only requires the monthly temperature data and the latitudinal coordinate of the location. The availability of the monthly temperature data from 78 stations was ensured by using the lapse rate method as mentioned in subsection 3.1, while the latitude of each station was known.

So following the Thornthwaite method, the monthly PET (mm) is obtained by:

$$PET = 16K\left(\frac{10T}{I}\right)^m \tag{18}$$

Where T is the monthly mean temperature (°C), I is a heat index, m is the coefficient depending on I: $m = 6.75 \times 10^{-7} I^2 + 1.79 \times 10^{-2} I + 0.492$, and K is a correction coefficient computed as a function of the latitude and month.

Following the same procedure as used for the SPI, the calculated D values can be aggregated at various time scales (in our case at: 1, 3, 6, 9, and 12 months).

Considering now the normalization of the water balance, the Log-logistic distribution can be used to fit the D series.

The probability density function of a three parameter Log-logistic distributed variable is defined as:

$$f(x) = \frac{\beta}{\alpha}\left(\frac{x-\gamma}{\alpha}\right)^{\beta-1}\left(1+\left(\frac{x-\gamma}{\alpha}\right)^{\beta}\right)^{-2} \tag{19}$$

where α, β and γ are scale, shape and origin parameters, respectively, for *D* values in the range ($\gamma > D < \infty$).

The parameters of the Log-logistic distribution can be derived, considering the L-moment procedure which according to Ahmad et al. (1988), constitutes the most robust and easy approach.

As the L-moments have been estimated, the parameters of the Pearson III distribution can be derived according to the following equations *(Singh et al., 1993)*.

$$\beta = \frac{2W_1 - W_0}{6W_1 - W_0 - 6W_2}, \tag{20}$$

$$a = \frac{(W_0 - 2W_1)\beta}{\Gamma\left(1+\frac{1}{\beta}\right)\Gamma\left(1-\frac{1}{\beta}\right)}, \quad (21)$$

$$\gamma = W_0 - a\Gamma\left(1+\frac{1}{\beta}\right)\Gamma\left(1-\frac{1}{\beta}\right) \quad (22)$$

Where $\Gamma(\beta)$ represents the gamma function of β

Thus, the probability distribution function of the D series, expressed by the log-logistic distribution is given by:

$$F(x) = \left[1 + \left(\frac{\alpha}{x-\gamma}\right)^{\beta}\right]^{-1} \quad (23)$$

Finally in the last step the SPEI series can easily be estimated as the standardized values of $F(x)$, relied on the approximate conversion of *Abramowitz and Stegun (1965).*

$$SPEI = W - \frac{C_0 + C_1 W + C_2 W^2}{1 + d_1 W + d_2 W^2 + d_3 W^3} \quad (24)$$

Where: $W = \sqrt{-2ln(P)}$ for $P \leq 0.5$, and P is the probability of exceeding a determined D value, $P = 1 - F(x)$. If $P > 0.5$, then P is replaced by $1 - P$ and the sign of the resultant SPEI is reversed.

The constants are:

$$C_0 = 2.515517, \qquad C_{1=}0.802853, \qquad C_2 = 0.010328$$

$$d_1 = 1.432788, \qquad d_2 = 0.189269, \qquad d_3 = 0.001308$$

It should be mentioned that the computational part of this method has been followed, according to the article-entitled, "The Standardized Precipitation Evapotranspiration Index (SPEI): a multi-scalar drought index" *(Vicente-Serrano et al., 2010).*

3.2.3 Computation of The Nonparametric Multivariate Standardized Drought Index (MSDI)

In this thesis, two different multivariate indices: MSDI(Pr-PET) and MSDI(SPI-SPEI) can be developed through constructing the joint distribution function of two univariate variables (precipitation and PET), and two univariate indices (SPI and SPEI), respectively. The nonparametric method, as proposed by *Hao and AghaKouchak* in 2014, has been selected, in order to derive these multivariate models. Furthermore, the two multivariate indices, have been calculated at time scales 1, 3, 6, 9 and 12 months, following the same procedure as used for the SPI.

More specifically, a nonparametric empirical method, expressed by Weibull *(Hirsch, 1981)* or by Gringorten *(Gringorten, 1963; Yue et al., 1999; Benestad and Haugen, 2007)* plotting position formula, can be applied in order to derive the empirical joint probability of drought-related variables (or indices).Therefore, denoting the drought-related variables precipitation and PET as two random variables X and Y respectively at a specific time scale, the empirical joint probability of the variables (x_k , y_k) can be calculated as:

$$P(x_k, y_k) = \frac{m_k}{n+1}, \quad \text{Weibull (Hirsch, 1981)} \tag{25}$$

where n is the number of the observation, and m_k is the number of occurrences of the pair $(x_{i,} y_i)$ for $x_i \leq x_k$ and $y_i \leq y_{k,}$ $(1 \leq i \leq n)$.

As the empirical joint probability of the drought-related variables, precipitation and PET has been estimated, the multivariate standardized drought model MSDI(Pr-PET) is formed, according to the following equation:

$$MSDI = \Phi^{-1}(P) \tag{26}$$

where φ is the standard normal distribution function.

Following the same procedure as described by the equations (25) and (26) for the drought indices SPI and SPEI, the second multivariate standardized model MSDI(SPI-SPEI) is derived.

It should be noticed that the nonparametric concept represents a modified version of the previous multivariate approach which was relied on the Copulas functions. The nonparametric method of MSDI, has been proposed by the authors “in order to avoid making assumptions regarding the distribution family, and to alleviate the computational burden in fitting parametric distributions” *(Hao and AghaKouchak, 2014).*

3.3 Correlation Analysis

In this thesis a correlation analysis, is performed among the indices, SPI, SPEI, MSDI(Pr-PET) and MSDI(SPI-SPEI) at time scales 1, 3, 6, 9 and 12. Main purpose of this analysis is to conduct a comprehensive comparison among the indices, providing scatter plots with their possible combinations at all time scales. The Pearson correlation coefficient r has been used as a statistical measure, in order to express the linear dependence among the indices. Furthermore, the Ordinary Kriging (OK) as an effective interpolation method (Best Linear Unbiased Estimator, BLUE) has been selected, providing a spatial insight of these correlations in Thessaly region at all time scales.

Ordinary Kriging, as a geostatistical method, differs from other spatial interpolation methods such as IDW (Inverse Distance Weighting) method, considering not only the distance between the measured points and the prediction location, but also the spatial covariance structure (autocorrelation) of the sample points.In case of Ordinary Kriging, the hypothesis of stationarity (that the mean and the variance of the values are constant across the spatial area) must be presumed.

A general equation of Ordinary Kriging method can be determined by the following equation:

$$\hat{z}(x_0) = \frac{1}{2n}\sum_{i=1}^{n} \lambda_i \, z(x_\mathrm{i}) \tag{27}$$

Where $\hat{z}(x_0)$ is the value to be estimated at location, x_0; $z(x_\mathrm{i})$ is the measured value at station, x_i; λ_i represents the weight of the measured value $z(x_\mathrm{i})$ at the i^{th} station, and n is the number of measured values.

The spatial dependence (autocorrelation) of the sample points is determined by fitting an experimental semivariogram. An experimental semivariogram $\gamma(\mathrm{h})$ can be defined as half the average squared difference between two neighbouring points, $\mathrm{Z}(x_\mathrm{i})$, $\mathrm{Z}(x_\mathrm{i}+\mathrm{h})$, separated by the distance h *(Goovaerts, 2000)*.

$$\hat{\gamma}(\mathrm{h}) = \frac{1}{2n}\sum_{i=1}^{n}[\mathrm{Z}(x_\mathrm{i}) - \mathrm{Z}(x_\mathrm{i}+\mathrm{h})]^2 \tag{28}$$

A spherical model has been selected to fit the data of the experimental variogram, according to the weighted least square technique. A spherical model can be expressed by the following equation:

$$g(h) = \begin{cases} 0 \;\; if \; h = 0 \\ c\left(\frac{3}{2}\frac{h}{R} - \frac{1}{2}\left(\frac{h}{R}\right)^3\right) \; if \; 0 < h \le R \\ c \; if \; h > R \end{cases} \tag{29}$$

Where c (sill) is the limiting value of the variogram model $g(h)$, and R (range) represents the distance at which, the values $\mathrm{Z}(x_\mathrm{i})$ and $\mathrm{Z}(x_\mathrm{i}+\mathrm{h})$ start to be uncorrelated.

The set of weights λ_i of equation (27) is determined by minimizing the estimation variance ($Var[\hat{z}(\mathrm{x}_0) - z(\mathrm{x}_0)]$), under the constraint of unbiasedness ($E[\hat{z}(\mathrm{x}_0)] = \mathrm{E}[z(\mathrm{x}_0)]$).

Finally, in order to test the goodness of fit of the estimations, a cross validation technique was conducted. Specifically, the statistical indices: Mean Error (ME), Root-Mean-Square Error (RMSE), Average Standard Error (ASE), Mean Standard Error (MSE), and the Root-Mean-Square Standardized Error (RMSSE) have been used in order to assess the effectiveness of the prediction model.

A more detailed explanation of this method can be found in *(Isaaks and Srivastava,1989; Cressie, 1993; Goovaerts, 1997; Kitanidis, 1997).*

3.4 Principal Components Analysis (PCA)

In this thesis the widely used indices SPI and SPEI have been selected as the most suitable indices in order to identify spatial patterns of droughts in the region of Thessaly for 42 hydrological years (October 1960 - September 2002), using the data from the 78 precipitation and temperature stations respectively.

It is understood, that the large size of dataset (78 Stations) for each index, complicates the process for a spatial characterization of droughts in Thessaly region. Therefore, the Principal Component Analysis as a statistical technique, applicable to many climatological fields is performed for the drought indices SPI and SPEI. Applying this method to the indices SPI and SPEI, a reduction in the dimensionality of their dataset can be accomplished, and a simplification of its interpretation can be ensured.

Specifically, “a Principal Component Analysis constitutes a statistical procedure that linearly transforms an original set of interrelated variables into a substantially smaller set of uncorrelated variables (principal components) that represents most of the information (variation) in the original set of variables” *(Dunteman, 1989).*

Therefore, p uncorrelated principal components $Z_1, Z_2 \dots Z_p$, can be derived as the linear combinations of the original variables: $X_1, X_2 \dots X_p$, according to the following equations:

$$\begin{cases} Z_1 = a_{11}X_1 + a_{12}X_2 + \dots + a_{1p}X_p \text{ with the constraint that: } a_{11}^2 + a_{12}^2 + \dots + a_{1p}^2 = 1 \\ Z_2 = a_{21}X_1 + a_{22}X_2 + \dots + a_{2p}X_p \text{ with the constraint that: } a_{21}^2 + a_{22}^2 + \dots + a_{2p}^2 = 1 \\ \vdots \\ Z_p = a_{p1}X_1 + a_{p2}X_2 + \dots + a_{pp}X_p \text{ with the constraint that: } a_{p1}^2 + a_{p2}^2 + \dots + a_{pp}^2 = 1 \end{cases} \quad (30)$$

- The $X_1, X_2 \dots X_p$ refer to the original variables (time series of each station) of the SPI (or SPEI) series.
- p is equal to the number of precipitation (or temperature) stations (in our case 78).
- The $a_{i,j}$ is the weight coefficient (eigenvector) of the variable X_j to the component Z_i. This coefficient (also called loading) reflects the contribution of the original variable X_j to the principal component Z_i.Hence, the produced component Z_i is really carried out to the same information as the variable X_j, when the absolute magnitude of the loading is large (i.e. approaching a value of ±1). Values close to zero indicate an insignificant correlation and therefore can be ignored.

The amount of variance λ_i explained by each component Z_i is called eigenvalue. The eigenvalue for each component Z_i is scaled according to the following inequality.

$$\lambda_1 \geq \lambda_2 \geq \dots \geq \lambda_p \geq 0 \quad (31)$$

Hence, the first eigenvalue λ_1, expresses the largest possible variance of the original p values, the second one retains as much of the remaining variance as possible, and so on.

Another useful property of the PCA method is that, the sum of the variances of the principal components (PCs) is equal to the sum of the variances of the original variables. This is very important, because the new principal components account for all of the variation in the original data.

The derivation of the eigenvalues and eigenvector of the PCs can be conducted by solving the following eigensystem:

$$(C - \lambda I)A = 0 \quad (32)$$

Where C is the variance-covariance matrix of the original variables (or the correlation matrix, if the original variables have been standardized), λ are the eigenvalues, I is an identity matrix and A are the eigenvectors.

It should be noticed that in this study, the observed variables have been standardized, and therefore the estimation of eigenvalues and eigenvectors of the PCs has relied on the correlation matrix C of the original variables. The correlation matrix can be defined as:

$$C = \begin{pmatrix} 1 & c_{12} & \dots & c_{1p} \\ c_{21} & 1 & \dots & c_{2p} \\ c_{p1} & c_{p2} & \dots & 1 \end{pmatrix} \quad (33)$$

Where $C_{ij} = C_{ji}$, is the correlation between X_i and X_j

Hence, the number of components extracted in PCA is equal to the number of observed variables.

Exploiting the property described in the relation (31), it is possible to work with a smaller number of components, retaining a significant amount of the total variation of the initial data; achieving in this way, some economy. The number of components that have to be maintained, without missing important information from the original data, is determined by the use of statistical criteria. The eigenvalue-one criterion *(Kaiser, 1960),* the scree test *(Cartell 1966)*, a criterion relied on the proportion of variance for each component, and a criterion associated with the cumulative proportion of variance explained by a k number of components, constitute some of the most popular criteria for selecting the most meaningful components.

It should be highlighted that there is no such thing as a simple and clear criterion that could be used in all cases *(Zwick and Velicer 1986; Thompson and Daniel 1996).* The determination of the most appropriate components can be achieved taking into account one or more criteria *(Hair et al., 1995),* but it would remain a matter of subjective choice, depending on the amount of data and the purposes of PCA method.

In this thesis, a number of principal components which define cumulatively at least the 75% of the total variance (cumulative variance) have been set as the most important, and therefore have been selected for a spatial characterization of droughts in Thessaly region.

This selection has been performed, according to the following approximation:

$$\left(\sum_{i=1}^{k} \lambda_i\right)/\mathrm{p} \geq \frac{3}{4} \quad (34)$$

Where k is the number of components explaining at least 75% of the total variance, p represents the number of the initial principal components (in our case 78), and λ_i is the eigenvalue (variance) for each component.

Once an appropriate number of components have been defined, the next step is to improve the interpretation for each of the remaining components. “This process often is facilitated by geometrically rotating the components, in order to obtain a sharper conceptual solution” *(Kellow, 2006).* Specifically, the rotation of the axes is a procedure during which the variance of the original components is redistributed in new components without affecting the total variation.The main purpose of this technique is to increase the distinctiveness among the loadings (forces the loadings to be either large or small) of the new components, providing an optimal simple structure and contributing to the best interpretation of each component.

In this study, an orthogonal rotation technique *(Varimax, Kaiser, 1958)* is applied in order to obtain more explainable spatial patterns of droughts in Thessaly region. It is relied on the assumption that the interpretability of a component can be measured by the variance of the square of its loadings. If the resulting variation is high, then some of the loadings tend to zero and some to one. Consequently, the philosophy of the rotation of the variation is based on the maximization of the sum of the variation for all components *(F.J. Manly, 2004)*.

It should be mentioned that the Principal Component Analysis, is performed at time scales 3 and 12, in order to identify spatial patterns associated with short (meteorological droughts) and medium term drought conditions (hydrological droughts), in Thessaly region. The spatiotemporal visualization of these patterns has been conducted by using the method of Ordinary Kriging as described in the previous subsection.

4 RESULTS AND DISCUSSION

4.1 SPI – SPEI – MSDI Indices

In this study the time series of meteorological drought indices SPI, SPEI, MSDI (Pr-PET) and MSDI(SPI-SPEI) were extracted for 42 hydrological years (October 1960 - September 2002), at time scales 1, 3, 6, 9 and 12 months, for each station in Thessaly region.

In this subsection, the results from station-2 which is located in the northwest side of Thessaly (Figure 2), will be used indicatively, analyzing the basic similarities /differences of SPI, SPEI, MSDI(Pr-PET) and MSDI(SPI-SPEI) series at the examined time scales (1, 3, 6, 9 and 12). In Appendix-B of the dissertation, the results of the stations: 62(Northeast), 57(Central), 6(Southwest) and 12(Southeast) are suggestively cited, representing four geographic sub-regions of Thessaly.

It should be pointed out that it was considered appropriate a shorter period of time than the initial to be used, in order to achieve best clarification of the results. Thus, the presentation of the results is conducted during the hydrological period from October 1982 to September 2002.

Concerning the results of station-2 (Figure 4), the monthly patterns of indices SPI, SPEI, MSDI(SPI-SPEI) seem to be quite similar at all time scales. Therefore, they can be characterized as 3 highly correlated indices, providing a similar behavior for the short and medium term drought conditions of the station. On the contrary, the MSDI(Pr-PET), differs significantly from the other indices and appears to be biased in negative values at all time scales. Regarding the results of the widely used indices SPI, SPEI, and the outcomes of the research of *Loukas and Vasiliades in 2004* which were based on the average SPI values for the period of time from 1960 to 1993 in Thessaly, the results of the index MSDI(Pr-PET) can be characterized as overrated and abnormal for the region, showing several prolonged drought episodes.

Examining the effectiveness of the measures SPI, SPEI and MSDI(SPI-SPEI) in detecting the extremely drought events ($\leq$ -2), of station-2, SPI and SPEI seem to be the more capable indices to capture these extremely conditions, while the multivariate model MSDI(SPI-SPEI) limited to identify only severely drought episodes (-1.5 to -1.99), at time scales 1, 3, 6, 9 and 12 months. Specifically, at time scale 1, the most extreme drought episode has been determined by the SPEI index (mid of 90s). As the time scales increase (time scales: 3-6-9-12) and more smoothed patterns of temporal variability can be derived, the most extreme drought events have been identified by the SPI index (early of 90s).

It is essential to underline once more, that the results above are suggestive and consequently the last indication about the indices SPI and SPEI is distinctive for station-2, and does not represent the results of the rest stations. For example, in stations where significant increasing trends in temperature were apparent, the most severe drought episodes in longer time scales have been identified by the SPEI index.

Furthermore, a drought classification for 42 hydrological years has been performed, taking into account the results of four indices, for all the stations, at all time scales. This classification involves the categories: Extremely Drought ($\leq$ -2), Severely Drought (-1.5 to -1.99), Moderately Drought (-1.0 to -1.49), Normal (-0.99 to 0.99), Moderately Wet (1.0 to 1.49), Severely Wet (1.5 to 1.99) and Extremely Wet ($2 \geq$) conditions.

In Table 4 are provided suggestively, the percentages of drought and rainfall events as detected by the four examined indices, at all time scales, for the station-2. It should be noticed that similar results were observed for all stations of the region while the drought classification of the stations 62, 57, 6 and 12 is presented in the Appendix-B. Analyzing the outcomes related to the drought episodes of station-2, the similar behavior of indices SPI and SPEI can be ascertained in this study for a second time. More specifically, the indices SPI and SPEI seem to have similar results in each of the three categories of drought (slightly more increased are the percentages of SPEI in the categories Moderate and Severe Drought, in most of the stations). In contrast, the MSDI(Pr-PET) differs significantly in the number of moderate and severe drought events compared to the other indices, accumulating higher rates in these categories. Moreover, it fails to detect extreme drought episodes at all time scales (similar behavior at all stations). Therefore, the choice of the variables of precipitation and PET for the formation of a competent drought index through a joint distribution concept, does not infer the desirable results. Finally, the MSDI(SPI-SPEI) index shows similar outcomes compared with SPEI index in the categories of Moderate Drought and Severe Drought. Furthermore, it should be highlighted that in this case as well, the weakness of the multivariate model to capture the extremely drought conditions of the station is obvious. (also 0 values at all stations in this category).

The empirical method used by the indices MSDI(Pr-PET) and MSDI(SPI-SPEI), and the characteristic way of their structure (through the joint distribution of two variables-indices), are the most possible reasons why the two multivariate models fail to detect the extreme drought episodes of the region.

Furthermore it is important to note that the four standardized meteorological drought indices, presented the three categories of drought events at all time scales with small or large discrepancies (not the same proportions in three categories, in most of cases), signifying that the drought classification of our study area has been depicted in a unique way (different structure) for each of the four meteorological drought measures. However the SPI, SPEI and MSDI(SPI-SPEI), as mentioned before, seem to be in consistency, aggregating similar rates with no large differences in most of cases. In contrast the MSDI(Pr-PET) is differentiated considerably compared to the other examined indices. A possible reason of this differentiation constitutes the probabilistic approach (empirical joint distribution concept) which has been used to combine the drought information from the hydro-climatic variables of precipitation and potential evapotranspiration. Therefore, this method can be characterized as ineffective in the process of monitoring and assessing droughts, considering the aforementioned variables.

Station-2 (Northwest)

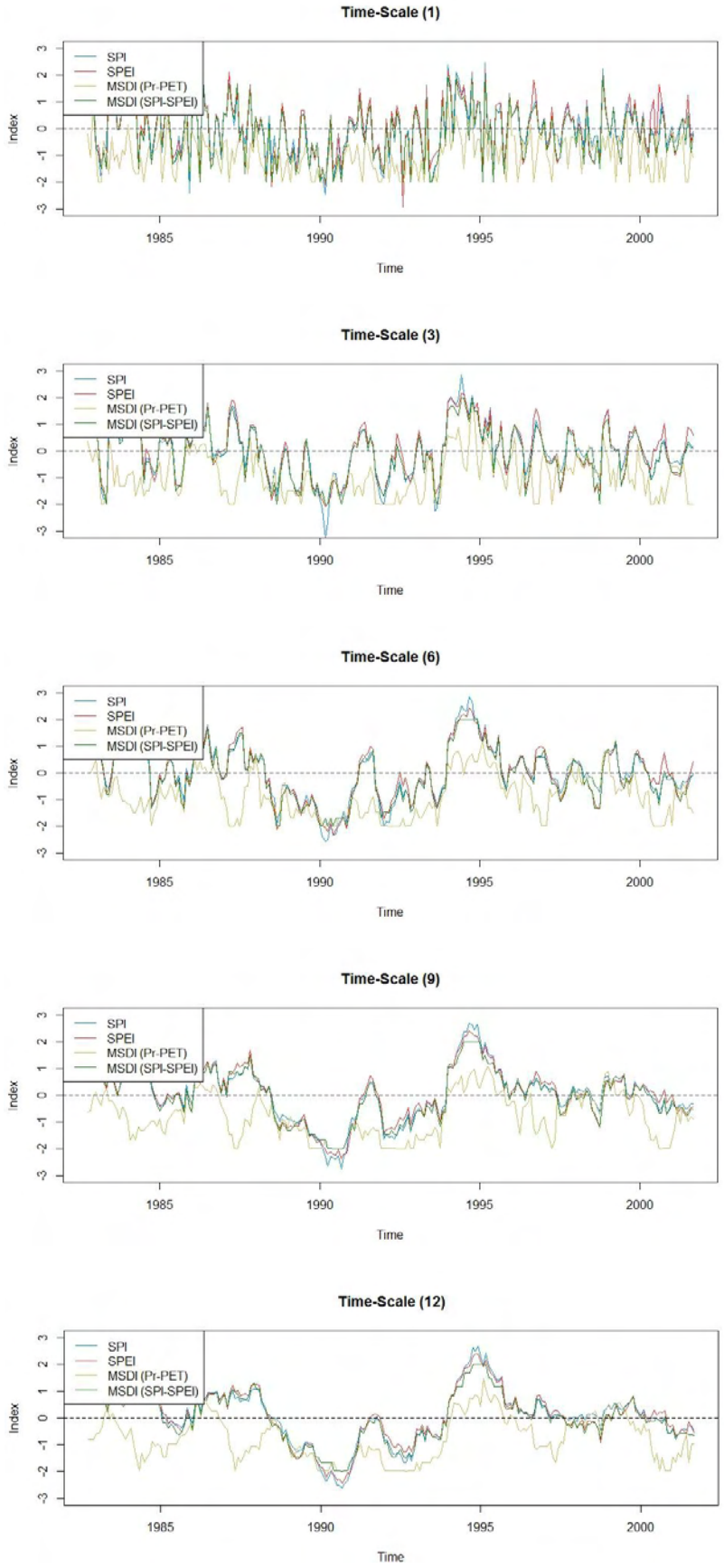

Figure 4: Time series plots of drought indices SPI (blue line), SPEI (red line), MSDI(Pr-PET) (yellow line), MSDI(SPI-SPEI) (green line), for 20 hydrological years (October 1982-September 2002) at time scales 1, 3, 6, 9 and 12 months.

Table 4: Drought classification for 42 hydrological years (October 1960 - September 2002), in Thessaly region, providing the percentages of drought events for indices SPI, SPEI, MSDI(Pr-PET), MSDI(SPI-SPEI) at time scales 1,3,6,9 and12 months.

Time-Scale (1)				
	SPI%	SPEI%	MSDI(Pr-PET)%	MSDI(SPI-SPEI)%
Extremely Wet	2	2	0	0
Severely Wet	5	6	0	4
Moderately Wet	8	11	2	9
Normal	71	64	53	68
Moderate Drought	9	12	23	13
Severe Drought	4	6	22	6
Extreme Drought	1	1	0	0
Time-Scale (3)				
	SPI%	SPEI%	MSDI(Pr-PET)%	MSDI(SPI-SPEI)%
Extremely Wet	1	1	0	0
Severely Wet	7	8	0	4
Moderately Wet	6	7	1	9
Normal	71	66	55	70
Moderate Drought	8	12	22	11
Severe Drought	4	5	22	6
Extreme Drought	3	1	0	0
Time-Scale (6)				
	SPI%	SPEI%	MSDI(Pr-PET)%	MSDI(SPI-SPEI)%
Extremely Wet	3	2	0	0
Severely Wet	4	6	0	4
Moderately Wet	7	8	1	9
Normal	72	69	55	69
Moderate Drought	7	8	24	11
Severe Drought	4	5	20	6
Extreme Drought	3	2	0	0
Time-Scale (9)				
	SPI%	SPEI%	MSDI(Pr-PET)%	MSDI(SPI-SPEI)%
Extremely Wet	3	2	0	0
Severely Wet	5	6	0	4
Moderately Wet	6	7	1	9
Normal	72	69	55	69
Moderate Drought	7	10	25	13
Severe Drought	3	3	19	5
Extreme Drought	4	3	0	0
Time-Scale (12)				
	SPI%	SPEI%	MSDI(Pr-PET)%	MSDI(SPI-SPEI)%
Extremely Wet	4	3	0	0
Severely Wet	3	3	0	4
Moderately Wet	8	10	1	8
Normal	69	67	52	68
Moderate Drought	11	12	23	13
Severe Drought	3	4	24	7
Extreme Drought	2	1	0	0

4.2 Correlation Analysis

In this subsection, a comprehensive comparative analysis, with the possible combinations of the four examined indices SPI, SPEI, MSDI(Pr-PET) and MSDI(SPI-SPEI) will be discussed. In Figure 5, the scatter plots among the indices of station-2 (Northwest) are indicatively presented, while in Appendix-C the outcomes of stations 62, 57, 6, and 12 are provided. Similar results have been observed at all time scales for the 78 stations of the region.

According to the results of station-2, the standardized indices SPI and SPEI, appear significantly correlated at all time scales. Furthermore, it is observed that as the time scale increases, the correlation between the indices SPI and SPEI becomes stronger and therefore a perfect correlation can be accomplished. This is reasonable, as in longer time scales the effect of PET is limited considerably when temporal trends of temperature are not noticeable; while for the parameter of precipitation this is no true.

Concerning the results of the MSDI(Pr-PET), the unconformity of the multivariate model with the other indices can be determined. Specifically, considerably lower correlation values (moderately to extremely low for most of the stations) compared to the other indices at all time scales, are presented for all the possible combinations of the model, indicating that the MSDI(Pr-PET) differs significantly from the indices SPI, SPEI and MSDI(SPI-SPEI). The small number of correlated observations, as was observed for several stations, in each pair of MSDI(Pr-PET), can be explained by the

tendency of model to approach many negative values as described in subsection 4.1.

Finally, the MSDI(SPI-SPEI) appears to be notably correlated with the indices SPI and SPEI, at all time scales. This can be explained by the fact that the multivariate model has been structured, combining the drought information of two strong interrelated indices (SPI and SPEI), ensuring highly correlated values for the pairs, MSDI(SPI-SPEI):SPI and MSDI(SPI-SPEI):SPEI.

Station-2 (Northwest)

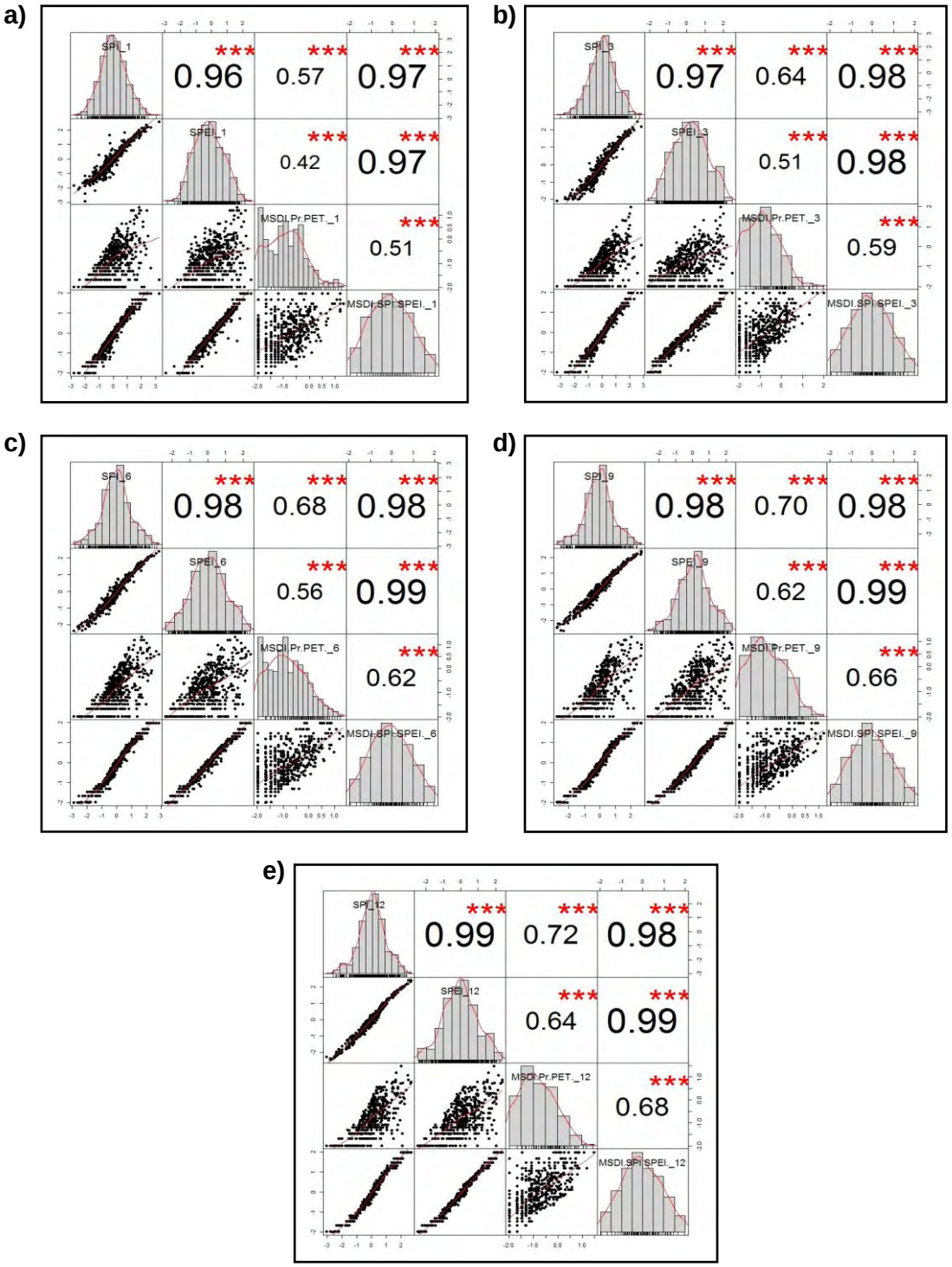

Figure 5: Cross correlation among the indices SPI,SPEI, MSDI(Pr-PET), MSDI(SPI-SPEI) for (a) 1-month, (b) 3-month, (c) 6-month, (d) 9-month, and (e) 12-month time scales.

Subsequently, the spatiotemporal correlation distribution for each pair of the analyzed indices will be discussed. Figure 6a shows the spatial patterns of Thessaly between SPI and SPEI. The results suggest a strong correlation between these indices at all time scales ($r \geq 0.75$), as expected. A remarkable characteristic of these patterns is that the western region which is characterized as mountainous seems to be more correlated than the central and eastern sides (plain areas) where many stations with lower elevation are located (Figure 2). This can be explained by the fact that the effect of PET in mountainous regions compared to the plain areas is lower, signifying that the indices SPI and SPEI respond mainly to the fluctuations of precipitation, and therefore more correlated values can be obtained for them.

Furthermore, it is important to reiterate again that the PET variability decreases in longer time scales, while this no true for the parameter of precipitation. Hence, the most correlated patterns for these indices have been derived at time scales 6, 9, and 12, while in shorter time scales, weaker correlation values have been extracted, verifying the above claim. It should be noted that the correlations values at time scales 9 and 12 compared to the time scale-6, appeared slightly lower. According to *Vicente-Serrano et al. (2010)* the correlation between the two indices may decrease in longer time scales when there are apparent rising trends in temperature.

Regarding the results of the MSDI(SPI-SPEI):MSDI(Pr-PET), moderately to extremely low correlation values predominate in all maps, at all time scales ($r \leq 0.72$) (Figure 6b). The limited number of correlated observations between the two multivariate models can be explained by the fact, that the MSDI(SPI-SPEI) seems to be in accordance (similar patterns) with the widely used indices SPI and SPEI, while the second model which is based on the combination of two hydro-climatic variables (precipitation, PET) is differentiated considerably, as it is biased in negative values; leading to abnormal results for the region.

a) **b)**

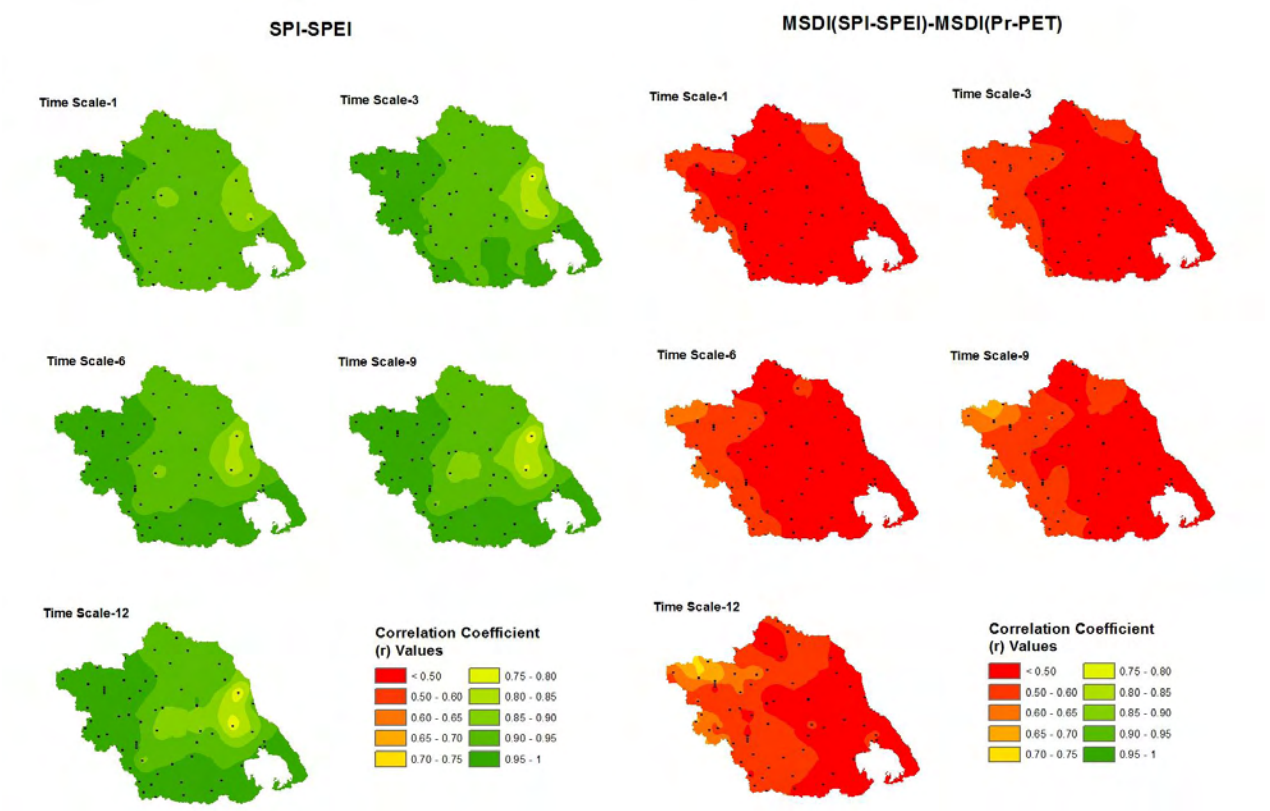

Figure 6: Spatial patterns of Thessaly, providing the correlation coefficient values between the indices: a) SPI-SPEI b) MSDI(SPI-SPEI)-MSDI(Pr-PET) at all time scales (1-3-6-9-12 months).

Figures 7a and 7b show the spatial patterns of the multivariate model MSDI (SPI-SPEI) with the SPI and SPEI, respectively. It is obvious that the multivariate model, is highly correlated with the interrelated indices SPI ($r \geq 0.81$) and SPEI ($r \geq 0.85$) at all time scales, providing quite similar patterns, in both cases. However, it is notable to mention that the MSDI(SPI-SPEI) seems to response slightly better with the SPEI index, indicating more correlated values in northern and eastern regions.

The highest correlated patterns for the two observed pairs, have been detected at longer time scales (time scale-9 and time scale-12).

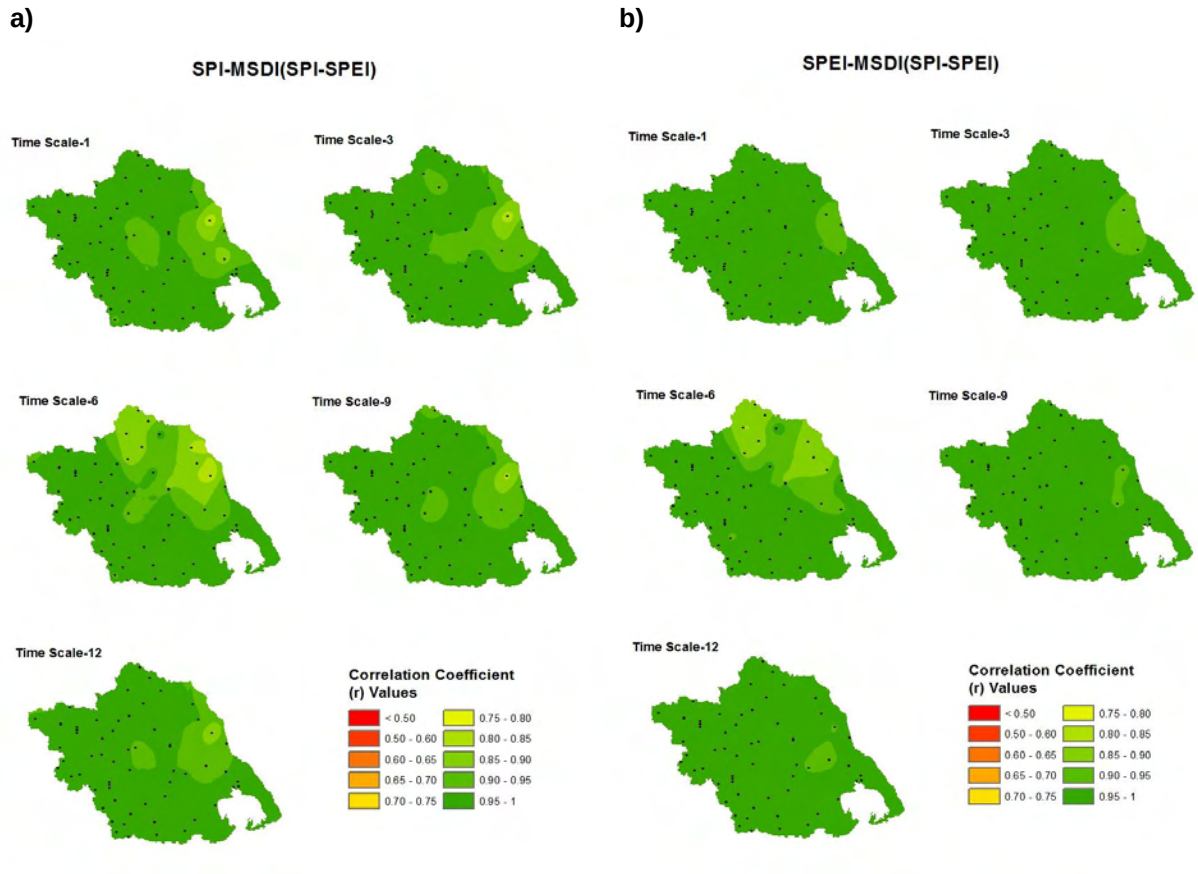

Figure 7: Spatial patterns of Thessaly, providing the correlation coefficient values between the indices: a) SPI-MSDI(SPI-SPEI) b) SPEI-MSDI(SPI-SPEI) at all time scales (1-3-6-9-12 months).

Examining the correlation strength of the multivariate model MSDI(Pr-PET) with the widely used indices SPI and SPEI (Figure 8a and Figure 8b), it is proved again the failure of the two hydro-climatic variables (precipitation and PET) to provide an effective meteorological drought measure through a joint distribution concept. Specifically, moderately to extremely low correlation values seem to prevail in both cases, at all time scales (a: $r \leq 0.72$, b: $r \leq 0.67$). Although the multivariate model corresponds better to the SPI index, this specific indication is of low interest as the inefficiency of the MSDI(Pr-PET) in drought monitoring of the region has been proved several times in this study.

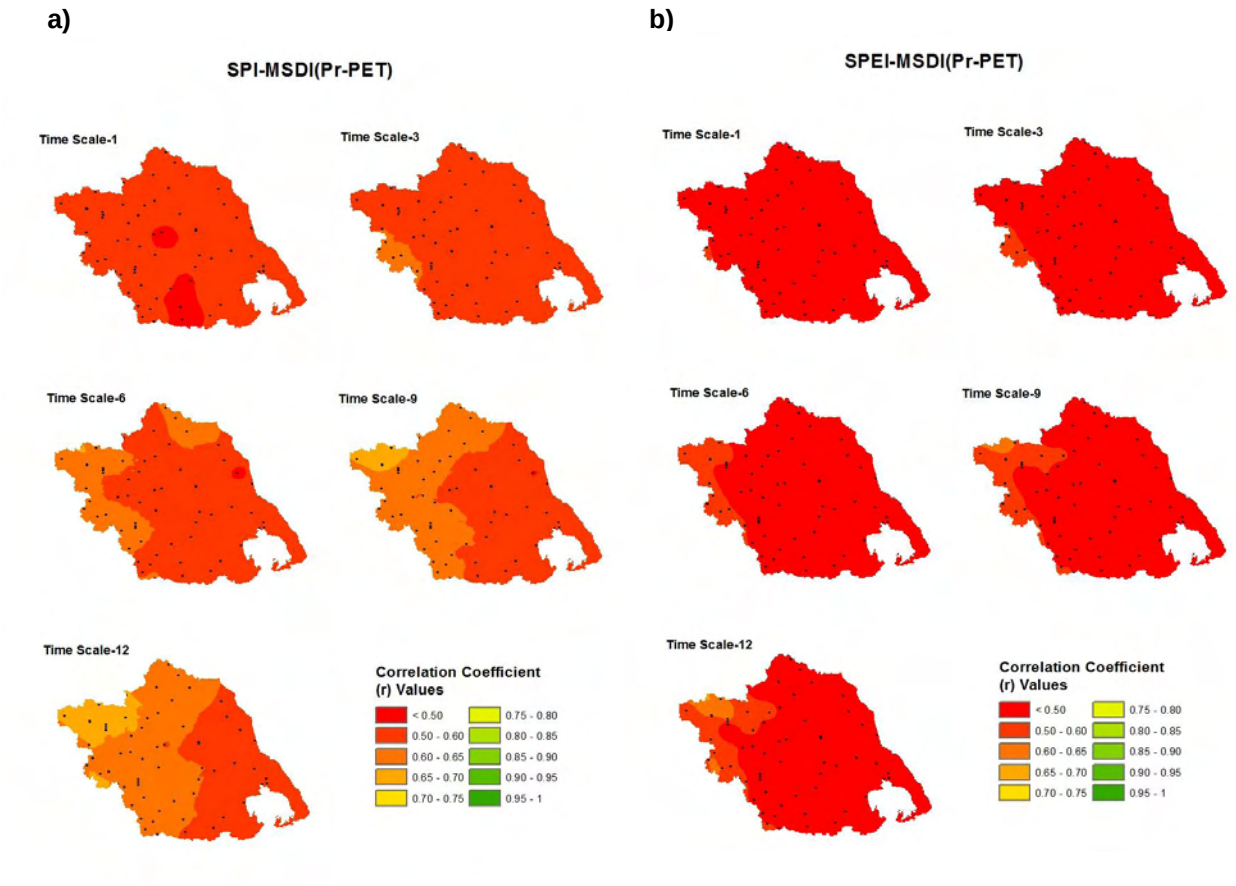

Figure 8: Spatial patterns of Thessaly, providing the correlation coefficient values between the indices: a) SPI-MSDI(Pr-PET) b) SPEI-MSDI(Pr-PET) at all time scales (1-3-6-9-12 months).

4.3 Principal Components Analysis

As the effectiveness of the four meteorological drought indices has been examined, the method of Principal Component Analysis can be performed to the most capable measures of our study area. Specifically, the SPI and SPEI series at time scales 3 and 12 have been used in order to obtain a spatial insight of the drought variability for the region of Thessaly.

Concerning the results in unrotated case at time scale-3, the PCA method identified 8 significant components for the SPI series and 6 for the SPEI index, defining cumulatively at least 75% of the total variance. The first components of the indices aggregate the highest values of loadings, depicting two spatially homogeneous patterns (Figures 9a and 9b). These patterns can be considered comparable with small differences in west, central and north sides, where the SPEI index shows more correlated values compared to SPI. Furthermore, the proportion of variance explained by the first principal components is the highest, representing the 57% and the 59.3% for the SPI and SPEI series, respectively (Table 5). This means that the temporal evolution of droughts in Thessaly region can be expressed by each index, using the values (scores) of the first significant component as was described in equation (30). Regarding the results for the less meaningful components, they are characterized by extremely low loadings (Figures 9a and 9b) and represent much lower proportion of variance related to the first ones (Table 5); with no particular interest for the drought variability of the region.

Examining the scores of the first unrotated components, the SPI and SPEI series seem to be in consistency, following similar patterns (Figures 11 and 12). These patterns are characterized by several severe drought episodes: at the mid of 60s, end of 60s, end of 70s, mid of 80s, end of 80s and in the beginning of 90s. The most severe drought events have been captured by the SPI index, and its minimum record value has been identified in 1990.

In Figures 10a, 10b the spatial patterns for the indices SPI and SPEI after an orthogonal rotation technique (Varimax), are provided. The results suggest that both indices aggregate strong correlation values at the southeast-coastland areas (SPI:RC2, SPEI:RC2) and in the northwest stations (SPI:RC6, SPEI:RC4). It is remarkable to mention that at these regions the spatial extent of SPEI index is wider, signifying that at these locations it is represented by higher loadings compared to SPI. The drought evolution of the low plain areas (central), is represented mainly by the SPEI index (RC1), indicating that the effect of temperature and therefore of PET is particularly noticeable at these areas. Finally, in the west side of Thessaly, three different high correlated areas have been depicted by both indices (SPI:RC4, SPI: RC3, SPEI:RC3).

The scores of the rotated components are presented in Figures 13 and 14. Particularly, in the southeast regions (SPI:RC2, SPEI:RC2) the two indices appear to be highly correlated, providing similar patterns. The main drought episodes were recorded in early of 60s, in the end of 70s, and in the beginning of 90s. The most extreme drought conditions have been identified by the SPI index. Examining the scores of the comparables components in northwest side, the RC6 of SPI index resembles the evolution of SPEI series (RC4), indicating once again the similar behaviour of these indices. Their temporal evolution shows several drought episodes, and the most extreme events have been captured by the SPI index in the beginning of 60s and in the mid of 80s. In central areas, the RC1 of SPEI index presented a slightly decreasing tendency towards drier periods during 90s. A remarkable drought event of great severity was recorded in the beginning of 00s. In the west side, the component RC4 of SPI series showed an intensification of severe drought events from mid of 60s to early 70s. The RC3 of the SPI index is characterized by consecutive severe drought episodes for the whole analyzed period. The most extreme drought event was detected in the mid of 60s. Furthermore several severe

drought events have been identified by the RC3 of SPEI index, and its minimum record value was observed in the beginning of 00s.

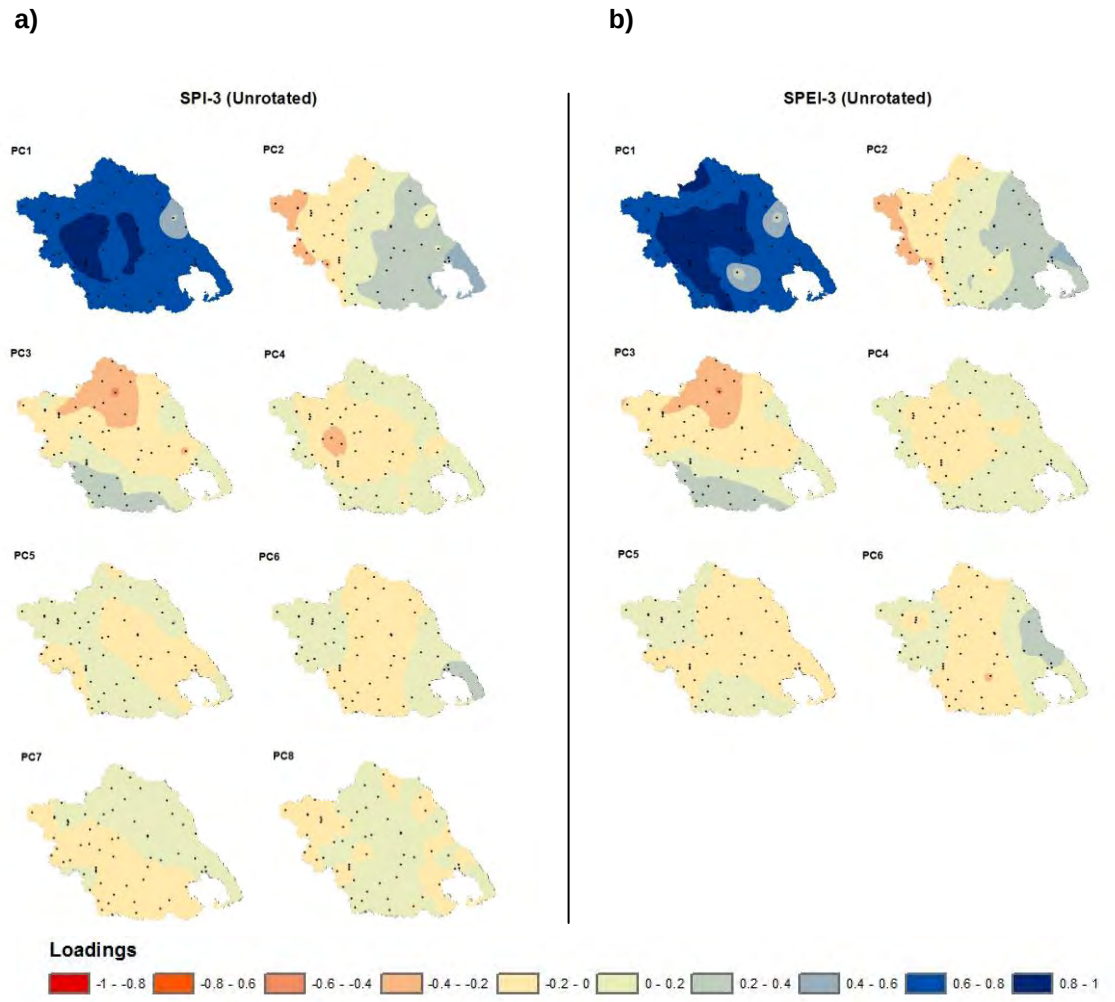

Figure 9: Spatial patterns of Thessaly, representing the loadings of unrotated components for a) 3-month SPI and b) 3-month SPEI.

Table 5: Proportion of Variance and Cumulative Variance (%) for each component of the SPI and SPEI indices at time scale-3, in unrotated case.

SPI-3 Unrotated Principal Components				SPEI-3 Unrotated Principal Components			
Id	**Variance**	**Variance (%)**	**Cumulative Variance (%)**	**Id**	**Variance**	**Variance (%)**	**Cumulative Variance (%)**
PC1	44.49	57	57	**PC1**	46.22	59.3	59.3
PC2	4.05	5.2	62.2	**PC2**	4.09	5.2	64.5
PC3	3.04	3.9	66.1	**PC3**	3.11	4	68.5
PC4	2.05	2.6	68.7	**PC4**	1.93	2.5	71
PC5	1.61	2.1	70.8	**PC5**	1.47	1.9	72.9
PC6	1.33	1.7	72.5	**PC6**	1.37	1.8	74.7
PC7	1.16	1.5	74				
PC8	1.09	1.4	75.4				

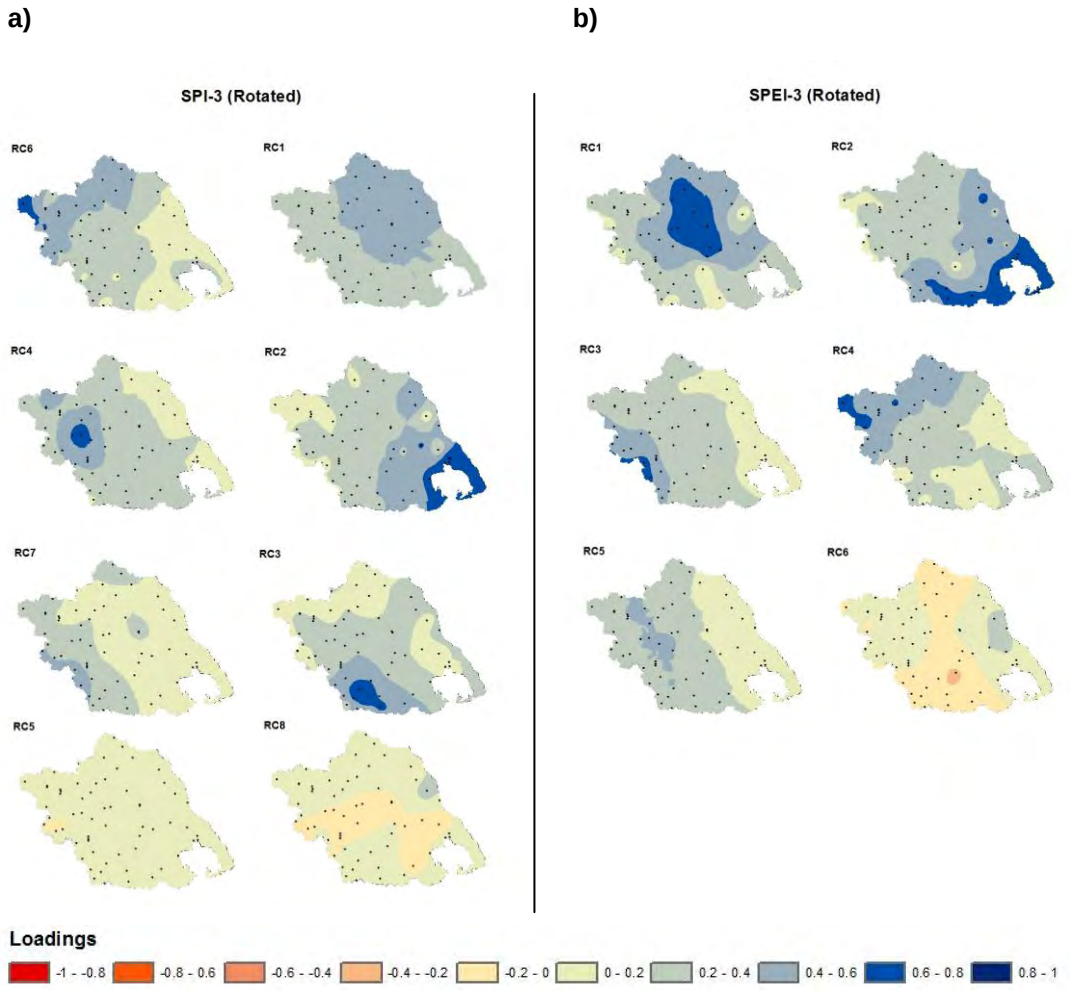

Figure 10: Spatial patterns of Thessaly, representing the loadings of rotated components for a) 3-month SPI and b) 3-month SPEI.

Table 6: Proportion of Variance and Cumulative Variance (%) for each component of the SPI and SPEI indices at time scale-3, in rotated case.

SPI-3 Rotated Principal Components				SPEI-3 Rotated Principal Components			
Id	**Variance**	**Variance (%)**	**Cumulative Variance (%)**	**Id**	**Variance**	**Variance (%)**	**Cumulative Variance (%)**
RC6	11.44	14.7	14.7	**RC1**	12.73	16.3	16.3
RC1	10.37	13.3	28	**RC2**	12.32	15.8	32.1
RC4	9.59	12.3	40.3	**RC3**	12.17	15.6	47.7
RC2	8.91	11.4	51.7	**RC4**	11.77	15.1	62.8
RC7	7.93	10.2	61.9	**RC5**	7.64	9.8	72.6
RC3	7.65	9.8	71.7	**RC6**	1.56	2	74.6
RC5	1.63	2.1	73.8				
RC8	1.30	1.7	75.4				

SPI-3 (Unrotated)

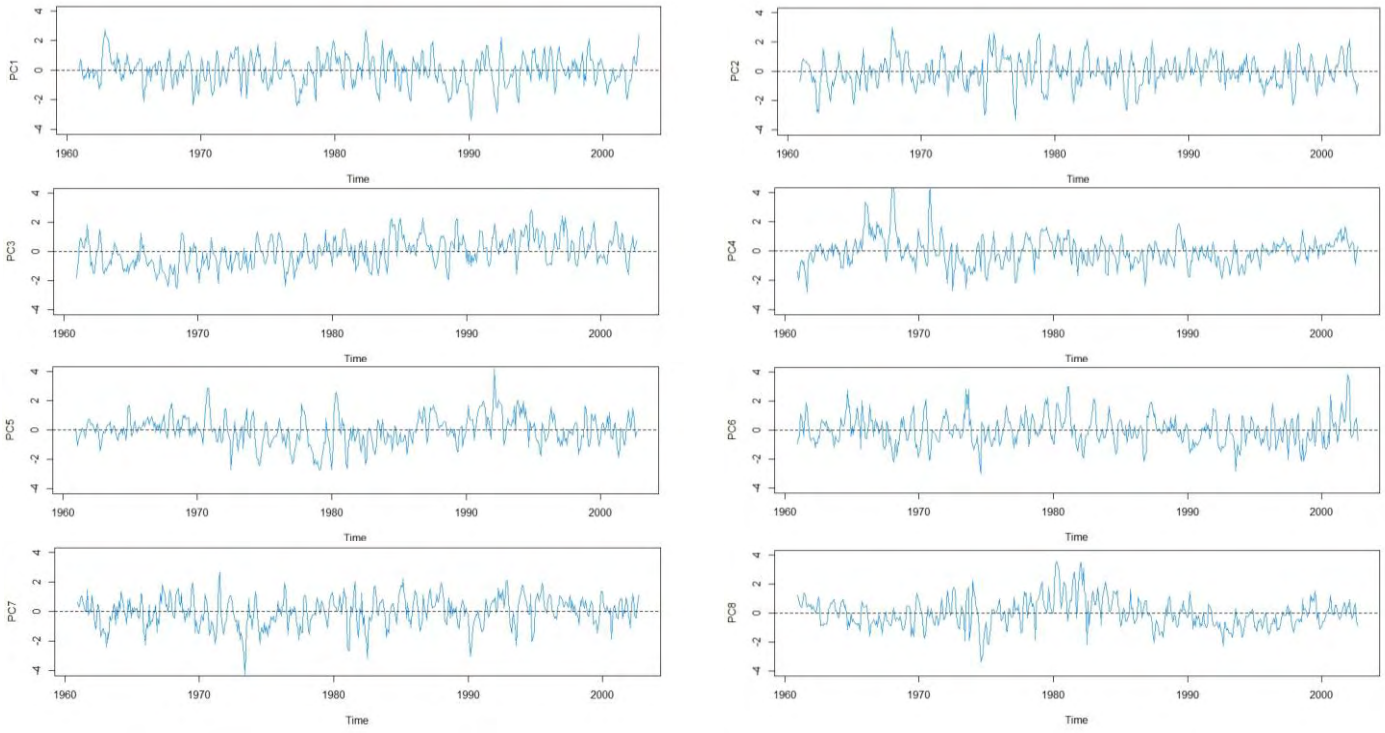

Figure 11: Scores of unrotated components for SPI index at time scale-3.

SPEI-3 (Unrotated)

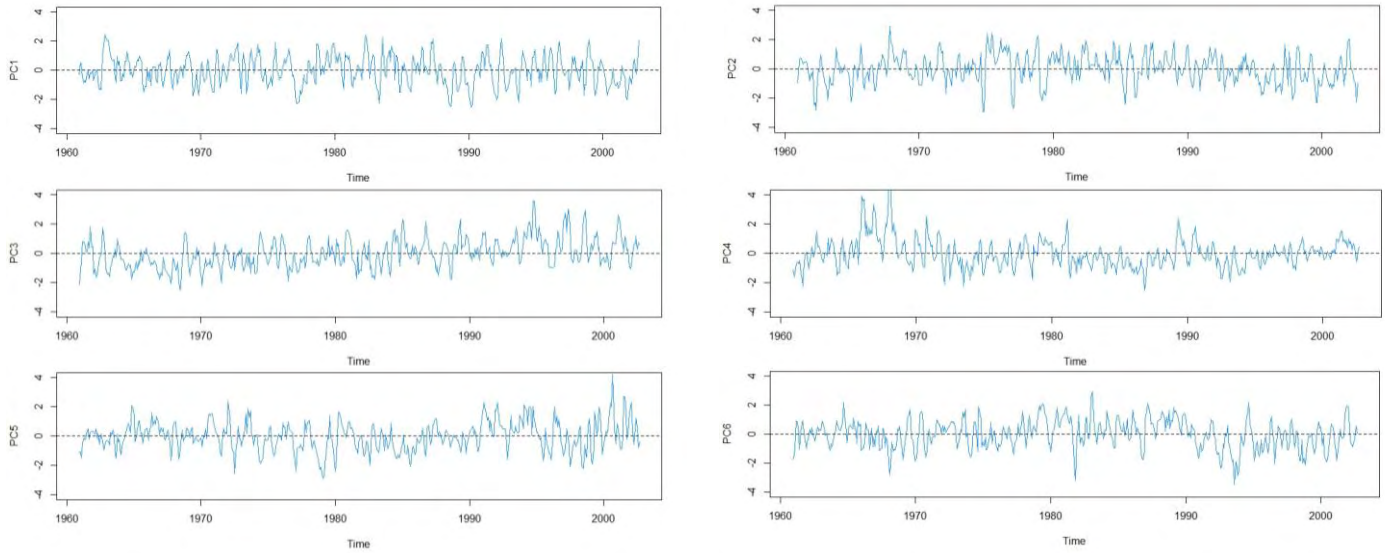

Figure 12: Scores of unrotated components for SPEI index at time scale-3.

SPI-3 (Rotated)

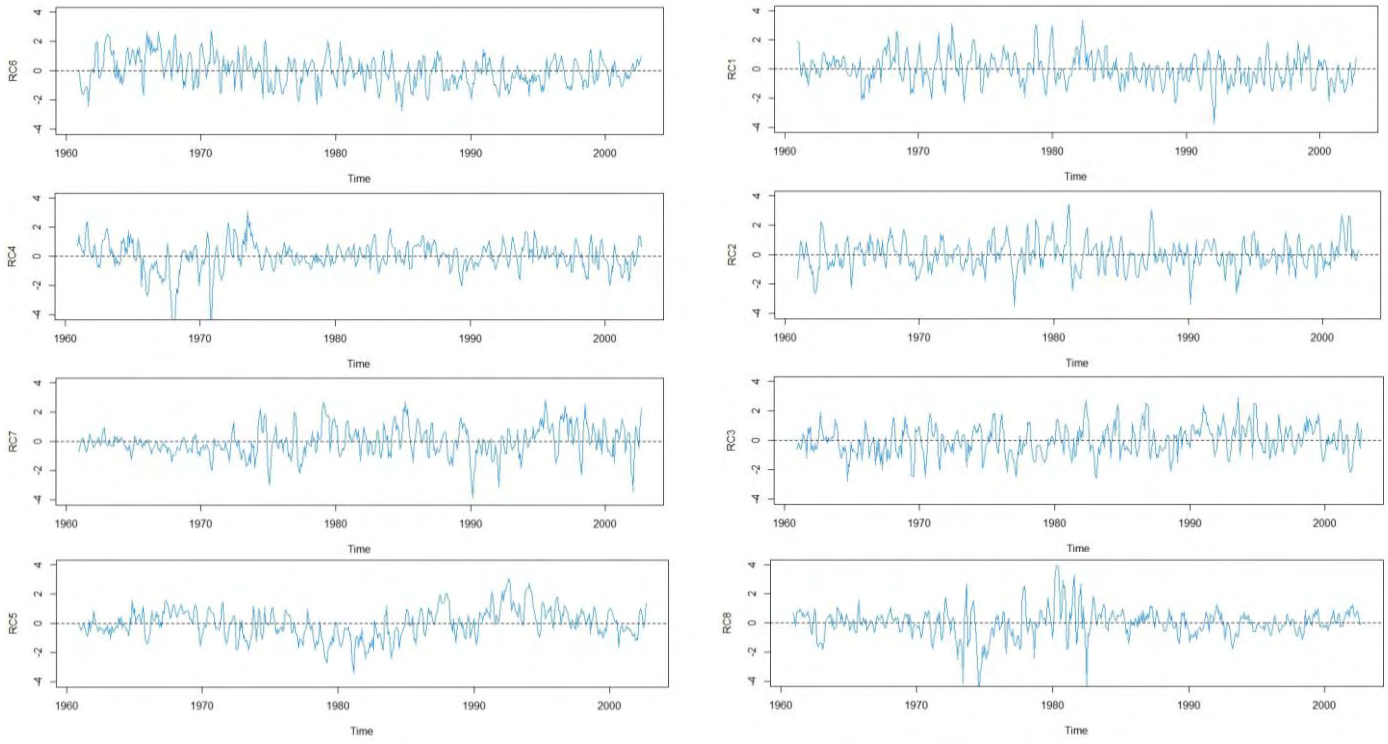

Figure 13: Scores of rotated components for SPI index at time scale-3.

SPEI-3 (Rotated)

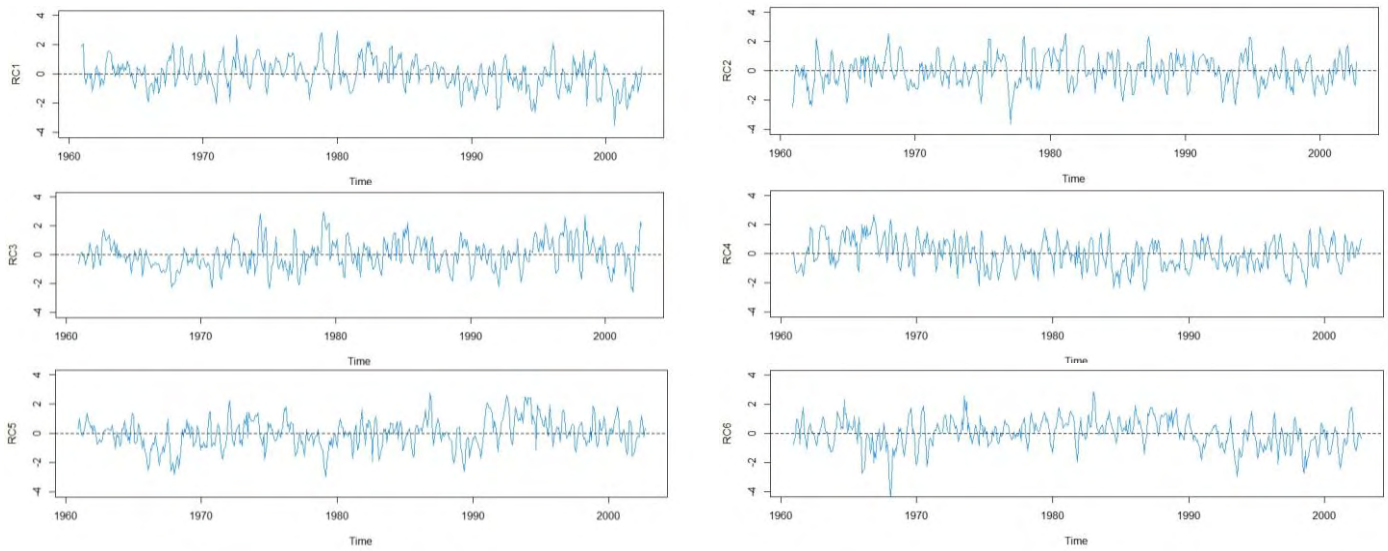

Figure 14: Scores of rotated components for SPEI index at time scale-3.

As far as the results of both indices at time scale-12 are concerned, similar outcomes can be inferred. According to the criterion of equation (34), 6 components have been ordered for each index. The first components explain the highest proportion of variance (Table 7); represented by high loadings, forming two spatially homogeneous patterns (Figures 15a and 15b). A wider extend of SPEI index is noticeable in central areas, indicating higher correlated values than SPI for these locations. Concerning the less significant components, they are represented by considerably lower loadings (Figures 15a and 15b), explaining in parallel lower proportions of variance compared to the former ones (Table 7); leading to spatial patterns of low interest.

Comparing the scores of two meaningful components, it is demonstrated the similar behaviour of two indices at longer time scale (Figures 17 and 18). Specifically, two distinctive severe periods have been revealed by both indices. The first period was recorded in the end of 70s and represents the most extreme drought event for the whole analyzed period. The second one occurred in the end of 80s and can be characterized as particularly severe, as it was prolonged in time. The results of the first components are consistent with the ones reported by *Loukas and Vasiliades in 2004* which were based on the monthly average SPI values, ensuring the proximity and the effectiveness of PCA method in our study area.

As the orthogonal rotation of the axes has been conducted, several distinguishing small regions have been appeared, providing useful information for the drought variability of Thessaly in a more local scale (Figures 16a and 16b). Specifically, both indices have identified spatial patterns of drought in: the western areas (SPI:RC1, SPEI:RC1), in the northwest and northern areas (SPI:RC2, SPEI:RC3) and in the southeast-coastland areas (SPI:RC3, SPEI:RC4). It should be noticed that in the west side of Thessaly and in northwest and northern regions the extent of SPI is larger related to SPEI. This can be explained by the fact that the stations at these regions response mainly to the variations of precipitation, as they are placed in the mountainous areas of Thessaly where the effect of PET can be considered negligible, indicating higher correlated values for the SPI index. On the other hand, the low-altitude stations in the southeast-coastland areas aggregate higher correlation values in case of SPEI (RC4) compared to SPI (RC3). Furthermore, as was observed at the time scale-3, the central (low elevation-plain) areas have been represented only by the SPEI index (RC2). Therefore, the inclusion of a temperature component (PET) especially in the drought monitoring of low-altitude regions is crucial for the identification of spatial drought patterns, at least in a local scale.

Examining the scores of the rotated components for both indices at time scale-12 (Figures 19 and 20), the first rotated components representing the west side of Thessaly (SPI:RC1, SPEI:RC1), indicated a remarkable extreme drought event in the end of 60s. This event was recorded by the SPI index with greater intensity, regarded to SPEI. In the northwest and northern areas, the comparable components of both indices (SPI:RC2, SPEI:RC3) revealed a slightly decreasing tendency towards drier periods from mid to late 80s. Comparing the southeast-coastland areas, the temporal evolution of component RC3 (SPI) resembles the RC4 obtained from SPEI series. However, different extreme events have been captured by both components (indices). Specifically the most extreme event for the SPI index was observed in the end of 70s, while the minimum value of SPEI index was recorded in the mid of 80s. All their episodes can be characterized prolonged in time. Finally, in central areas, the scores of RC2 for the SPEI series showed several prolonged drought events and the most severe episode was detected in the mid of 60s.

The strength of loadings of each station for the two indices (SPI, SPEI), at the examined time scales (3-month, 12-month), is presented in Appendix-D.

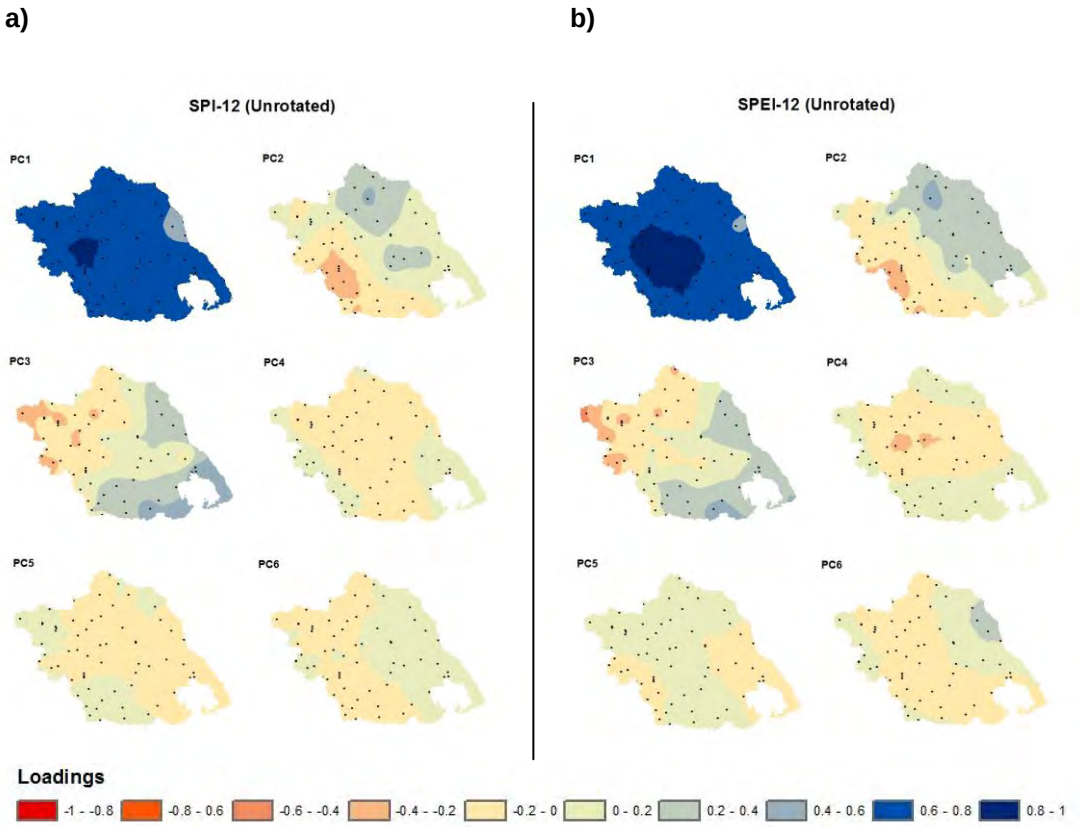

Figure 15: Spatial patterns of Thessaly, representing the loadings of unrotated components for a) 12-month SPI and b) 12-month SPEI.

Table 7: Proportion of Variance and Cumulative Variance (%) for each component of the SPI and SPEI indices at time scale-12, in unrotated case.

SPI-12 Unrotated Principal Components				SPEI-12 Unrotated Principal Components			
Id	**Variance**	**Variance (%)**	**Cumulative Variance (%)**	**Id**	**Variance**	**Variance (%)**	**Cumulative Variance (%)**
PC1	41.05	52.6	52.6	**PC1**	43.16	55.3	55.3
PC2	5.39	6.9	59.5	**PC2**	5.44	7	62.3
PC3	4.36	5.6	65.1	**PC3**	4.33	5.5	67.8
PC4	3.02	3.9	69	**PC4**	2.72	3.5	71.3
PC5	2.79	3.6	72.6	**PC5**	2.43	3.1	74.4
PC6	1.77	2.3	74.9	**PC6**	1.79	2.3	76.7

a) b)

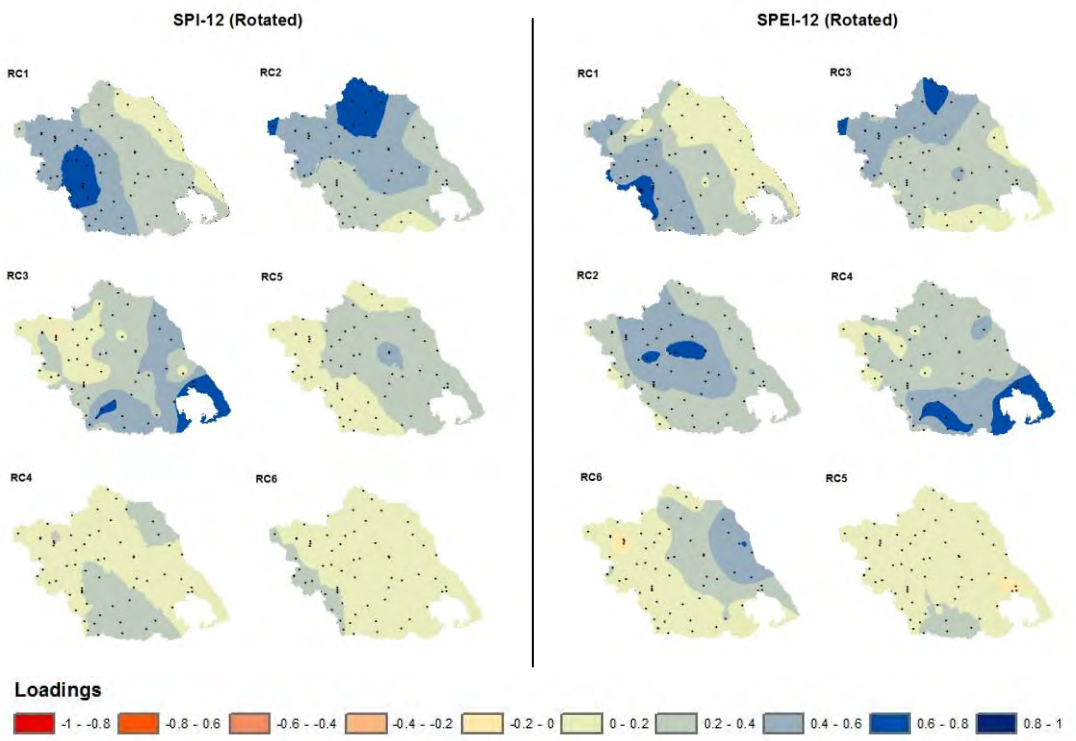

Figure 16: Spatial patterns of Thessaly, representing the loadings of rotated components for a) 12-month SPI and b) 12-month SPEI.

Table 8: Proportion of Variance and Cumulative Variance (%) for each component of the SPI and SPEI indices at time scale-12, in rotated case.

SPI-12 Rotated Principal Components				SPEI-12 Rotated Principal Components			
Id	Variance	Variance (%)	Cumulative Variance (%)	Id	Variance	Variance (%)	Cumulative Variance (%)
RC1	18.54	23.8	23.8	RC1	16.03	20.5	20.5
RC2	16.69	21.4	45.2	RC3	12.65	16.2	36.7
RC3	9.78	12.5	57.7	RC2	12.42	15.9	52.6
RC5	4.87	6.2	63.9	RC4	10.86	13.9	66.5
RC4	4.67	6	69.9	RC6	4.55	5.9	72.4
RC6	3.81	4.9	74.8	RC5	3.36	4.3	76.7

SPI-12 (Unrotated)

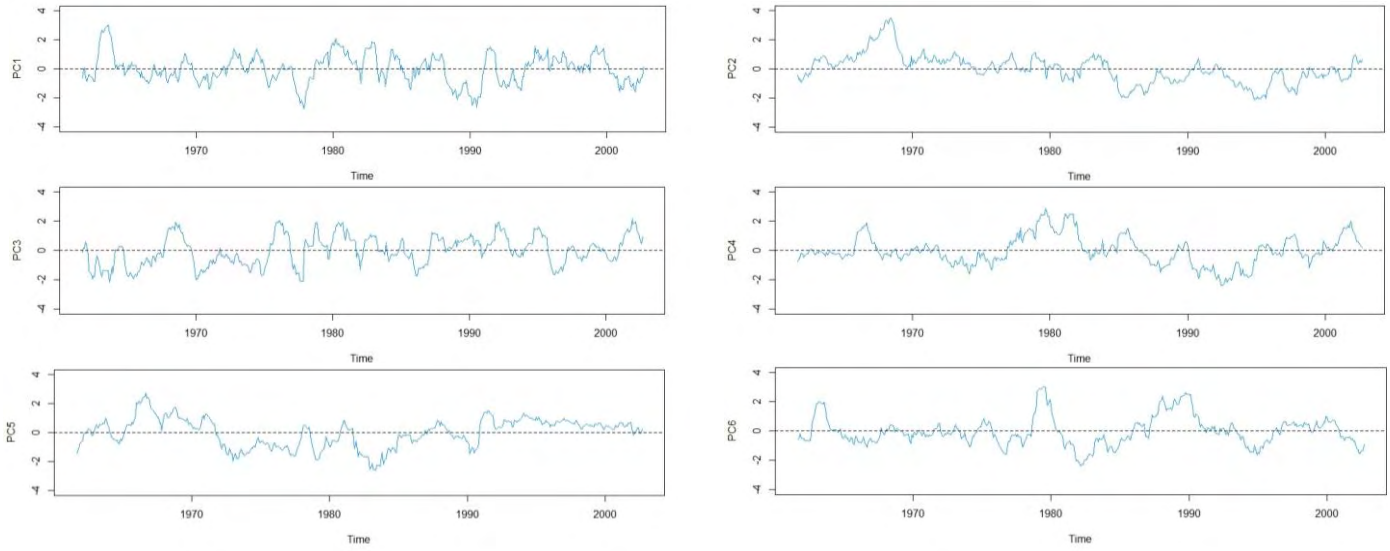

Figure 17: Scores of unrotated components for SPI index at time scale-12.

SPEI-12 (Unrotated)

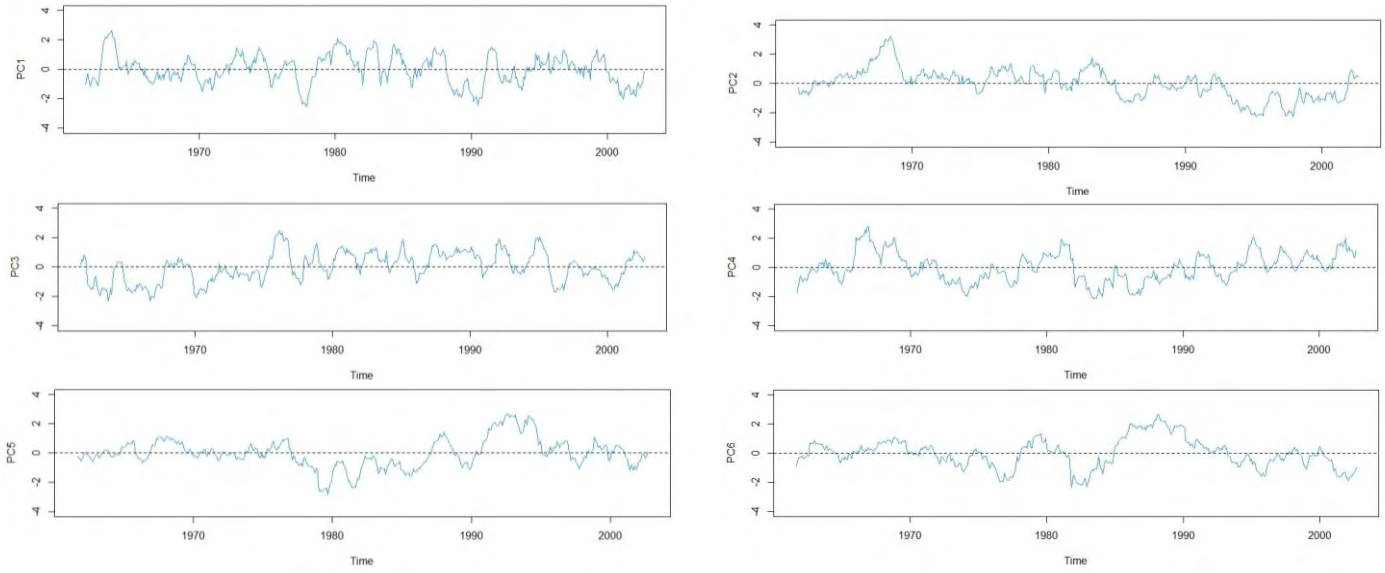

Figure 18: Scores of unrotated components for SPEI index, at time scale-12.

SPI-12 (Rotated)

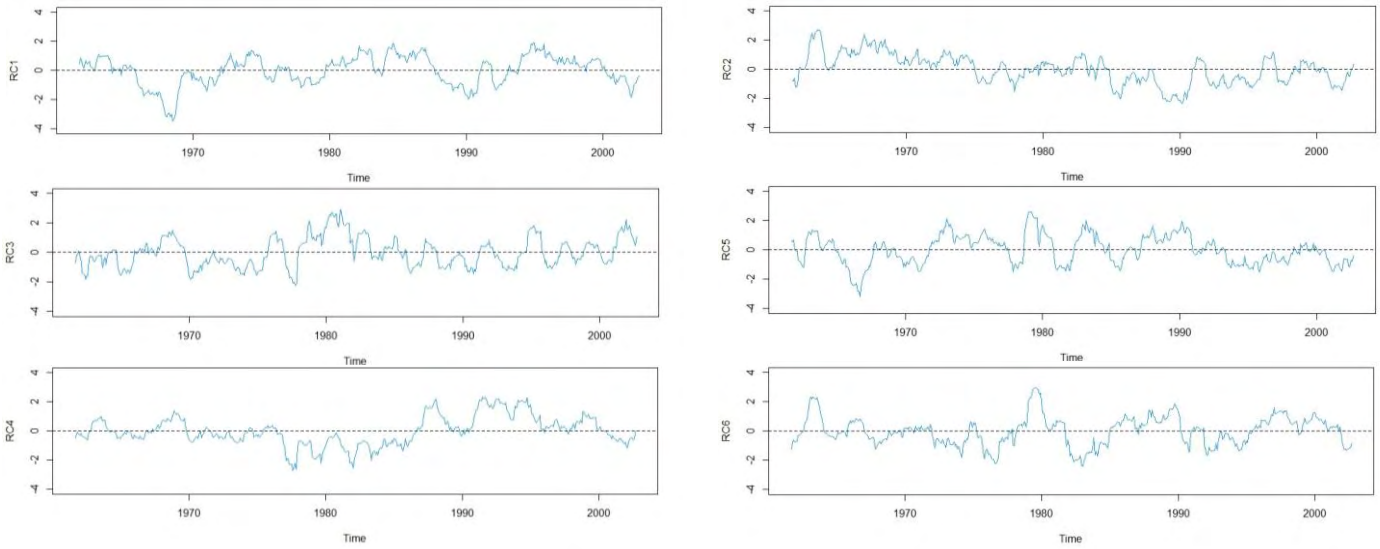

Figure 19: Scores of rotated components for SPI index, at time scale-12.

SPEI-12 (Rotated)

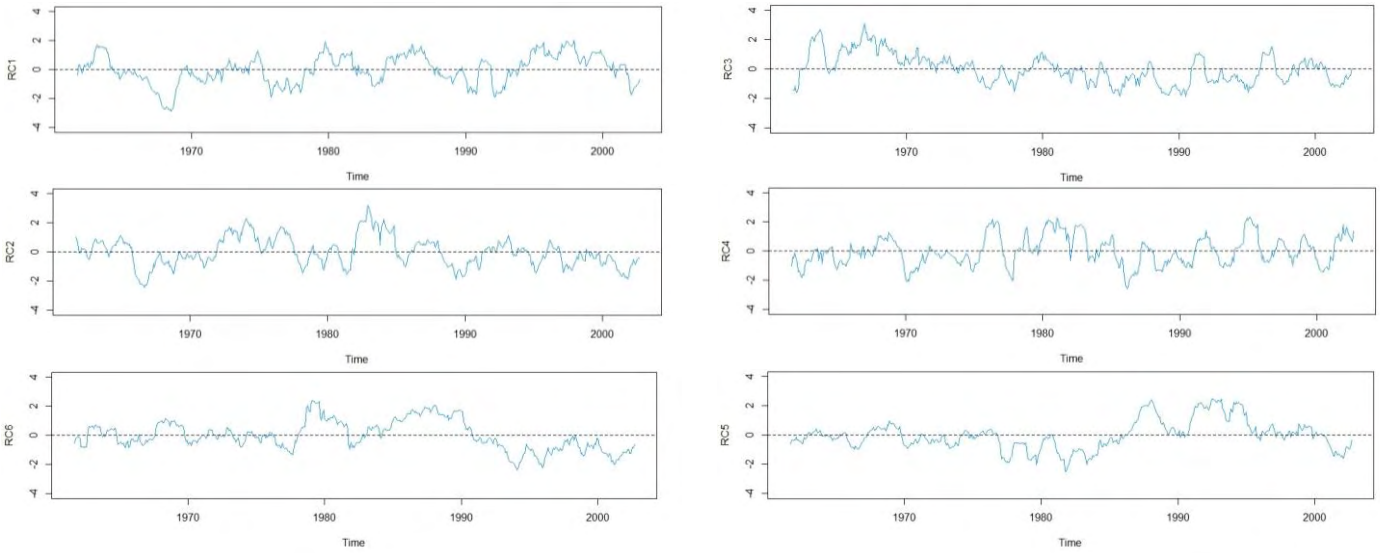

Figure 20: Scores of rotated components for SPEI index, at time scale-12.

5 CONCLUSIONS

The main objective of this study was to examine the effectiveness of four meteorological drought indices with different structure, detecting the drought events in Thessaly region. Specifically, the recommended index SPI, its enhanced version SPEI, and two multivariate models which combine probabilistically two hydro-climatic variables (precipitation and PET) and two drought indices (SPI and SPEI) respectively, have been used for the drought analysis of the area. It should be mentioned that the lapse rate method has been applied, overcoming the problem with the limited number of temperature stations of the region. Hence, 78 temperature and precipitation stations uniformly distributed over Thessaly provide the monthly data for the estimation of the aforementioned indices. In order to assess the short and medium term drought conditions, the four indices were calculated at time scales 1, 3, 6, 9, and 12 months.

The time series analysis and the drought classification for each station showed that the indices SPI and SPEI represent the most suitable measures for the drought monitoring of the region, appearing similar patterns and similar rates in each category of drought events. Small differences between them have been identified in stations where increasing trends of temperature were apparent, strengthening the ability of SPEI index in the detection of the most severe drought events relative to SPI.

Examining the results of the two multivariate models, the MSDI(Pr-PET) appeared to be biased in negative values, overestimating the number of moderate and severe drought episodes of the region compared to the other indices. On the other hand, the second multivariate model MSDI(SPI-SPEI) was found to be in consistency with the widely used indices SPI and SPEI, displaying similar patterns at all time scales. The outcomes of the drought classification indicated a similar behavior of the model with the SPEI index in the categories Moderate and Severe droughts. Furthermore, it was shown the weakness of the two produced multivariate indices to determine the extremely drought conditions of the region.

A more comprehensive comparison among the indices was conducted, examining their linear dependence, and providing the spatiotemporal distribution of correlation values for all the possible combinations of the indices. The results suggested a strong correlation between the SPI and SPEI at all time scales. Also the discordance of MSDI(Pr-PET) with the other indices was confirmed again, presenting in several stations moderately to extremely low correlation values, while the second multivariate model appeared highly correlated with the interrelated indices SPI and SPEI. According to the outcomes of the spatiotemporal correlation analysis, it was recognized that the MSDI(SPI-SPEI) response better with the SPEI index, providing the highest coefficient values in our study area. Moreover, it was observed that in mountainous areas (west side) where the effect of potential evapotranspiration it is not noticeable, the indices SPI and SPEI appeared to have more correlated coefficient values compared to the plain areas (central side). This means that the two indices in high-altitude regions respond mainly to the fluctuations of precipitation. Additionally, it should be noted that the weakest correlation values were presented at time scales 1 and 3, indicating the importance of PET in the short term drought conditions.

In the last part of this thesis a Principal Component Analysis (PCA) was conducted for the most efficient indices SPI and SPEI at time scales 3 and 12. According to this methodology, a reduction in the dimensionality of the initial SPI and SPEI series can be achieved, providing information for the drought variability of the region and thus, it can be construed as a new index for the aforementioned meteorological drought measures.

Regarding the results of this analysis, two similar homogeneous spatial patterns extracted for both indices, expressing in a similar way the temporal evolution of droughts in Thessaly for the 42 hydrological years. Examining the short term drought conditions (time scale-3), the most severe drought events were recorded in the end of 70s and in the beginning of 90s. Assessing the hydrological drought conditions (time scale-12), two distinctive severe periods were detected by both indices. The first period was recorded in the end of 70s and the second one in the end of 80s.

The PCA procedure was supported using the orthogonal Varimax technique. The results suggested that the identification of spatial drought patterns in Thessaly is closely related to the geomorphology of the region. Specifically, it was indicated that more correlated values in the low-elevation regions where the effect of PET is noticeable, were mainly represented by the components of SPEI index. On the contrary, in the high-elevation regions where the parameter of precipitation dominates, the components of SPI appeared to aggregate higher loadings than SPEI.

Except for the PCA method, an alternative way to provide spatial patterns of droughts can be performed to the SPI and SPEI series, using a non-hierarchical cluster analysis (K-means analysis). According to this statistical process, the most similar observations can be enclosed in the same group, while observations with different characteristics can be set separately; providing K different clusters of greatest possible distinction *(Santos et al., 2010)*. Therefore, a comparison between both methods can be conducted. Furthermore, the spatial and temporal characteristics of SPI and SPEI series can be assessed developing Drought Severity-Area-Frequency (SAF) annual and monthly curves, taking into account the hydrological period: October 1960-September 2002. This probabilistic approach is of great interest, concerning the planning and the decision-making of the water resources management of the region, as the plain of Thessaly constitutes the most productive agricultural region of Greece and the constant indications of increasing temperature in the recent years are characterized as particularly alarming. The aforementioned analyses will be topics of a future work.

REFERENCES

Abramovitz, M., & Stegun, I. (1965). Handbook of Mathematical Functions. National Bureau of Standards, Applied Mathematics Series – 55, Washington, D.C.

Ahmad, M. I., Sinclair, C. D., & Werritty, A. (1988). Log-logistic flood frequency analysis. Journal of Hydrology, 98(3-4), 205-224.

Anagnostopoulou, C. (2003). A contribution of drought analysis in Greece. Aristotle University of Thessaloniki. Ph. D. Dissertation, Thessaloniki, Greece.

Angelidis, P., Maris, F., Kotsovinos, N., & Hrissanthou, V. (2012). Computation of drought index SPI with alternative distribution functions. Water resources management, 26(9), 2453-2473.

Beguería, S., Vicente-Serrano, S. M., & Angulo-Martínez, M. (2010). A multiscalar global drought dataset: the SPEIbase: a new gridded product for the analysis of drought variability and impacts. Bulletin of the American Meteorological Society, 91(10), 1351-1356.

Benestad, R. E., & Haugen, J. E. (2007). On complex extremes: flood hazards and combined high spring-time precipitation and temperature in Norway. Climatic Change, 85(3-4), 381-406.

Bifulco, C., Rego, F., Dias, S., & Stagge, J. H. (2014). Assessing the association of drought indicators to impacts. The results for areas burned by wildfires in Portugal. In Proceedings of the VII International Conference on Forest Fire Research, Coimbra, Portugal (pp. 1054-1060).

Cattell, R. B. (1966). The scree test for the number of factors. Multivariate behavioral research, 1(2), 245-276.

Cressie, N. (1993). Statistics for spatial data (revised ed.). Wiley, New York.

Dunteman, G.H. (1989). Principal component analysis. Series: Quantitative applications in the social sciences. Vol. 69. Newbury Park, CA: Sage Publishers.

Edwards, D.C., & McKee, T.B. (1997). Characteristics of 20th century drought in the United States at multiple time 15 scales. Climatology Report Number 97-2, Colorado State University, Fort Collins, Colorado.

Goovaerts, P. (1997). Geostatistics for natural resources evaluation. Oxford University Press on Demand, New York.

Goovaerts, P. (2000). Geostatistical approaches for incorporating elevation into the spatial interpolation of rainfall. Journal of hydrology, 228(1), 113-129.

Gringorten, I. I. (1963). A plotting rule for extreme probability paper. Journal of Geophysical Research, 68(3), 813-814.

Guarín, A., & Taylor, A. H. (2005). Drought triggered tree mortality in mixed conifer forests in Yosemite National Park, California, USA. Forest Ecology and Management, 218(1), 229-244.

Gudmundsson, L., Rego, F. C., Rocha, M., & Seneviratne, S. I. (2014). Predicting above normal wildfire activity in southern Europe as a function of meteorological drought. Environmental Research Letters, 9(8), 084008.

Guttman, N. B. (1991). A sensitivity analysis of the Palmer Hydrologic Drought Index. Water Resources Bulletin, 27, 797–807.

Guttman, N. B. (1993). The use of L-moments in the determination of regional precipitation climates. Journal of Climate, 6(12), 2309-2325.

Guttman, N. B. (1998). Comparing the Palmer Drought Index and the Standardised Precipitation Index. American Water Resources Association, 34, 113–121.

Guttman, N. B. (1999). Accepting the standardized precipitation index: a calculation algorithm. JAWRA Journal of the American Water Resources Association, 35(2), 311-322.

Hair Jr, J. F., Anderson, R. E., Tatham, R. L., & William, C. (1995). Black (1995), Multivariate data analysis with readings. New Jersey: Prentice Hall.

Hao, Z., & AghaKouchak, A. (2013). Multivariate standardized drought index: a parametric multi-index model. Advances in Water Resources, 57, 12-18.

Hao, Z., & AghaKouchak, A. (2014). A nonparametric multivariate multi-index drought monitoring framework. Journal of Hydrometeorology, 15(1), 89-101.

Hao, Z., & Singh, V. P. (2015). Drought characterization from a multivariate perspective: A review. Journal of Hydrology, 527, 668-678.

Hayes, M. J., Svoboda, M. D., Wilhite, D. A., & Vanyarkho, O. V. (1999). Monitoring the 1996 drought using the standardized precipitation index. Bulletin of the American Meteorological Society, 80(3), 429-438.

Hayes, M. (2000). Revisiting the SPI: clarifying the process. Drought Network News, 12(1), 13–14. [available online at http://enso.unl.edu.ndmc/center/dnn/winspr.pdf] [accessed in 2000].

Hayes, M.J., Alvord, C., & Lowrey J. (2007). Drought Indices. Feature Article, Intermountain West Climate Summary, 3(6): 2-6.

Hirsch, R.M. (1981). Estimating Probabilities of Reservoir Storage for the Upper Delaware River Basin. U.S. Geological Survey, Open File Report 81-478.

Horridge, M., Madden, J., & Wittwer, G. (2005). The impact of the 2002–2003 drought on Australia. Journal of Policy Modeling, 27(3), 285-308.

Isaaks, E. H., & Srivastava, R. M., (1989). An introduction to applied geostatisics. Oxford University Press, New York.

Kaiser, H. F. (1958). The varimax criterion for analytic rotation in factor analysis. Psychometrika, 23(3), 187-200.

Kaiser, H. F. (1960). The application of electronic computers to factor analysis. Educational and psychological measurement, 20(1), 141-151.

Kao, S. C., & Govindaraju, R. S. (2010). A copula-based joint deficit index for droughts. Journal of Hydrology, 380(1), 121-134.

Kellow, J. T. (2007). Using principal components analysis in program evaluation: some practical considerations. Journal of MultiDisciplinary Evaluation, 3(5), 89-107.

Keyantash, J., & Dracup, J. A. (2002). The quantification of drought: an evaluation of drought indices. Bulletin of the American Meteorological Society, 83(8), 1167-1180.

Keyantash, J. A., & Dracup, J. A. (2004). An aggregate drought index: Assessing drought severity based on fluctuations in the hydrologic cycle and surface water storage. Water Resources Research, 40(9), W09304.

Kitanidis, P. K. (1997). Introduction to geostatistics: applications in hydrogeology. Cambridge University Press.

Loukas, A., & Vasiliades, L. (2004). Probabilistic analysis of drought spatiotemporal characteristics in Thessaly region, Greece. Natural Hazards and Earth System Science, 4(5/6), 719-731.

Manly, B. F. (2004). Multivariate statistical methods: a primer. CRC Press. Boca Raton, FL.

Marengo, J. A., Nobre, C. A., Tomasella, J., Oyama, M. D., Sampaio de Oliveira, G., de Oliveira, R., Camargo, H., Alves, L.M., Brown, I. F. (2008). The Drought of Amazonia in 2005. Journal of Climate, 21(3), 495-516.

Mavromatis, T. (2007). Drought index evaluation for assessing future wheat production in Greece. International Journal of Climatology, 27(7), 911-924.

McKee, T. B., Doesken, N. J., & Kleist, J. (1993). The relationship of drought frequency and duration to time scales. In Proceedings of the 8th Conference on Applied Climatology. Boston, MA: American Meteorological Society.

OFDA (Office of Foreign Disaster Assistance). (1990). Annual Report. Office of Foreign Disaster Assistance. Washington D.C.

Palmer, W. C. (1965). Meterological Drought. U.S. Department of Commerce. Weather Bureau, p. 58.

Santos, J. F., Pulido-Calvo, I., & Portela, M. M. (2010). Spatial and temporal variability of droughts in Portugal. Water Resources Research, 46(3).

Singh, V. P., Guo, H., & Yu, F. X. (1993). Parameter estimation for 3-parameter log-logistic distribution (LLD3) by Pome. Stochastic Hydrology and Hydraulics, 7(3), 163-177.

Spinoni, J., Naumann, G., Carrao, H., Barbosa, P., & Vogt, J. (2014). World drought frequency, duration, and severity for 1951–2010. International Journal of Climatology, 34(8), 2792-2804.

Stagge, M. S. R., & Van Lanen, H. A. (2015). Links between meteorological drought indices and yields (1979–2009) of the main european crops. DROUGHT-R&SPI Project, Technical Report, No.36.

Tallaksen, L. M., Stahl, K., & Wong, G. (2011). Space-time characteristics of large-scale droughts in Europe derived from streamflow observations and watch multi-model simulations. WATCH Project, Technical Report, No.48.

Tannehill, J. R. (1947). Drought, its causes and effects. Drought, its causes and effects. Princecton University Press, Princecton NJ.

Thom, H. C. (1958). A note on the gamma distribution. Monthly Weather Review, 86(4), 117-122.

Thompson, B., & Daniel, L. G. (1996). Factor analytic evidence for the construct validity of scores: A historical overview and some guidelines.

Thornthwaite, C. W. (1948). An approach toward a rational classification of climate. Geographical review, 38(1), 55-94.

Tsakiris, G., Loukas, A., Pangalou, D., Vangelis, H., Tigkas, D., Rossi, G., & Cancelliere, A. (2007). Drought characterization. Drought management guidelines technical annex, 85-102.

Tsakiris, G., Pangalou, D., & Vangelis, H. (2007). Regional drought assessment based on the Reconnaissance Drought Index (RDI). Water resources management, 21(5), 821-833.

UNISDR (United Nations International Strategy for Disaster Reduction Secretariat). (2011). Global Assessment Report on Disaster Risk Reduction. Geneva, Switzerland.

Vicente-Serrano, S. M., Beguería, S., & López-Moreno, J. I. (2010). A multiscalar drought index sensitive to global warming: the standardized precipitation evapotranspiration index. Journal of climate, 23(7), 1696-1718.

Vogt, J.V., Barbosa, P., Hofer, B., Magni, D., De Jager, A., Singleton, A., Horion, S., Sepulcre, G., Micale, F., Sokolova, E., Calcagni, L., Marioni, M., & Antofie, T.E. (2011a). Developing a European Drought Observatory for Monitoring, Assessing and Forecasting Droughts across the European Continent. In AGU Fall Meeting Abstracts 1, NH24A-07.

Vogt, J. V., Safriel, U., Von Maltitz, G., Sokona, Y., Zougmore, R., Bastin, G., & Hill, J. (2011b). Monitoring and assessment of land degradation and desertification: towards new conceptual and integrated approaches. Land Degradation & Development, 22(2), 150-165.

Wilhite, D. A., & Glantz, M. H. (1985). Understanding: the drought phenomenon: the role of definitions. Water international, 10(3), 111-120.

Wilhite, D. A. (1992). Drought. Encyclopedia of Earth System Science, 2, 81–92. Academic Press, San Diego.

Wilhite, D. A. (2000). Drought as a Natural Hazard: Concepts and definitions. Drought: A Global Assessment, 1(1), 3-18. Routledge, London.

Wilhite, D. A., & Pulwarty, R. S. (2005). Drought and Water Crises: Science, Technology, and Management Issues, 389-398. CRC Press, Boca Raton, Florida.

WMO (World Meteorological Organization). (1975). Drought and Agriculture. World Meteorological Organization Technical Note No 138, 392, Geneva, Switzerland.

Wu, H., Svoboda, M. D., Hayes, M. J., Wilhite, D. A., & Wen, F. (2007). Appropriate application of the standardized precipitation index in arid locations and dry seasons. International Journal of Climatology, 27(1), 65-79.

Yue, S., Ouarda, T. B. M. J., Bobée, B., Legendre, P., & Bruneau, P. (1999). The Gumbel mixed model for flood frequency analysis. Journal of hydrology, 226(1), 88-100.

Zwick, W.R., & Velicer, W.F. (1986). Comparison of five rules for determining the number of components to retain. Psychological bulletin, 99(3), 432.

APPENDIX-A

Spatial Distribution of Seasonal Rainfall in Greece

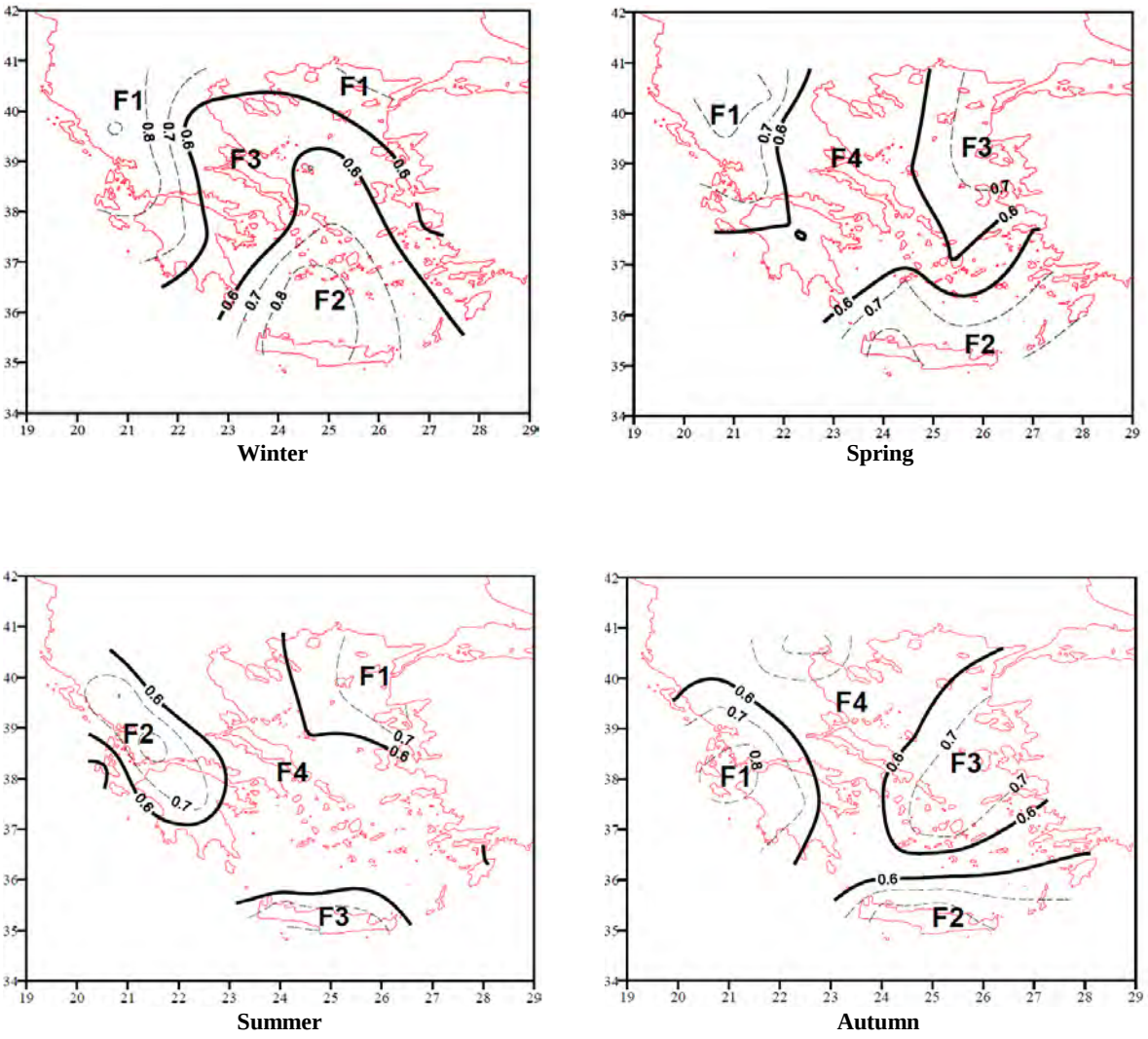

Figure 21: Spatial Distribution of seasonal rainfall in Greece providing the isolines of the loadings of the produced Factors; examining the hydrological period: 1958-1997 (Anagnostopoulou, 2003).

APPENDIX-B

SPI-SPEI-MSDI

Station-62 (Northeast)

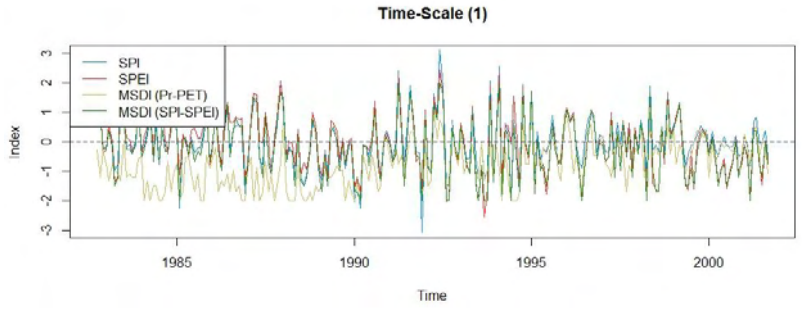

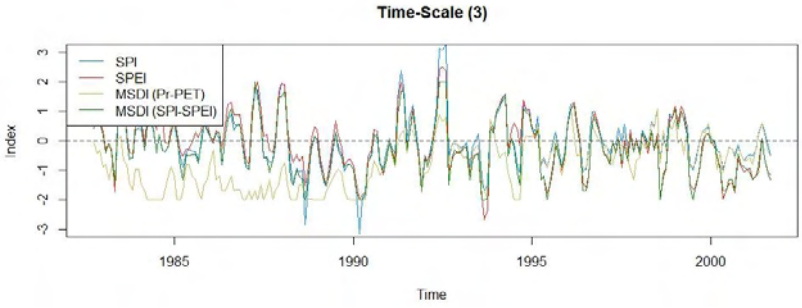

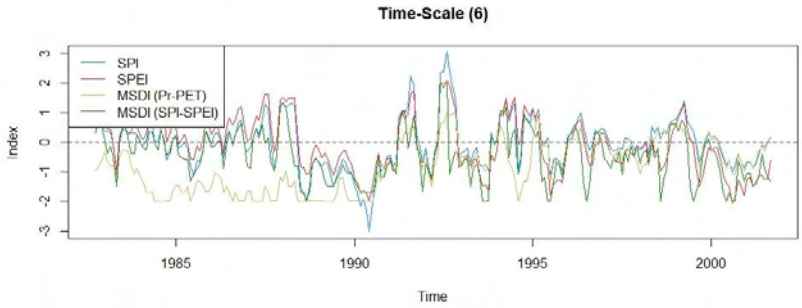

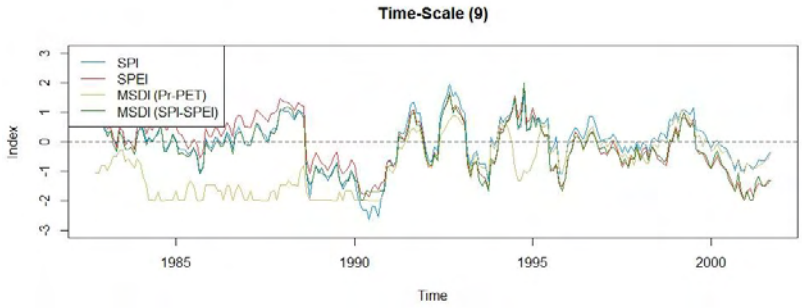

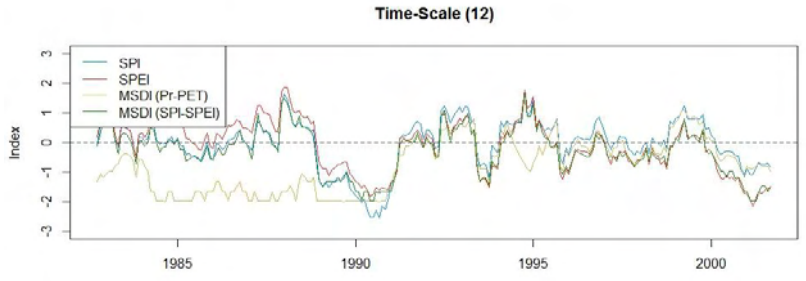

Figure 22: Time series plots of drought indices SPI (blue line), SPEI (red line), MSDI(Pr-PET) (yellow line), MSDI(SPI-SPEI) (green line), for 20 hydrological years (October 1982-September 2002) at time scales 1, 3, 6, 9 and 12 months.

Station-57 (Central)

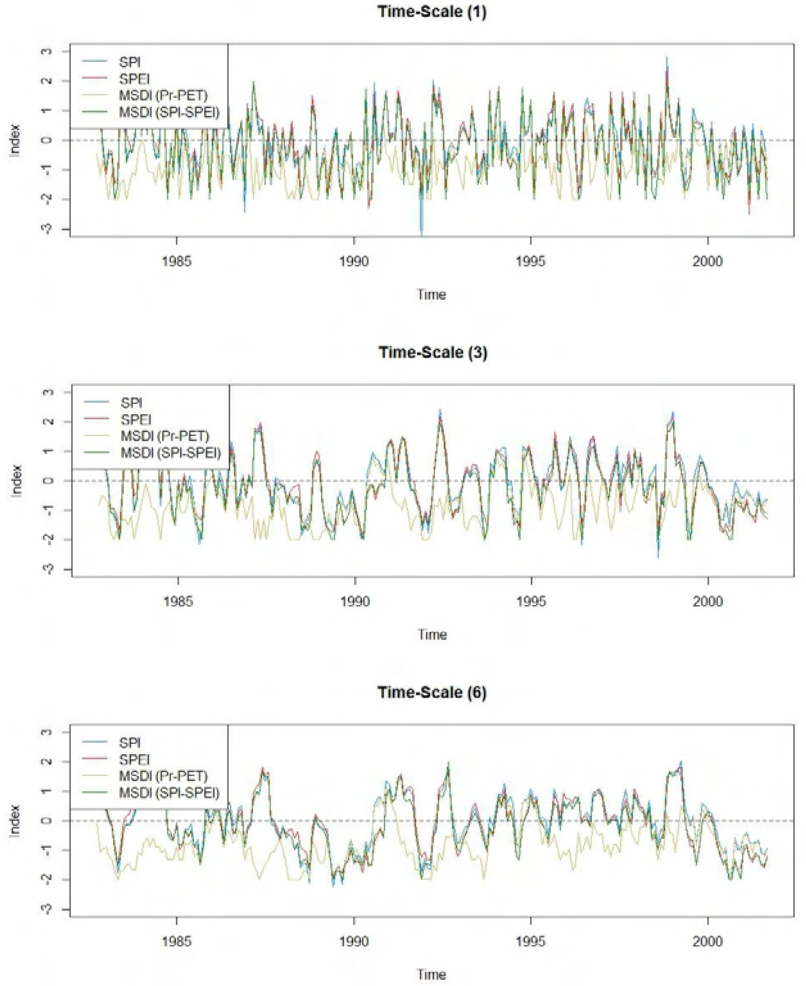

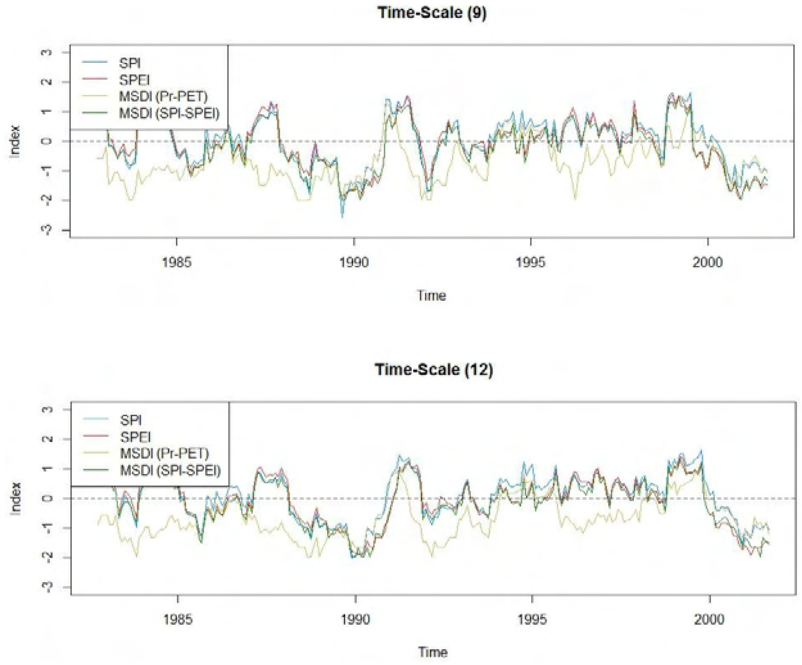

Figure 23: Time series plots of drought indices SPI (blue line), SPEI (red line), MSDI(Pr-PET) (yellow line), MSDI(SPI-SPEI) (green line), for 20 hydrological years (October 1982-September 2002) at time scales 1, 3, 6, 9 and 12 months.

Station-6 (Southwest)

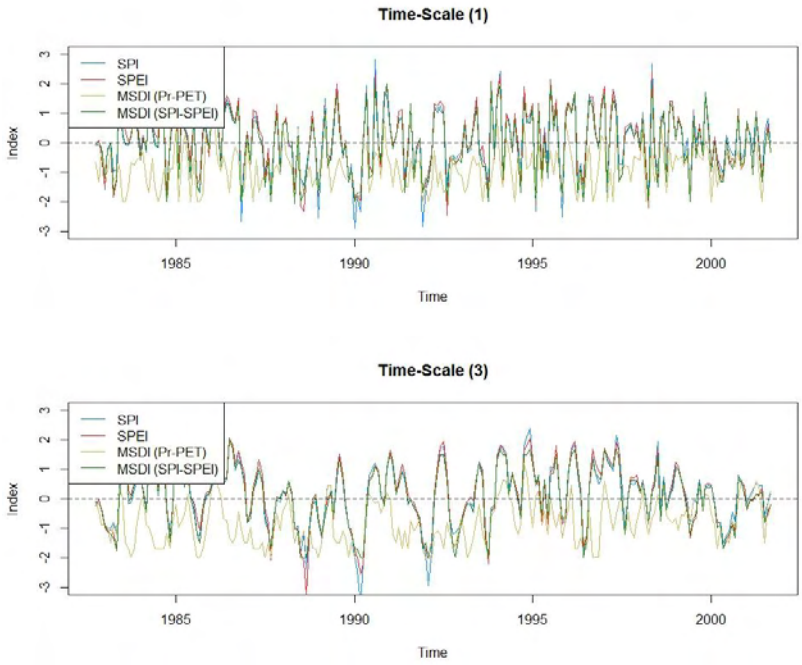

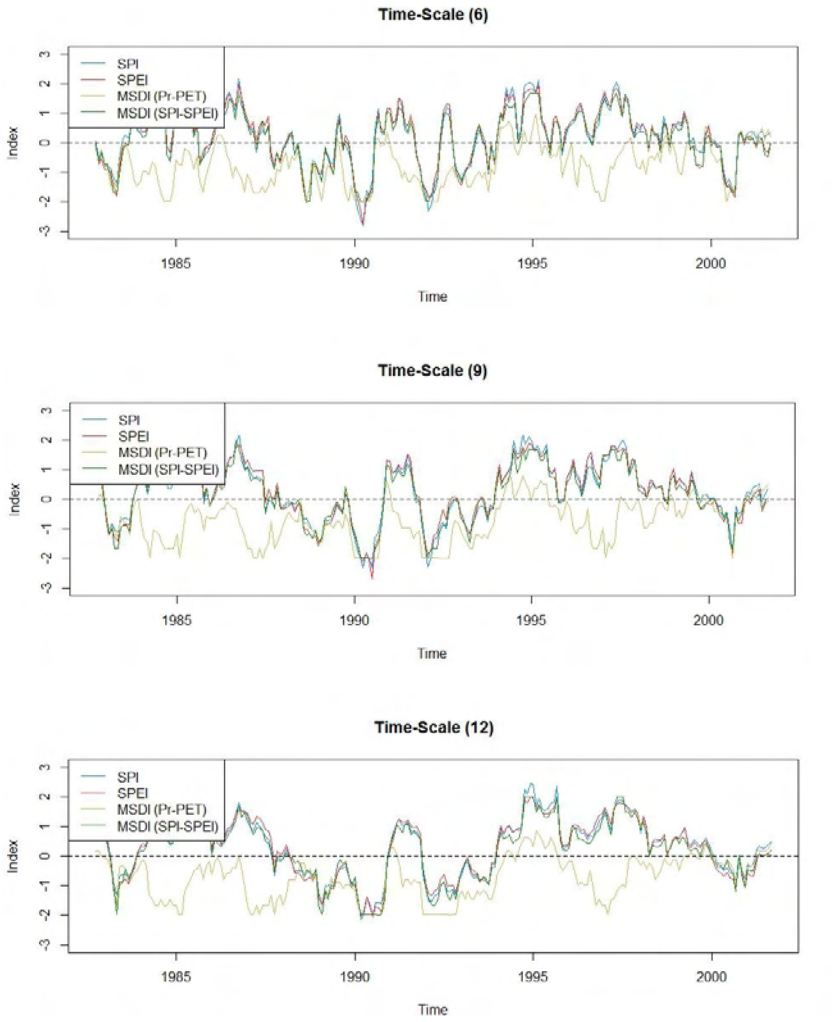

Figure 24: Time series plots of drought indices SPI (blue line), SPEI (red line), MSDI(Pr-PET) (yellow line), MSDI(SPI-SPEI) (green line), for 20 hydrological years (October 1982-September 2002) at time scales 1, 3, 6, 9 and 12 months.

Station-12 (Southeast)

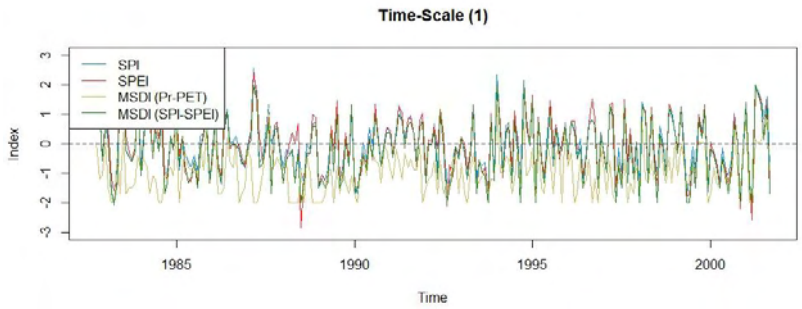

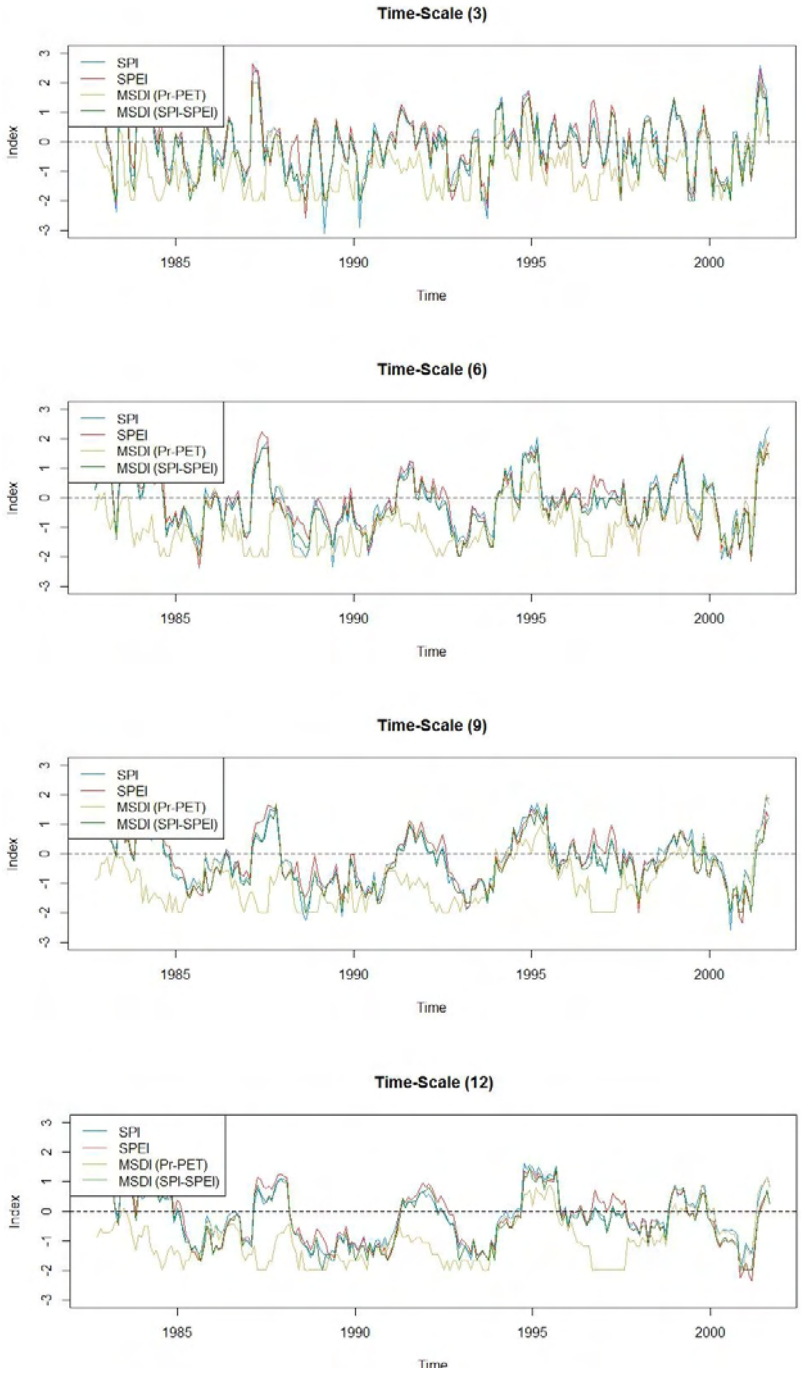

Figure 25: Time series plots of drought indices SPI (blue line), SPEI (red line), MSDI(Pr-PET) (yellow line), MSDI(SPI-SPEI) (green line), for 20 hydrological years (October 1982-September 2002) at time scales 1, 3, 6, 9 and 12 months.

Table 9: Drought classification for 42 hydrological years (October 1960 - September 2002), in Thessaly region, providing the percentages of drought events for indices SPI, SPEI, MSDI(Pr-PET), MSDI(SPI-SPEI) at time scales 1, 3, 6, 9, and 12 months.

Station 62 (Northeast)

Time-Scale (1)				
	SPI%	**SPEI%**	**MSDI(Pr-PET)%**	**MSDI(SPI-SPEI)%**
Extremely Wet	3	2	0	0
Severely Wet	2	4	0	4
Moderately Wet	9	10	1	9
Normal	72	67	57	66
Moderate Drought	9	10	25	13
Severe Drought	3	6	17	8
Extreme Drought	2	1	0	0

Time-Scale (3)				
	SPI%	**SPEI%**	**MSDI(Pr-PET)%**	**MSDI(SPI-SPEI)%**
Extremely Wet	2	2	0	0
Severely Wet	4	5	0	4
Moderately Wet	9	10	1	8
Normal	72	66	59	66
Moderate Drought	8	10	20	14
Severe Drought	3	5	20	8
Extreme Drought	2	2	0	0

Time-Scale (6)				
	SPI%	**SPEI%**	**MSDI(Pr-PET)%**	**MSDI(SPI-SPEI)%**
Extremely Wet	3	2	0	0
Severely Wet	3	5	0	1
Moderately Wet	10	11	0	5
Normal	71	67	61	66
Moderate Drought	6	10	18	18
Severe Drought	4	4	22	10
Extreme Drought	3	1	0	0

Time-Scale (9)				
	SPI%	**SPEI%**	**MSDI(Pr-PET)%**	**MSDI(SPI-SPEI)%**
Extremely Wet	3	2	0	0
Severely Wet	3	4	0	4
Moderately Wet	7	10	0	7
Normal	72	68	61	69
Moderate Drought	8	10	19	12
Severe Drought	3	5	20	8
Extreme Drought	3	1	0	0

Time-Scale (12)				
	SPI%	**SPEI%**	**MSDI(Pr-PET)%**	**MSDI(SPI-SPEI)%**
Extremely Wet	2	2	0	0
Severely Wet	5	5	0	4
Moderately Wet	6	7	0	7
Normal	70	67	61	68
Moderate Drought	10	12	18	13
Severe Drought	3	6	21	8
Extreme Drought	4	1	0	0

Table 10: Drought classification for 42 hydrological years (October 1960 - September 2002), in Thessaly region, providing the percentages of drought events for indices SPI, SPEI, MSDI(Pr-PET), MSDI(SPI-SPEI) at time scales 1, 3, 6, 9, and 12 months.

Station-57 (Central)

Time-Scale (1)				
	SPI%	**SPEI%**	**MSDI(Pr-PET)%**	**MSDI(SPI-SPEI)%**
Extremely Wet	1	1	0	0
Severely Wet	6	7	0	4
Moderately Wet	8	10	0	9
Normal	70	65	53	67
Moderate Drought	9	10	27	11
Severe Drought	4	6	19	9
Extreme Drought	1	1	0	0

Time-Scale (3)				
	SPI%	**SPEI%**	**MSDI(Pr-PET)%**	**MSDI(SPI-SPEI)%**
Extremely Wet	2	1	0	0
Severely Wet	3	5	0	4
Moderately Wet	12	12	0	8
Normal	69	64	53	69
Moderate Drought	6	11	25	12
Severe Drought	5	6	22	7
Extreme Drought	3	1	0	0

Time-Scale (6)				
	SPI%	**SPEI%**	**MSDI(Pr-PET)%**	**MSDI(SPI-SPEI)%**
Extremely Wet	2	1	0	0
Severely Wet	4	6	0	3
Moderately Wet	10	11	0	8
Normal	67	64	52	70
Moderate Drought	10	12	26	13
Severe Drought	4	5	22	6
Extreme Drought	3	1	0	0

Time-Scale (9)				
	SPI%	**SPEI%**	**MSDI(Pr-PET)%**	**MSDI(SPI-SPEI)%**
Extremely Wet	2	1	0	0
Severely Wet	4	6	0	3
Moderately Wet	9	11	1	8
Normal	70	64	52	70
Moderate Drought	8	11	25	11
Severe Drought	5	6	22	8
Extreme Drought	2	1	0	0

Time-Scale (12)				
	SPI%	**SPEI%**	**MSDI(Pr-PET)%**	**MSDI(SPI-SPEI)%**
Extremely Wet	2	1	0	0
Severely Wet	2	6	0	3
Moderately Wet	13	9	0	9
Normal	66	66	53	69
Moderate Drought	9	11	22	11
Severe Drought	5	8	25	8
Extreme Drought	3	0	0	0

Table 11: Drought classification for 42 hydrological years (October 1960 - September 2002), in Thessaly region, providing the percentages of drought events for indices SPI, SPEI, MSDI(Pr-PET), MSDI(SPI-SPEI) at time scales 1, 3, 6, 9, and 12 months.

Station-6 (Southwest)

Time-Scale (1)				
	SPI%	**SPEI%**	**MSDI(Pr-PET)%**	**MSDI(SPI-SPEI)%**
Extremely Wet	3	2	0	0
Severely Wet	4	5	0	5
Moderately Wet	8	10	1	9
Normal	72	66	54	68
Moderate Drought	7	11	25	12
Severe Drought	3	5	20	6
Extreme Drought	3	1	0	0

Time-Scale (3)				
	SPI%	**SPEI%**	**MSDI(Pr-PET)%**	**MSDI(SPI-SPEI)%**
Extremely Wet	3	3	0	0
Severely Wet	5	5	0	4
Moderately Wet	6	8	0	9
Normal	71	68	52	70
Moderate Drought	10	10	27	11
Severe Drought	3	4	21	6
Extreme Drought	2	2	0	0

Time-Scale (6)				
	SPI%	**SPEI%**	**MSDI(Pr-PET)%**	**MSDI(SPI-SPEI)%**
Extremely Wet	4	1	0	0
Severely Wet	4	7	0	4
Moderately Wet	8	8	0	9
Normal	71	68	53	71
Moderate Drought	8	10	25	10
Severe Drought	3	5	22	6
Extreme Drought	2	1	0	0

Time-Scale (9)				
	SPI%	**SPEI%**	**MSDI(Pr-PET)%**	**MSDI(SPI-SPEI)%**
Extremely Wet	2	0	0	0
Severely Wet	6	7	0	5
Moderately Wet	8	11	0	9
Normal	68	65	54	70
Moderate Drought	12	12	24	10
Severe Drought	2	3	22	6
Extreme Drought	2	2	0	0

Time-Scale (12)				
	SPI%	**SPEI%**	**MSDI(Pr-PET)%**	**MSDI(SPI-SPEI)%**
Extremely Wet	2	0	0	0
Severely Wet	7	7	0	4
Moderately Wet	7	12	0	9
Normal	67	61	53	69
Moderate Drought	14	16	25	12
Severe Drought	3	3	22	6
Extreme Drought	0	1	0	0

Table 12: Drought classification for 42 hydrological years (October 1960 - September 2002), in Thessaly region, providing the percentages of drought events for indices SPI, SPEI, MSDI(Pr-PET), MSDI(SPI-SPEI) at time scales 1, 3, 6, 9, and 12 months.

Station-12 (Southeast)

Time-Scale (1)				
	SPI%	**SPEI%**	**MSDI(Pr-PET)%**	**MSDI(SPI-SPEI)%**
Extremely Wet	2	2	0	0
Severely Wet	4	4	0	5
Moderately Wet	9	11	0	8
Normal	70	66	52	66
Moderate Drought	11	12	25	14
Severe Drought	4	4	23	7
Extreme Drought	0	1	0	0

Time-Scale (3)				
	SPI%	**SPEI%**	**MSDI(Pr-PET)%**	**MSDI(SPI-SPEI)%**
Extremely Wet	3	3	0	0
Severely Wet	3	4	0	4
Moderately Wet	10	10	1	9
Normal	68	66	51	68
Moderate Drought	10	11	25	12
Severe Drought	4	5	23	7
Extreme Drought	2	1	0	0

Time-Scale (6)				
	SPI%	**SPEI%**	**MSDI(Pr-PET)%**	**MSDI(SPI-SPEI)%**
Extremely Wet	2	2	0	0
Severely Wet	5	5	0	4
Moderately Wet	6	8	1	8
Normal	72	69	53	69
Moderate Drought	9	8	23	12
Severe Drought	3	6	23	7
Extreme Drought	3	2	0	0

Time-Scale (9)				
	SPI%	**SPEI%**	**MSDI(Pr-PET)%**	**MSDI(SPI-SPEI)%**
Extremely Wet	3	2	0	0
Severely Wet	4	5	0	4
Moderately Wet	8	10	1	9
Normal	70	67	52	69
Moderate Drought	9	10	23	12
Severe Drought	4	4	24	6
Extreme Drought	2	2	0	0

Time-Scale (12)				
	SPI%	**SPEI%**	**MSDI(Pr-PET)%**	**MSDI(SPI-SPEI)%**
Extremely Wet	4	3	0	0
Severely Wet	3	3	0	4
Moderately Wet	8	10	1	8
Normal	70	66	52	68
Moderate Drought	11	12	23	13
Severe Drought	3	4	24	7
Extreme Drought	1	2	0	0

APPENDIX-C

Correlation Analysis

Station 62 (Northeast)

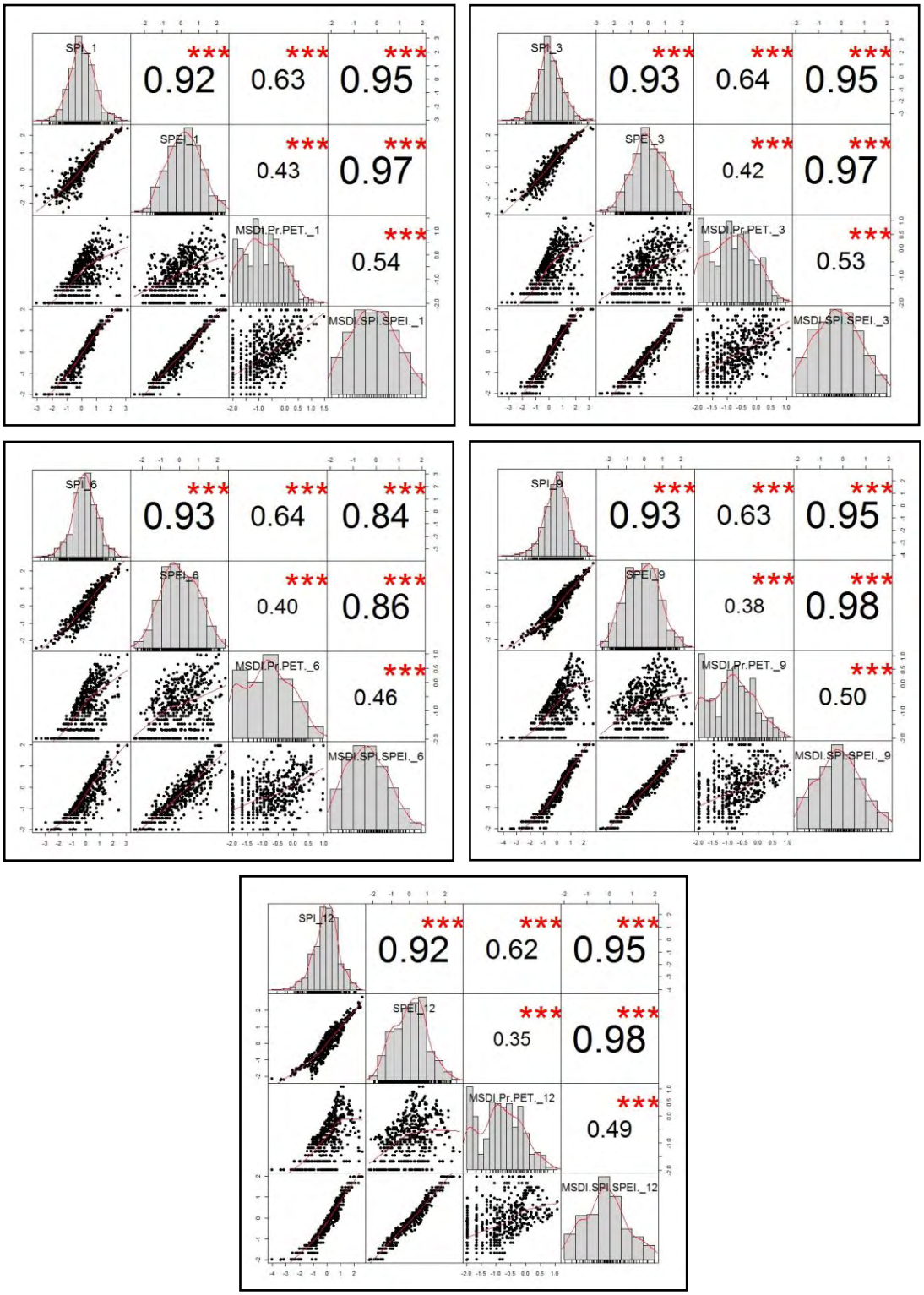

Figure 26: Cross correlation among the indices SPI,SPEI, MSDI(Pr-PET), MSDI(SPI-SPEI) for (a) 1-month, (b) 3-month, (c) 6-month, (d) 9-month, and (e) 12-month time scales.

Station-57 (Central)

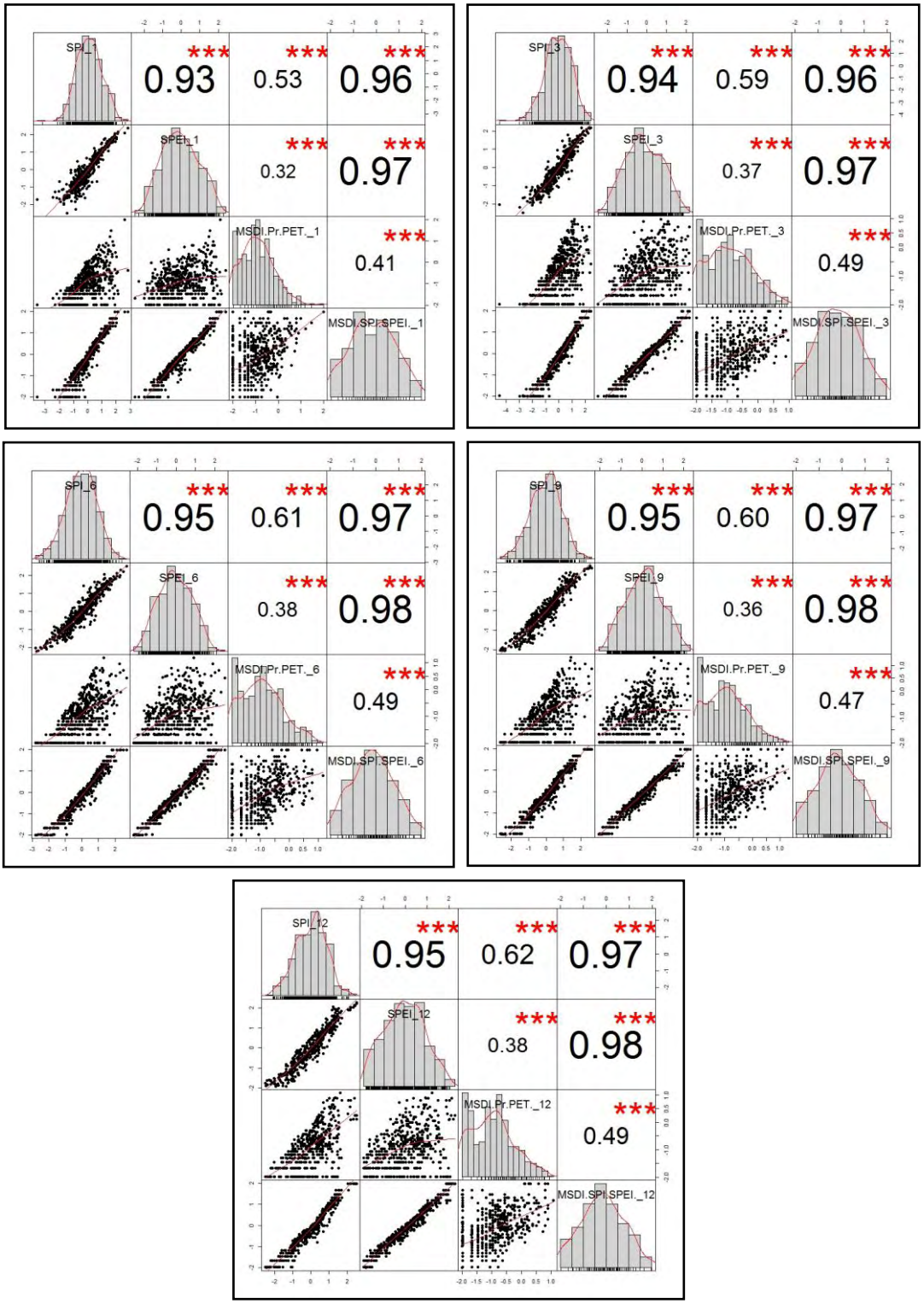

Figure 27: Cross correlation among the indices SPI,SPEI, MSDI(Pr-PET), MSDI(SPI-SPEI) for (a) 1-month (b) 3-month, (c) 6-month, (d) 9-month, and (e) 12-month time scales.

Station-6 (Southwest)

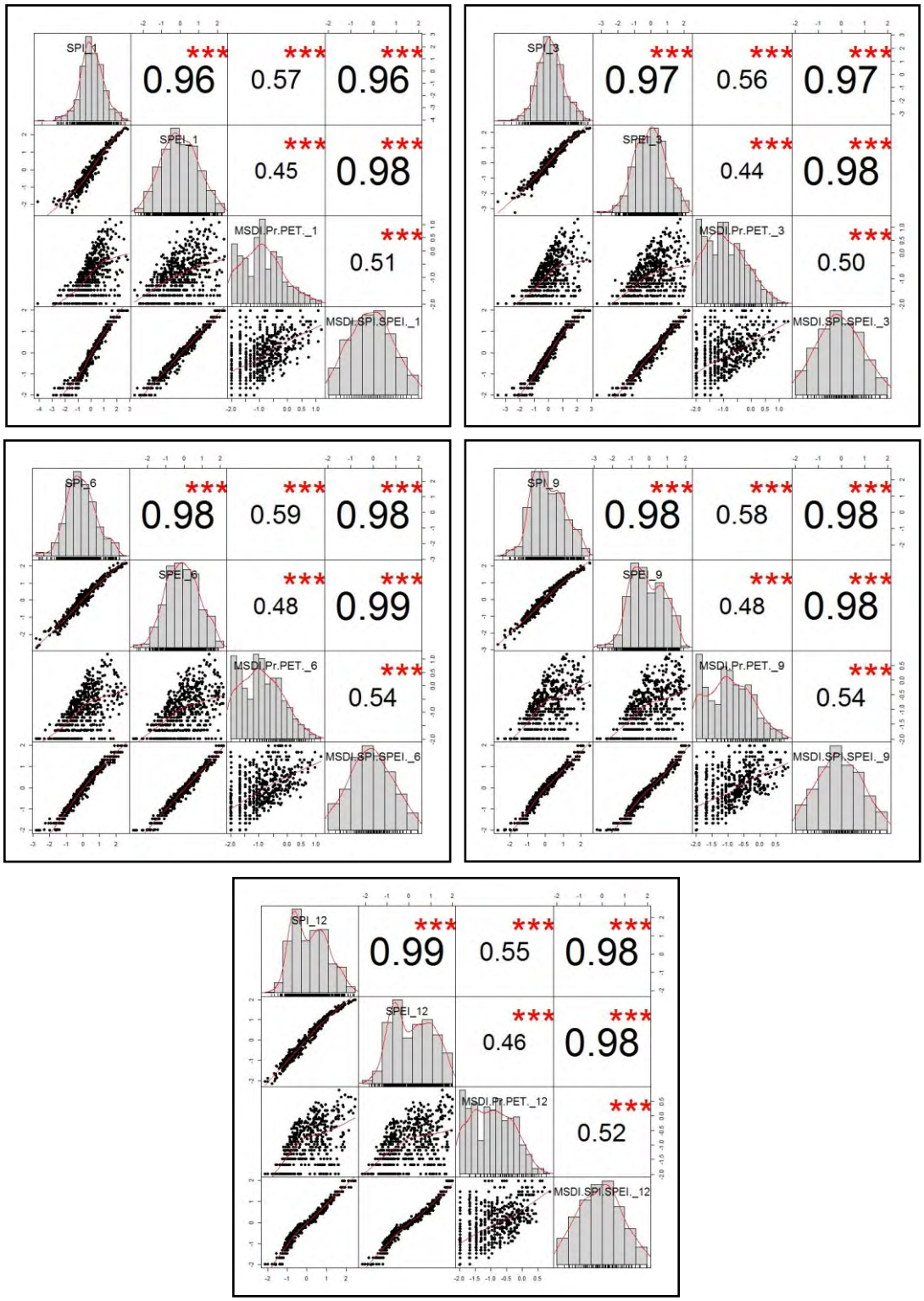

Figure 28: Cross correlation among the indices SPI,SPEI, MSDI(Pr-PET), MSDI(SPI-SPEI) for (a) 1-month, (b) 3-month, (c) 6-month, (d) 9-month, and (e) 12-month time scales.

Station-12 (Southeast)

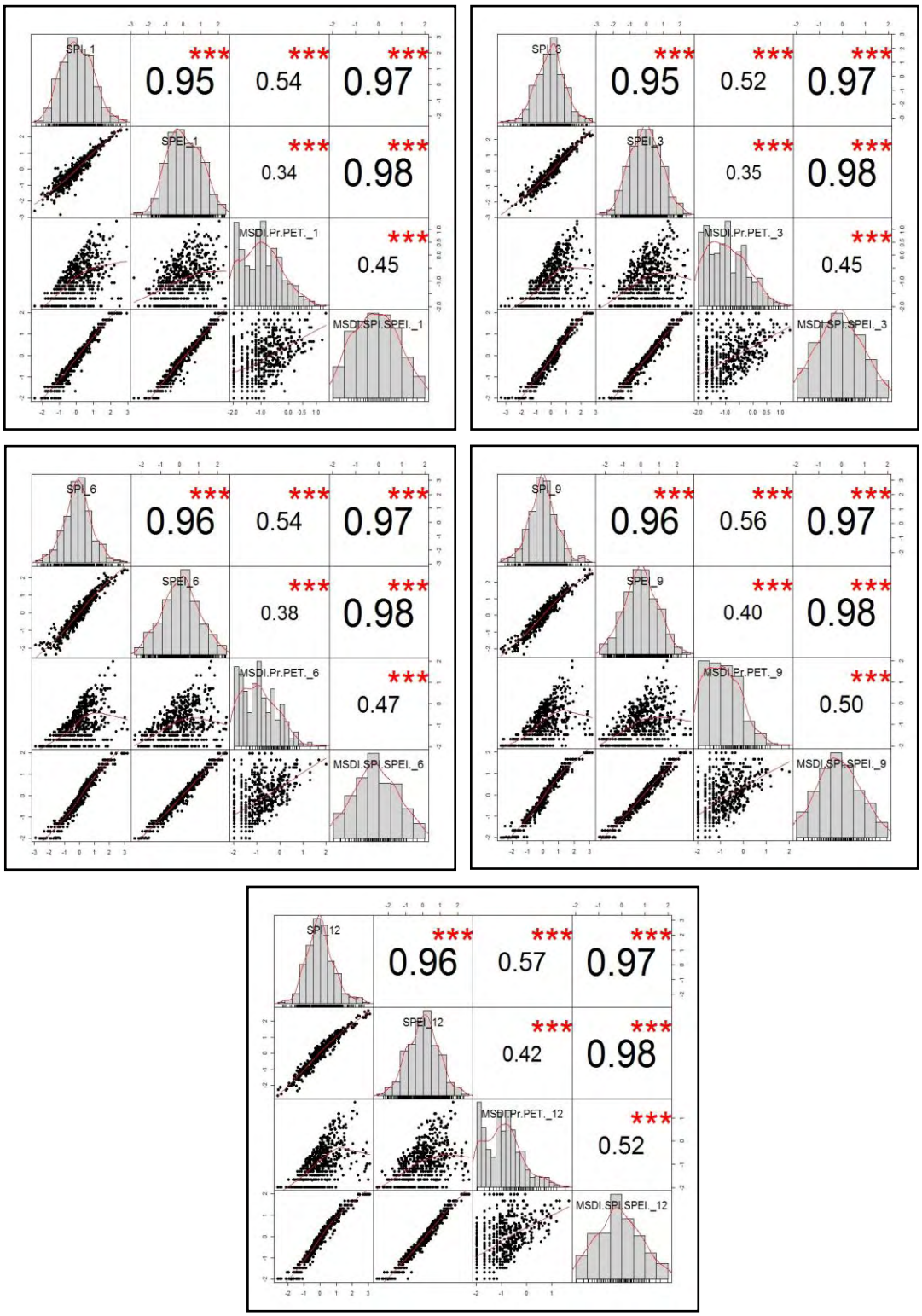

Figure 29: Cross correlation among the indices SPI,SPEI, MSDI(Pr-PET), MSDI(SPI-SPEI) for (a) 1-month, (b) 3-month, (c) 6-month, (d) 9-month, and (e) 12-month time scales.

APPENDIX-D

Principal Component Analysis (PCA)

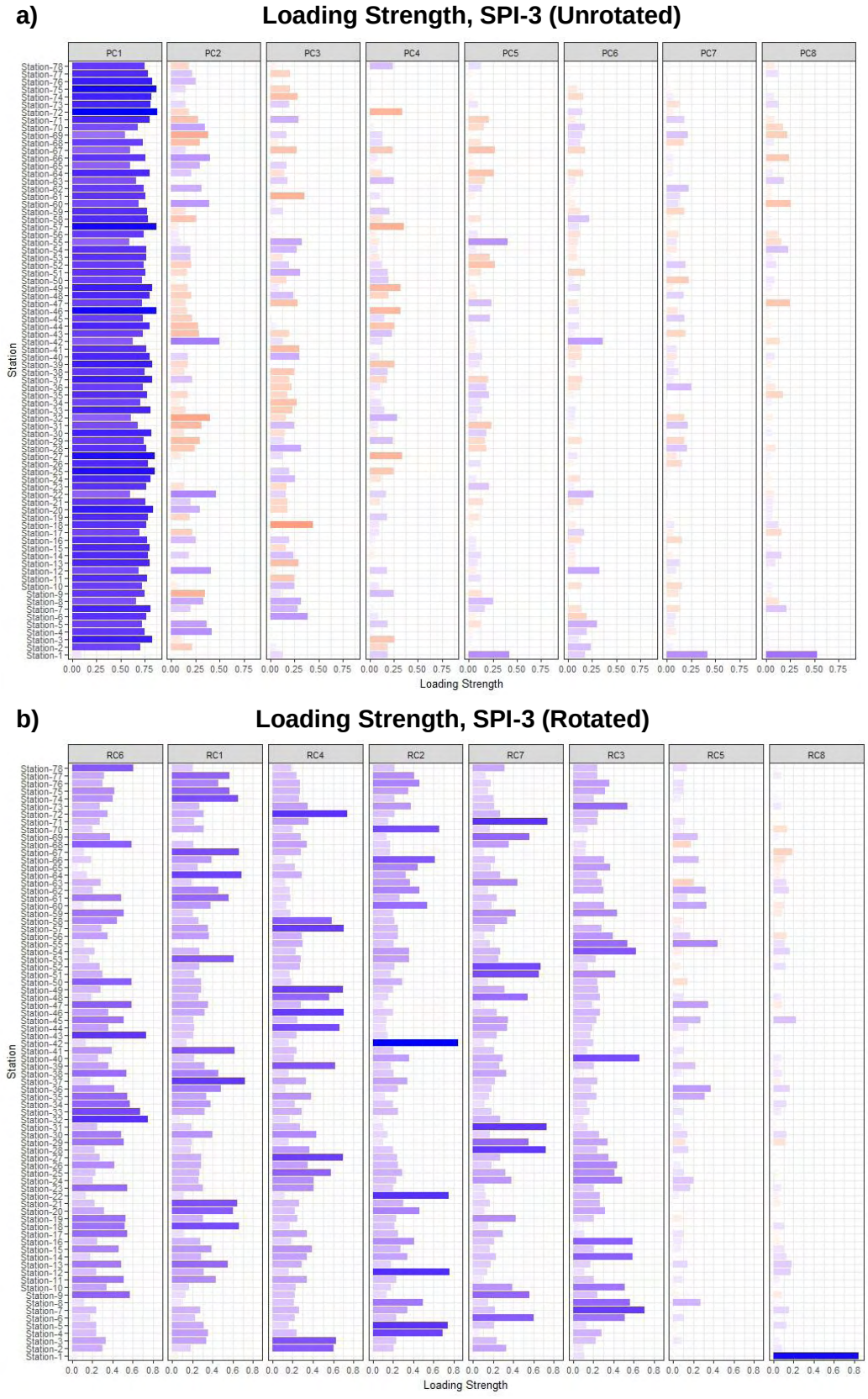

Figure 30: Loading strength for each station, of 8 meaningful components, analyzing the SPI index at time scale-3 in a) unrotated case b) rotated case.

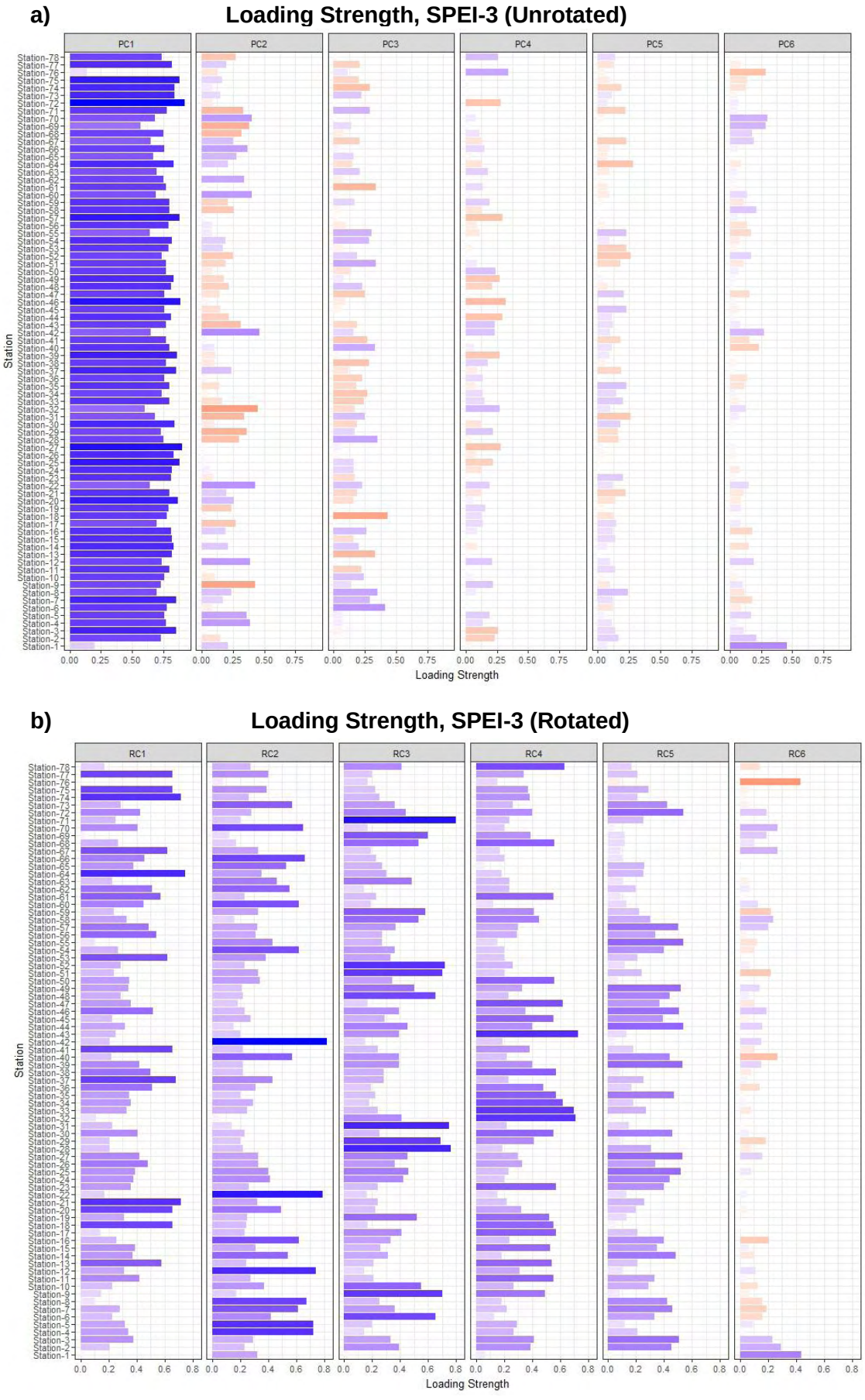

Figure 31: Loading strength for each station, of 6 meaningful components, analyzing the SPEI index at time scale-3 in a) unrotated case b) rotated case.

Figure 32: Loading strength for each station, of 6 meaningful components, analyzing the SPI index at time scale-12 in a) unrotated case b) rotated case.

Figure 33: Loading strength for each station, of 6 meaningful components, analyzing the SPEI index at time scale-12 in a) unrotated case b) rotated case.